EFFECT OF BLEND RATIO OF h-LLDPE WITH LDPE ON THE PROCESSABLITY AND THE MECHANICAL PROPERTIES OF BLOWN FILMS

BY

SARFARAZ AHMED FURQUAN

A Thesis Presented to the

DEANSHIP OF GRADUATE STUDIES

KING FAHD UNIVERSITY OF PETROLEUM & MINERALS

DHAHRAN, SAUDI ARABIA

In Partial Fulfillment of the
Requirements for the Degree of

MASTER OF SCIENCE

In

MECHANICAL ENGINEERING

MAY 2009

KING FAHD UNIVERSITY OF PETROLEUM & MINERALS

DHAHRAN 31261, SAUDI ARABIA

DEANSHIP OF GRADUATE STUDIES

This thesis, written by **Sarfaraz Ahmed Furquan** under the direction of his thesis advisor and approved by his thesis committee, has been presented to and accepted by the Dean of Graduate Studies, in partial fulfillment of the requirements for the degree of **MASTER OF SCIENCE IN MECHANICAL ENGINEERING**.

Thesis Committee

Dr. Khaled Mezghani (Advisor)

Dr. AbdelRahman N. Shuaib (Member)

Dr. Khaled A. Al-Dheylan (Member)

27/06/2009

Dr. Amro M. Al- Qutub
Department Chairman

Dr. Salam A. Zummo
Dean of Graduate Studies

3/2/10

Date

Dedicated to

my Beloved Parents, Brothers and Sister

ACKNOWLEDGEMENTS

"In the name of Allah, The Most Gracious and The Most Merciful"

All praise and thanks are to Almighty Allah, The Most Beneficent and Magnificent for endowing me with perseverance, courage and patience to complete my M.S. and thesis work. May peace and blessings be upon the prophet Muhammad (PBUH), his family and his companions.

My due acknowledgements to King Fahd University of Petroleum & Minerals for providing me this opportunity to accomplish my M.S. and thesis research work. I would also like to thank King Abdul Aziz Center for Science & Technology for funding this research project.

I would like to express my profound gratitude and appreciation to my advisor Dr. Khaled Mezghani for his continuous support and guidance throughout my research work. It was his motivation and inspiration that helped me in getting through all the difficult stages of my work. With due respect, I would like to acknowledge the encouragement and guidance from my committee members Dr. AbdelRehman N. Shuaib and Dr. Khaled Al- Dheylan.

I would like to extend my thanks to all the ME department lab engineers and faculty members, especially Mr. Saleh, Mr. Habib and Mr. Faheemuddin for their help in learning the instrument operations and valuable support. With great appreciation I would like to thank all the ME workshop personnel for their contribution in making the accessories for the experimental setup. Many thanks to Mr. Mohammed Ayub for his

kind help in acquiring the standard, which played a crucial role in accomplishment of my thesis.

I thank all my fellow graduate students in the department and also the other graduate students at KFUPM. To name them all would be difficult, and thus to name a few, acknowledgements to Siraj, Safdar, Shiraz bhai, Hasan, Hussain, Murtuza bhai, Asrar bhai, Najid, Irfan, Zahed bhai, Razwan bhai, Nazeer bhai, Fareed bhai and Faheem bhai for making my stay at KFUPM a memorable and enjoyable one..

Special thanks to my parents, brothers and sister for their encouragement, support and constant prayers for my success. Sincere thanks to all my relatives residing in Saudi Arabia for their support an encouragement during my entire course of study at KFUPM.

.

TABLE OF CONTENTS

LIST OF TABLES

LIST OF FIGURES

Nomenclature

h-LLDPE	Hexene Linear low Density Polyethylene
LDPE	Low Density Polyethylene
HDPE	High Density Polyethylene
DR	Draw Ratio
BR	Blow Ratio
MD	Machine Direction
TD	Transverse Direction
FLH	Frost Line Height
WAXS	Wide Angle X-ray Scattering
SAXS	Small Angle X-ray Scattering
TEM	Transmission Electron Microscopy
AFM	Atomic Force Microscopy
FTIR	Fourier– Transform Infrared Dichroism
DSC	Differential Scanning Calorimetry
UTS	Ultimate Tensile Strength
σ_y	Tensile Stress at Yield
ϵ_F	Tensile Strain at Break - Ductility
T_E	Toughness – Energy at Break
STD	Standard Deviation
F_{PN}	Normalized Peak Force (N)

E_{PN}	Normalized Energy to Peak Force (J)
F_{FN}	Normalized Failure Force (N)
ΔL_{FN}	Normalized Failure Deformation (mm)
E_{FN}	Normalized Failure Energy (J)
TR	Tear Resistance
TR_N	Normalized Tear Resistance

THESIS ABSTRACT (ENGLISH)

NAME: SARFARAZ AHMED FURQUAN

TITLE: EFFECT OF BLEND RATIO OF h-LLDPE WITH LDPE ON THE PROCESSABILITY AND THE MECHANICAL PROPERTIES OF BLOWN FILMS

MAJOR: MECHANICAL ENGINEERING

DATE: MAY 2009

The h-LLDPE is well known for its superior mechanical properties but at the same time is very difficult to process. On the other hand LDPE is much better in processing but has lower mechanical properties. Thus a blend of h-LLDPE/LDPE is an option which could improve processability and at the same time provide better mechanical properties. Of the two, h-LLDPE and LDPE, h-LLDPE is difficult to process and thus in this research, the processability and the mechanical characteristics of h-LLDPE/LDPE blends are studied. The processability window and polymer degradation studies for h-LLDPE were established for different die temperatures (210, 230, 250 and 270°C), and it was found that the optimum die temperature was 230°C. Also, effects of draw ratio (DR) and blow ratio (BR) on the mechanical properties of the blown films were studied. Mechanical tests such as tensile and Elmendorf tear test were conducted in both MD (machine) and TD (transverse) directions. Also, impact tests were carried out. Different mechanical tests of blown film samples at different DRs of 7, 21, 36, 49, 64 and 86 were accomplished. The DR 21 which resulted in higher impact resistance to failure of films was selected as the optimum DR. Other blown films of h-LLDPE were produced at different BRs of 1.12, 1.4 and 1.78 and mechanically tested. The study showed that the optimum BR should be in the range of 1.4 to 1.78; therefore an average value of 1.6 was selected. Consequently with the selected values of die temperature (230°C), draw ratio (21), and blow ratio (1.6) the effect of blending h-LLDPE with LDPE was studied.

Pure h-LLDPE, LDPE and their blends (5%, 10%, 15%, 20% and 50%) were processed, and the effect of blending was studied using thermal, birefringence and mechanical techniques. The crystallinity for different blends was determined using DSC instrument. The cyrstallinity values were found to be in the range of 40% close to that of pure h-LLDPE and were not affected by the blend ratio. The birefringence of the blends has been studied using an optical microscope and an index of orientation has been reported. There is an increase in MD orientation when the blend ratio increases ($-3x10^{-3}$ to $5x10^{-3}$) from 0 to 50%, and then the birefringence decreases. Mechanical tests such as tensile, impact and elmendorf tear test were also conducted on the blended films. With addition of up to 20% LDPE, many mechanical properties of the blend showed

improvement. There was a 20% enhancement in MD yield strength by small addition of LDPE without any decrease in the MD ductility. The MD toughness also displayed an increment of around 43% in its properties with this small addition of LDPE. The enhancement in TD tensile strength was more than 75% with very low blend ratio of 10% LDPE. The TD ductility slightly improved in comparison to pure h-LLDPE. TD toughness showed a small increase up to a blend ratio of 50%. A 20% improvement was observed in the impact peak force with very small addition of LDPE. In case of impact failure energy there was some decrease with respect to the blend ratio. The tear resistance also showed some kind of deterioration in the MD direction, but there was a large improvement for tear resistance in the TD direction. The TD tear resistance improved by almost 100% by addition of LDPE for the low blend percentages up to 20%.

In general, the study of blend effect of h-LLDPE/LDPE on mechanical properties of blown films showed improvement up to 20% blends. In addition the torque requirement for the film process was reduced with the increase of blend ratio, except at 5% blend ratio.

MASTER OF SCIENCE DEGREE

KING FAHD UNIVERSITY OF PETROLEUM & MINERALS

Dhahran, Saudi Arabia

THESIS ABSTRACT (ARABIC)

الاسم: سرفراذ احمد فرقان

العنوان : تأثير مزيج من نسبة ه - مع البولي إثيلين المنخفض الكثافة الخطي المعنية للتجهيز والخصائص الميكانيكية في مهب الأغشية

التخصص: الهندسة الميكانيكية

التاريخ:

وح - الخطي هو معروف جيدا لخواصه الميكانيكية الامتفوقة ولكن في نفس الوقت من الصعب جدا معالجته .وبالتالي مزيج من h-LLDPE/LDPE هو الخيار الذي يمكن أن يحسن للتجهيز وفي نفس الوقت توفير أفضل الخصائص الميكانيكية. من الاثنين ، ه- البولي إثيلين منخفض الكثافة الخطي ، و ه - الخطي يصعب معالجتهما ، وبالتالي في هذا البحث ، التجهيز والخصائص الميكانيكية للمزيج h-LLDPE/LDPE تم دراستها . نافذة التجهيز وانحلال البولي مرات تم دراستها ل ه – الخطي والتي أسست لدرجات حرارة مختلفة (210,230,250,270 درجة مئوية) ووجد أن درجه الإخماد المثلى هي 230 أيضا تأثير نسبه السحب ونسبه النفخ على الخواص الميكانيكه تم دراستها اختبارات ميكانيكية مثل الشد والتمزيق أجريت في كل من اتجاه الماكينة والاتجاه العرضي أيضا, اختبارات التصادم نفذت أيضا . الاختبارات الميكانيكية المختلفة لعينات مختلفة 7 ، 21 ، 36 ، 49 ، 64 و 86 تم انجازه. الدي أر 21 والذي أعطى نتيجة مقاومه للصدمات أكبر في فشل الأغشية التي تم اختيارها كدرجه مثلى للدي أر.الأغشية ه - الخطي أنتجت في براس مختلفة من 1.12 و 1.4 و 1.78 ميكانيكيا تم اختبارها . وأظهرت الدراسة أن ألبي أر الأمثل ينبغي أن يكون في نطاق بين 1.4 و 1.78 ، وبالتالي على قيمة متوسط 1.6 تم اختياره .بناء على ذلك ومع الدرجة الخامدة المختارة (230) ونسبه السحب (21) ونسبه النفخ(1.6) تم دراسة تأثير مزج ه - مع منخفض الكثافة الخطي .

H-LLDPE/LDPE النقي ومزيجه (5%,10%,15%,20%,50%) تم معالجته. وتم دراسة تأثير المزيج باستخدام الانكسار الحراري والتقنيات ألميكانيكيه. البلورية لأمزجه متلفه تم تحديدها باستخدام الدي أس سي.وجدأن قيم البلورية في نطاق 40% قريبه للقيم النقية لل H-LLDPE وكذلك لا تتأثر بنسبة المزج. الانكسار للأمزجة تمت دراسته باستخدام الميكروسكوب الضوئي و مؤشر التوجه تم وصفة.هناك زيادة في اتجاه الماكينة عندما تزيد نسبه المزج (3-^10*3-إلى 5^10*5) من 0 إلى 50% عندها فان الانكسار يقل , اختبارات ميكانيكية مثل الشد والأثر والتمزيق أجريت على الأغشية المخلوطة. مع إضافة ما يصل إلى 20 ٪ ل د ب ي ، العديد من الخصائص الميكانيكية للمزيج أظهرت تحسنا. كانت هناك زيادة

بنسبة 20 ٪ في اتجاه الماكينة من قبل قوة العائد بإضافة صغيرة من البولي إثيلين المنخفض الكثافة من دون أي نقصان في ليونة الماكينة .والمتانة أيضا عرض ت زيادة قدرها حوالي 43 ٪ في خصائصها مع هذا بإضافة صغيرة من البولي إثيلين المنخفض الكثافة.

زيادة في قوة الشد في الاتجاه العرضي كان أكثر من 75 ٪ مع نسبة 10% منخفضة جدا مزيج من البولي إثيلين المنخفض الكثافة, ليونة الاتجاه العرضي أظهرت تحسن طفيف مقارنة ح نقية الخطي. الاتجاه العرضي للمتانة الصغيرة أظهرت زيادة تصل إلى نسبة 50 ٪ من الخليط. وتحسن بنسبة 20 ٪ لوحظ في ذروة قوة التأثير مع إضافة قليل من البولي إثيلين المنخفض الكثافة . في حالة عدم تأثير الطاقة كان هناك بعض الانخفاض فيما يتعلق نسبة خليط. المقاومة أظهرت نوعا من التدهور في اتجاه الماكينة ، ولكن كان هناك تحسن كبير للمقاومة في الاتجاه العرضي. المقاومة في الاتجاه العرضي تحسنت تقريبا بنسبه 100% عن طريق إضافة منخفض الكثافة لمزيج نسب منخفضة تصل إلى 20 ٪.

على h-LLDPE/LDPE بشكل عام تم دراسة تأثير مزيج من الخواص الميكانيكية للأغشية و أظهرت تحسنا بمزج ما يصل إلى 20 ٪. وبالإضافة إلى ذلك تم تخفيض عزم الدوران المطلوب لمعالجة الأغشية مع زيادة نسبة خليط، في ما عدا5 ٪ نسبة مزيج

درجة الماجستير في العلوم

جامعة الملك فهد للبترول و المعادن

الظهران المملكة العربية السعودية

CHAPTER 1

INTRODUCTION

1.1 Background

Polyethylene (PE) is the most commercially used polymer in the form of films. PE is primarily chosen from the set of polymers due to its low price and easy processability. PE comes in different grades according to its density and molecular structure (branching). It has been classified into three main categories, namely, the high density (HDPE), the low density (LDPE), and the linear low density (LLDPE). HDPE has a density in the range of 935 – 965 Kg/m^3; it is densely packed with a low degree of branching which exhibits stronger intermolecular forces and tensile strength. LDPE is characterized by a density in the range of 918 – 935 Kg/m^3. The molecules in it are less tightly packed with a high degree of short and long chain branching, thereby exhibiting less crystalline structure. LLDPE has a density in the range of 915 – 925 Kg/m^3 with a significant number of short branches. LLDPE, which is produced via copolymerization process is further divided into three different branch types; butene, hexene and octene LLDPE depending on the co monomer used. Within the family of PE resins low density PE (LDPE) and linear low density PE (LLDPE) resins have found an extensive application in the packaging area using film blowing process. The mechanical properties of the PE films depend significantly on variables such as the extent and type of branching, the crystal structure and the molecular weight. When comparing LDPE and LLDPE, it has been observed that the LDPE offers a very good processability with lower mechanical properties; on the

other hand LLDPE exhibits better mechanical properties with lower procesability. The above argument is supported by the results of Wong *et al.* [1]. These PE films which are being used for numerous applications play an important role in packaging industry and their demand for vast range of mechanical properties is met by blending different types of resins. These films are produced by film blowing process. This process is the same as a regular extrusion process up until the die. The extrusion process can be attained by a single screw or a double screw extruder. The die is an upright cylinder with a circular opening similar to that of a pipe die. The pellets are fed into the extruder barrel through a metered feeder at a constant mass flow rate. The extruder screws are driven by a motor and its speed can be changed as desired. The pellets melt in the extruder and then the melt is pushed out through an adaptor die located at the exit of the extruder. The melt then flows through a melt pump which supplies the molten plastic to the die at a constant mass flow rate. This melt then flows through the die channel and squeezes out through the die opening. The molten plastic is then pulled upwards from the die by a pair of nip rolls high above the die as shown in Figure 1.1. In the centre of the die there is an air inlet from which compressed air can be forced into the centre of the extruded circular profile, creating a bubble. This expands the extruded circular cross section by some ratio (a multiple of the die diameter), thus decreasing the wall thickness. This ratio is called the "blow-up ratio" and can be adjusted to different multiples of the original diameter. There is also an external air cooling ring attached to the die which cools the bubble from the outer surface. The nip rolls flatten the bubble into a double layer film. This film is then spooled on a drum [2-4]. The product qualities of these films are immensely dependent on its morphological and mechanical properties. The structure and mechanical properties are

in turn dependent on the processing variables and the molecular characteristics of the resin.

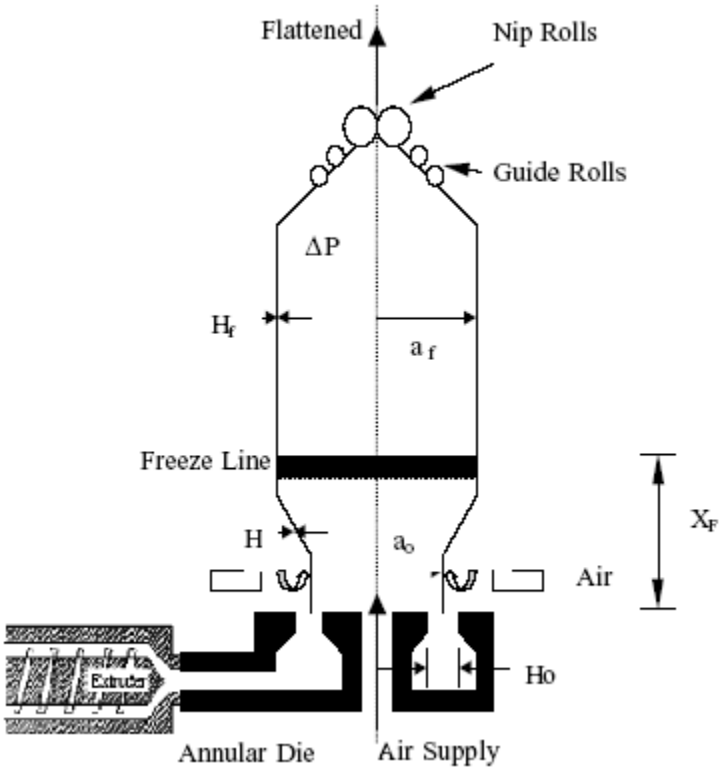

Figure 1.1. Schematic diagram of Film Blowing [5].

The various processing parameters which influence the quality of the film can be classified as the temperature profile, the melt temperature at the die, the pressure of the melt at the die, pressure inside the bubble, melt flow rate of the material at the outlet, take off velocity, cooling air flow rate, viscosity of the material and the die gap. The air pressure inside the bubble affects the properties of the film by imparting molecular orientation in the hoop direction. By changing the speed of the nip rollers the take off velocity is varied leading to variation in wall thickness and bubble stability of the film. This also changes the properties of the film in the machine direction due to stretching of

the film in longitudinal direction. Physically it means that, by increasing the speed of the nip rolls more length of film can be produced from the same mass content. Cooling air blown around the bubble causes the film to solidify or crystallize and freeze the orientation imparted due to biaxial stretching. The amount of cooling air plays an important role in locking the orientation within the film. The die gap needs to be more than the film thickness required as it will be stretched in both directions to create molecular orientation. Branching is known to have a significant effect on the rheology of polymeric melts, especially on the extensional behavior of the polymers. Hence the viscosity of the material to a large extent affects the processability and mechanical properties of the films.

Although different film markets have different performance requirements, superior tear, tensile, and dart impact strength are always desired. It has been recognized that film performance is strongly dependent upon the orientation of both the crystalline phase and amorphous chains, which in turn are largely influenced by the fabrication process and polymer chain microstructure. The morphology and property differences among high density PE (HDPE), low density PE (LDPE), and linear low density PE (LLDPE) films have also been demonstrated and explained in several recent publications [6-13], but the combined effect of these polymers is still in the initial stages. In this research the effect of process parameters, molecular type, and blend ratio on the film processability and its mechanical properties was studied.

1.2 Objectives

PE is well known for its easy processability and is widely used in making films. Among different grades of PE, the LDPE offers a very good processability with lower mechanical

properties; on the other hand LLDPE exhibits better mechanical properties with lower processability. By blending these two grades of PE, the processability of the polymer and the product quality of the film can be significantly improved. The aim of this research is to study the effect of process parameters, molecular type, and blend ratio on the film processability and its mechanical properties. Different blend ratios of h-LLDPE (hexene-Linear Low Density Polyethylene) with LDPE will be experimentally processed and characterized to study the effect of blending.

1.3 Processability and Process Parameters

In this present study the films were produced using twin screw extruder and the film blowing die. Saudi Basic Industries Corporation (SABIC) made LDPE and h-LLDPE polymer pellets were used for film fabrication. Three different grades of LDPE were extruded and the grade with the highest drawability was used for further studies. The blends of different composition of h-LLDPE and LDPE were made by melt mixing them in a Polylab twin screw extruder with the aid of two feeders. The pure h-LLDPE and LDPE were subjected to the same extrusion conditions in order to establish the same thermal and deformation history for all samples . The pure LDPE and h -LLDPE polymer pellets were extruded and their bubble stability window was obtained at different die temperatures ranging from 210° C to 270° C for each material. This bubble stability window gave the range of BRs (Blow Ratio) and DRs (Draw Ratio) for which the bubble remained stable. The die temperature at which the bubble stability window was largest for the pure h-LLDPE material was set as the die temperature for the remaining tests. The test samples of pure LDPE and h-LLDPE processed at different die temperatures were subjected to thermal tests of differential scanning calorimetry (DSC) so as to study the

polymer degradation at these temperature ranges. The processability of the polymer was determined in terms of the torque required for extruding the material. The processability in terms of torque required for extruding the material significantly depends on the type of the material and the blend ratio.

1.3.1 Draw Ratio and Blow Ratio

Pure h-LLDPE was used for film fabrication and the effect of DR on its film properties was studied. The DR was varied by varying the take up speed of the nip rolls. The films produced at different DRs were then tested in tension for the tensile properties and for tear in machine direction (MD) and transverse direction (TD). The effect of DR on the impact strength was studied using the Instron 9250G impact testing machine. The amount of crystalline content at different DRs was determined using the DSC experiments. The orientation developed in the films was observed using the birefringence technique with help of an optical microscope. The DR at which the biaxially tested films had the maximum impact strength for failure was selected to be the optimum DR. In a similar way the BR was varied keeping the temperature and the DR constant and its effect on the film properties was studied. Tensile, impact, tear, crystallinity and orientation tests were conducted on these films and the BR with the maximum impact strength for failure was selected as the optimum BR. Now, with these set of optimum processing parameters of die temperature, DR and BR the effect of blend ratio was studied.

1.3.2 Blend Ratio

Pure h-LLDPE and LDPE were extruded to produce films at the same processing conditions. The maximum possible processing conditions of h-LLDPE were selected for processing the blends and the two pure materials. The blends were then prepared by

adding small amounts of LDPE polymer to the h-LLDPE pellets. The blending was achieved with the help of two separately controlled feeders. The different blend ratios of h-LLDPE/LDPE studied have been listed in Table 1.1. Films at different blend ratios were collected and its effect on tensile, impact, tear, crystalline and the orientation properties was studied. The range of blend ratios for which the impact strength was maximum was then determined. This provided a cost effective processing conditions for film blowing of h-LLDPE/LDPE blends by decreasing the power consumption in terms of the torque required for extrusion process.

Table 1.1. Blending Percentages of LDPE to h-LLDPE.

Host Material LLDPE		Blending Percentage of LDPE				
Branch Type	ID	5%	10%	15%	20%	50%
Hexene	HL	HL5	HL10	HL15	HL20	HL50

CHAPTER 2

LITERATURE REVIEW

2.1 Process Parameters

2.1.1 Extrusion temperature

Extrusion temperature has a significant effect on the orientation, elongational viscosity and bubble stability of the blown films. Van Gurp *et al.* [1994] [[14]] from their studies concluded that the crystallization morphology consisted of twisted lamellae in amorphous matrix, and this twist was less at low extrusion temperatures which resulted in higher crystalline orientation. For LDPE/LLDPE blends (10% and 20% of LDPE) processed at two different temperatures, Micic et al [2000] [[9]], observed that the elongational viscosity curves of the LLDPE rich blends revealed stronger strain hardening characteristics at higher processing temperatures. Due to this, the bubble stability increased at elevated temperatures. They also highlighted the limited use of shear viscosity curves in predicting bubble stability as a function of temperature. The models developed by Muke *et al.* [2003] [[5]] for film blowing process had the temperature as the most critical parameter which influenced the characteristics of blown polypropylene (PP) films. However, Ghaneh-Fard [1999] [[15]], in their study concluded that the extrusion temperatures did not significantly effect the modulus of LDPE film. This disagreement was associated with different range of processing conditions and experimental procedure. Thus the effect of

extrusion temperature on the bubble stability of the film is still a subject of interest and it is being studied by researchers and our proposed study will help in evaluating the influence of extrusion temperature on bubble stability.

2.1.2 Draw Ratio

Draw Ratio (DR) is the ratio of the velocity of the nip rolls (or the films) to the velocity of the extruded melt. By changing the speed of the nip rollers the take off velocity is varied leading to variation in wall thickness and bubble stability of the film. DR was varied to obtain the operating window for bubble stability by Wong *et al.* [1998] [[1]] and Fang *et al* [2003] [[16]]. Operating window is defined as the range of DR and BR for which the bubble is stable. It is the bounded region of DRs and BRs which produce a stable bubble during the processing of these polymers. From their study, LDPE was observed to have a wider operating window when compared to LLDPE. Similar bubble stability operating window was obtained for LDPE blends by Micic *et al.* [1998] [[8]]. Kim *et al.* [2004] [[17]] evaluated the bubble instabilities (such as draw resonance, helicoidal instabilities and frost line height instability) originating in the bubble over a wide range of take up ratios. They concluded that the draw resonance, helicoidal instability and eccentricity decreased as take up ratio were increased. Ghaneh-Fard [1999] [[15]] from their study revealed that with increase in DR the Machine Direction (MD) and Transverse Direction (TD) moduli slightly decreased for LDPE and LLDPE.

2.1.3 Blow Ratio

Wong *et al.* [1998] [[1]] and Fang *et al.* [2003] [[16]] varied the BR to obtain an operating window for bubble stability of LDPE, LLDPE (hexene) and m-PE (hexene and butene) polymers. Similar bubble stability operating window was obtained for LDPE blends by

Micic *et al.* [1998] [8]. Their study revealed a range of BR's and DR's for which the bubble remained stable. Kim *et al*. [2004] [17] evaluated the bubble instabilities (such as draw resonance, helicoidal instabilities and frost line height instability) originating in the bubble over a wide range of blow up ratios. Their study revealed that the helicoidal instabilities and the eccentricity decreased as the BR was increased. The polymers LDPE, LLDPE and m-LPE have been studied and the order of bubble stability was LDPE, LLDPE and LmPE. Ghaneh-Fard [1999] [15] from his study revealed that with increase in BR the Machine Direction (MD) and Transverse Direction (TD) moduli slightly decreased for LDPE and LLDPE. It was very difficult for them to interpret their results and was attributed to the strong interaction between DR and BR. Thus, the relation between the DR and BR and their effect on the mechanical properties of the film is still unclear and our study will help in highlighting the effect of these parameters.

The Frost Line Height (FLH) can be varied by varying the BR and DR. This is the line at which the melt solidifies and which is slightly above the film blowing die exit. Wong *et al.* [1998] [1] and Fang et al [2003] [16], varied the FLH to study the processability of LDPE, LLDPE (hexene) and m-PE (hexene and butene) polymers. It was shown that the wider the range of FLH, the higher was the processability in terms of bubble stability. Their results showed that LDPE was observed to have a higher range of FLH and wider operating window compared to LLDPE. They concluded that the higher the storage modulus, the more stable was the film. The storage modulus was attributed to be strongly dependent on the Molecular Weight Distribution (MWD) and as well on the long chain branches. Stable polymer melts were produced by those polymers which contained higher elongational properties. However, Ghaneh-Fard [1999] [15], in their study concluded that

the FLH did not significantly effect the modulus of film, which contradicts the results of Wong *et al.* [1].

2.2 Blend Ratio

The morphology and property differences among HDPE, LDPE, and LLDPE films have also been demonstrated and explained in several recent publications [6-13], but the combined effect of these polymers is still in the initial stages. Huizenga *et al.* [1990] [6], blended LDPE and LLDPE in different ratios (10, 20, 30, 40, 50, 60, and 70%) and studied its effect on mechanical properties such as ultimate strength, toughness, elongation at break and secant modulus. LDPE (hexene and octene) was blended with LLDPE and it was shown that the mechanical properties increased with increase in LLDPE content of the blend ratio. Also, the hexene (molecular type) was shown to have higher mechanical properties at blend ratios greater than 50% of LLDPE. Lu and Sue [2001] [18] characterized and compared the morphologies of films blown from LDPE, LLDPE, and their blends. The film made from the LDPE/LLDPE blend possessed the highest degree of crystal orientation. It was also observed that blending resulted in anisotropy in the mechanical properties of the films. Now, it still remains to be seen if there is any effect of LLDPE (butene, hexene and octene – branch type) when blended with LDPE. Also, it needs to be studied, whether small percentages less than 10% improve the mechanical strength of the blends. Micic *et al.* [1998] [8, 9] considered two different blends of LLDPE mixed with 10% and 20% of LDPE and processed them at two different processing temperatures. They determined that the elongational viscosity curves of the LLDPE rich blends revealed stronger strain hardening characteristics at a high temperature and exhibiting better bubble stability. Micic *et al.* [2000] [9] also

studied the effect of LDPE concentration on the shear and elongational viscosity of LLDPE/LDPE blends. The LDPE blend did not have a significant effect on the shear viscosity, while profoundly infuenced the elongational property of LLDPE. Miller *et al.* [2001] [10] investigated the rheological and mechanical properties for blends of recycled high-density polyethylene (HDPE) and virgin polyolefins and correlated the relative shear viscosity and relative stiffness of these blends. Fang *et al*. [2005] [11] studied the thermal and rheological properties to determine immiscibility of mPE/LDPE blends with different molecular structures. They suggested that by increasing the lengths of short chain in mPE can promote miscibility of mPE/LDPE blends. Silvestre *et al*. [2006] [12] performed the analysis of the structure orientation, morphology, relaxation time and optical properties of blown films of mLLDPE, LDPE and their blends. The presence of LDPE favorably modified the optical properties of mLLDPE blown films. The presence of LDPE in the film also modified the melt relaxation time and (permitting the use of lower extrusion temperatures) the nucleation process. Jagannath *et al.* [2006] [7] incorporated starch into LDPE blown films to convert it to a biodegradable film and then investigated the effect of starch on the mechanical properties (elongation, tensile strength, tear strength, seal strength, & bursting) and barrier properties (water vapour & oxygen transmission rate) of LDPE blown films. Their investigations revealed that the mechanical properties decreased with increase in starch concentration whereas the barrier properties increased with increase in starch concentration. In most of the above cases, the procedure for blending used is not revealed. There are two ways for blending the material, one by mixing the two polymers in solid state and feed the mixture through the hopper. This type of mixing would result in inhomogeneity in the melt. The alternate

method is to use two feeders simultaneously. This would have a better control on the feeding with a uniform concentration distribution resulting in a much better homogeneity in the material. In our study, the polymers will be blended by melt mixing with the aid of two feeders which will be connected externally to the mixing element of the extruder. Here, it is important that the blends are properly prepared by controlling the mixing process, as there is a good chance of having an inhomogeneous mixing in the first type of mixing.

2.3 Processability

Processability of the material is defined in various ways such as, energy consumption, bubble stability, torque required to turn the extruder screws, etc. Wong *et al.* [1998] [1] studied the ease of processability in terms of energy consumption on LDPE, LLDPE (hexene) and m-PE (hexene, butene) polymers by varying the process parameters. It was shown that the processability in terms of energy consumption was least for LDPE and the highest for LLDPE. Processability was also defined in terms of range of frost line heights (FLH) for which the bubble is stable, the wider the range of FLH, the greater was the processability of the polymer. Micic *et al.* [1998] [8] and Fang et al [2003] [16] investigated the processability of LLDPE/LDPE blends in terms of bubble stability by varying the haul off speed and lay flat width. They concluded that the strain hardening characteristics of the polymer played an important role in processability improvement in terms of bubble stability. Kim *et al*. [2004] [17] also evaluated the bubble instabilities such as draw resonance, helicoidal instabilities and frost line height instability over a wide range of take-up ratio, blow up ratio and frost line height. The polymers LDPE, LLDPE and metallocene-catalyzed linear polyethylene (LmPE) produced by Ziegler-

Natta catalyst have been studied and the order of bubble stability was LDPE, LLDPE and LmPE.

2.4 Mechanical Properties

2.4.1 Tensile, Impact and Tear Test

Good mechanical properties of any product are always desired. For films, the desired properties are the tensile, tear and impact strength. These properties are influenced by a variation in processing factors and molecular type of the polymer. Huizenga *et al.* [1990] [6] performed mechanical tests on blends of LDPE and LLDPE and used it as a selection tool for selecting an optimum blend ratio for better processability and higher mechanical properties (ultimate strength, toughness, elongation at break and secant modulus). It was shown that the mechanical properties increased with increase in LLDPE content of the blend ratio. Also, the hexene (molecular type) was shown to have higher mechanical properties at blend ratios richer in LLDPE content greater than 50%. Ghaneh-Fard [1999] [15] investigated the effect of process parameters on the mechanical properties of the films. LDPE and LLDPE were tested and the MD and TD modulus was shown to be greater in LLDPE when compared to LDPE. Jagannath *et al.* [2006] [7] investigated the effect of mechanical properties (elongation, tensile strength, tear strength, seal strength, & bursting) and barrier properties (water vapour & oxygen transmission rate) by incorporation of starch into LDPE blown films. Their investigations revealed that the mechanical properties decreased with increase in starch concentration whereas the barrier properties increased with increase in starch concentration. Miller *et al*. [2001] [10] investigated the mechanical properties for blends of recycled high-density polyethylene (HDPE) and virgin polyolefins and correlated the relative shear viscosity and relative

stiffness of these blends. Lu and Sue [2002] [18] characterized and compared the morphologies of films blown from LDPE, LLDPE, and their blends. It was also observed that blending resulted in anisotropy in the mechanical properties of the films.

2.5 Characterization

2.5.1 Film Orientation

The orientation in films is characterized using Wide Angle X-ray Scattering (WAXS), Small Angle X-ray Scattering (SAXS), Transmission Electron Microscopy (TEM), Atomic Force Microscopy (AFM), Fourier – transform Infrared (FTIR) dichroism, polarized Raman spectroscopy and birefringence. Van Gurp *et al.* [1994] [14] studied the effect of extrusion temperature on the orientation in the LDPE blown films. They concluded that, among the four different techniques used, WAXS was the best in qualitatively revealing the crystalline orientational distribution. Silvestre *et al*. [2006] [12] performed the analysis of the structure orientation, morphology, relaxation time and optical properties on blown films of mLLDPE, LDPE and their blends. Blend films exhibited unclear and distinct spherulite structures. The blend films had a lower orientation compared to LDPE films. Lu and Sue [2002] [18] characterized and compared the morphologies of films blown from LDPE, LLDPE, and their blends. The film made from the LDPE/LLDPE blend possessed the highest degree of crystal orientation. The underlying mechanisms of morphology development due to blending and strategies for minimizing the undesirable anisotropy in LDPE/LLDPE blended films have been proposed.

2.5.2 Elongational Viscosity

Baird [1999] [19] defined the kinematics of shear flow or extensional flow and the associated material functions. The kinematics of most processing flows was shown as extensional rather than shear in nature, and, hence, the performance of polymers was more readily accounted for through extensional viscosity measurements. Micic *et al.* [1998] [8] evaluated the elongational viscosity of LLDPE/LDPE blends by varying the extrusion temperatures. They determined that the elongational viscosity curves of the LLDPE rich blends revealed stronger strain hardening characteristics at a higher temperature; therefore, exhibiting better bubble stability at these temperatures. The stronger stain hardening was linked to the faster evolution of material time (relaxation time) at elevated temperatures. They defined the bubble stability in terms of strain hardening parameter which was the ratio of elongational viscosity for different span of time. Their complex shear viscosity curves were of limited use in predicting the bubble stability as a function of temperature. Thus, the strain hardening characteristics of the polymer played an important role in processability improvement in terms of bubble stability. Munstedt *et al*. [2006] [20] characterized two polyethylene (LDPE and LLDPE) and two polypropylene (PP) melts in uniaxial elongational flow. Significant differences with respect to strain hardening were observed between the two polymers. For the PPs it was shown that the elongational behavior found in uniaxial elongation was qualitatively reflected in biaxial deformation too. Strain hardening was of great importance for the geometrical uniformity of the processed items for both PP and PE materials. Micic et al [2000] [9] investigated the effect of different LDPE components as well as their concentration on shear and elongational viscosity of LLDPE/LDPE blends. The LDPE

blend did not have a significant effect on the shear viscosity, while profoundly infuenced the elongational property of LLDPE. They observed that the molecular structure of parent polymer and blend composition play an important role in the rheology of these blends and consequently on the performance during the film blowing process. Fang et al [2003] [16] and Miller *et al*. [2001] [10] correlated the rheological properties and processability of various polyethylenes during film blowing process. Their work was similar to Munstedt et al [20] in correlating the uniaxial elongation and strain rates to the bubble stability during the film blowing process.

2.5.3 Crystallinity

The degree of crystallinity is determined using Differential Scanning Calorimetry (DSC). Ghaneh-Fard [1999] [15] produced films over a wide range of DR, BR, polymer flow rate and extrusion temperature and tested them using DSC. He found no significant difference in the degree of crystallinity or shape of the DSC scans. It appeared from his results that DSC was not sensitive enough to detect very small changes in the crystallinity. It has been reported in literature that the ultimate tensile properties are independent of the degree of crystallinity. However, yield stress of PE samples was observed to be primarily influenced by the degree of crystallinity.

CHAPTER 3

EXPERIMENTAL PROCEDURE

3.1 Extrusion and Film Blowing

A Thermo Haake twin screw extruder as shown in Figure 3.1 was used to produce the films. This extruder was designed with an L/D ratio of 40. All the heating zones and the screw speeds were externally controlled with a computer. The temperatures of the melt were measured using thermocouple sensors and the pressure at the extruder exit was measured with a pressure sensor. The torque required to turn the screw was being electronically reported on the computer. The pellets are fed into the extruder barrel through a metered feeder at a constant mass flow rate. The extruder screws are driven by a motor and its speed can be changed as desired. The pellets melt in the extruder and then the melt is pushed out through an adaptor die located at the exit of the extruder. The melt then flows through a melt pump which supplies the molten plastic to the die at a constant mass flow rate. This melt then flows through the die channel and squeezes out through the die opening. The molten plastic is then pulled upwards from the die by a pair of nip rolls high above the die as shown in Figure 1.1. In the centre of the die there is an air inlet from which compressed air can be forced into the centre of the extruded circular profile, creating a bubble. This expands the extruded circular cross section by some ratio (a multiple of the die diameter), thus decreasing the wall thickness. This ratio is called the "blow ratio" and can be adjusted to different multiples of the original diameter. There is also an external air cooling ring attached to the die which cools the bubble from the outer

surface. The nip rolls flatten the bubble into a double layer film. This film is then spooled on a drum. The twin screw extruder had seven controllable heating zones upto the extruder exit. A temperature profile of 120/150/180/200/200/200/200 °C was maintained in the extruder. It had three mixing zones with mixing elements. The material feeding was achieved with the help of a controlled feeder. This feeder was also being controlled by the same computer. By increasing the temperature profile values the processability increases but this would lead to polymer degradation at higher temperatures. At the same time, for low extrusion temperature profile values the torque required to turn the screw was too high. The melting temperature of LLDPE is around 120°C. For very low extrusion temperature profiles, the torque required to turn the screw increases, and the motor gets tripped off with the equipment shutting down. Thus, the above temperature profile was selected by taking into account the processability, polymer degradation and the equipment limitations concerns. Keeping this temperature profile as constant the other parameters were optimized to obtain a maximum mass flow rate. This was achieved by varying the processing parameters such as the screw speed and the melt pump speed. The extruder speed was varied from 0-12 rpm and was found that the torque required to turn the screw was maximum at the speed of 12 rpm with h-LLDPE material at a constant pressure of 14 to 16 bar at the extruder die exit. The melt pump was varied from 0 to 30 rpm feeding rate and was found to give a consistent flow rate at 10 rpm with 230 °C temperatures. Thus the melt pump speed was set to a constant feeding rate of 10 rpm at 230 °C to pump the material to the film blowing die. The maximum mass flow rate at these feed rates was around 8 g/min. An extruder screw speed of 12 rpm was used and a constant pressure of 14 to 16 bar was maintained at the extruder die exit.

Figure 3.1. Thermo Haake extruder for film blowing.

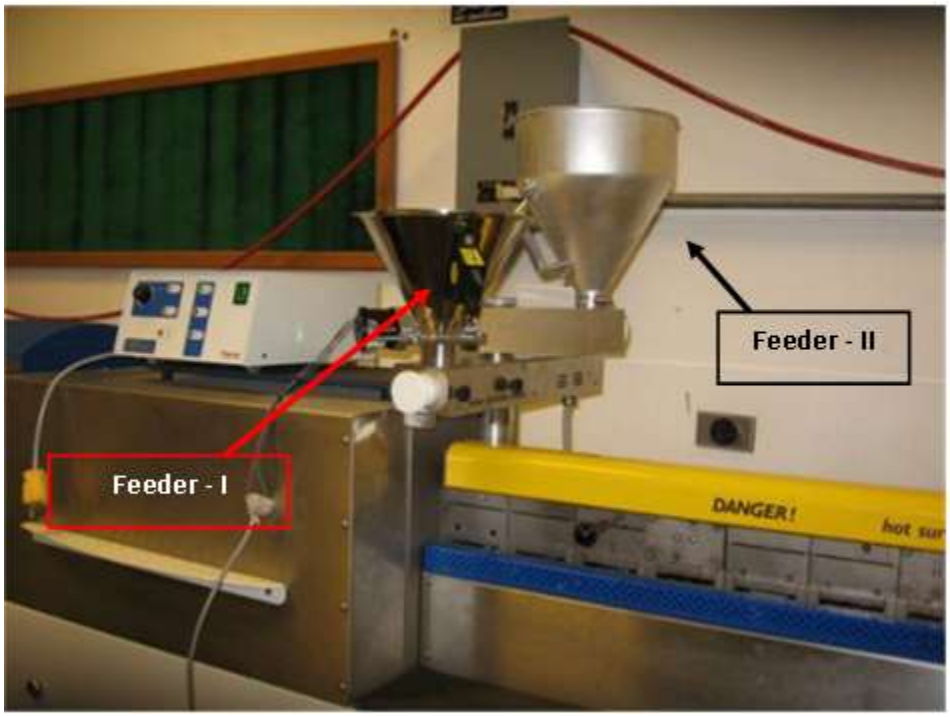

Figure 3.2. Two feeders for blending h-LLDPE/LDPE.

For blending, a separate feeder was used in addition to the previous one as shown in Figure 3.2. The pellets were simultaneously fed into the extruder barrel from the same point of entry. This kind of blending using two different feeders will give a better control on the homogeneity of the blend when compared to manual mixing of the material and feeding through a single feeder. The first feeder was used to feed the h-LLDPE pellets and the second feeder for LDPE pellets. The feed rates were controlled and calibrated so as to obtain the blend ratios of 5%, 10%, 15%, 20% and 50% of LDPE to the main material h-LLDPE. The calibration plots of feeder-I (h-LLDPE) and feeder-II (LDPE) are shown in Figure 3.3 and Figure 3.4 respectively.

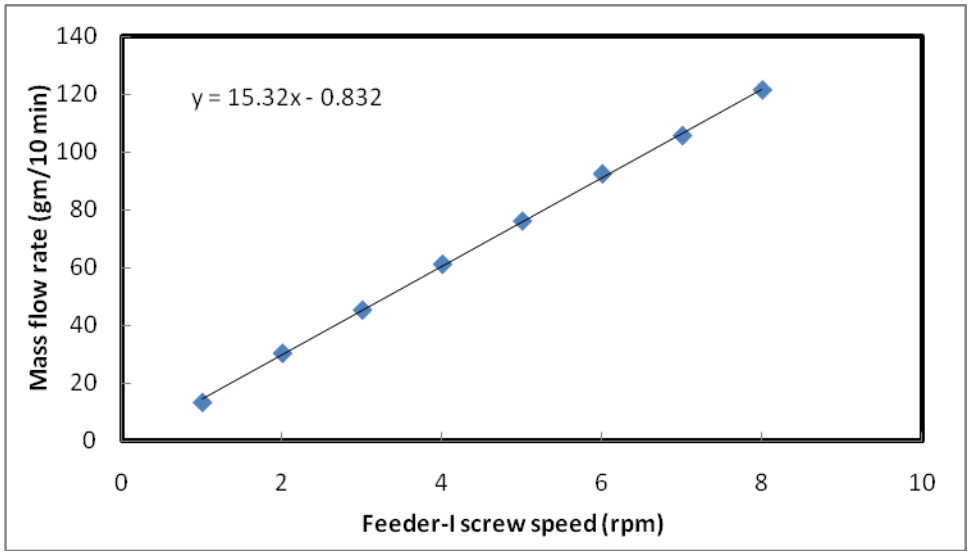

Figure 3.3. Calibration plot of feeder-I (LLDPE).

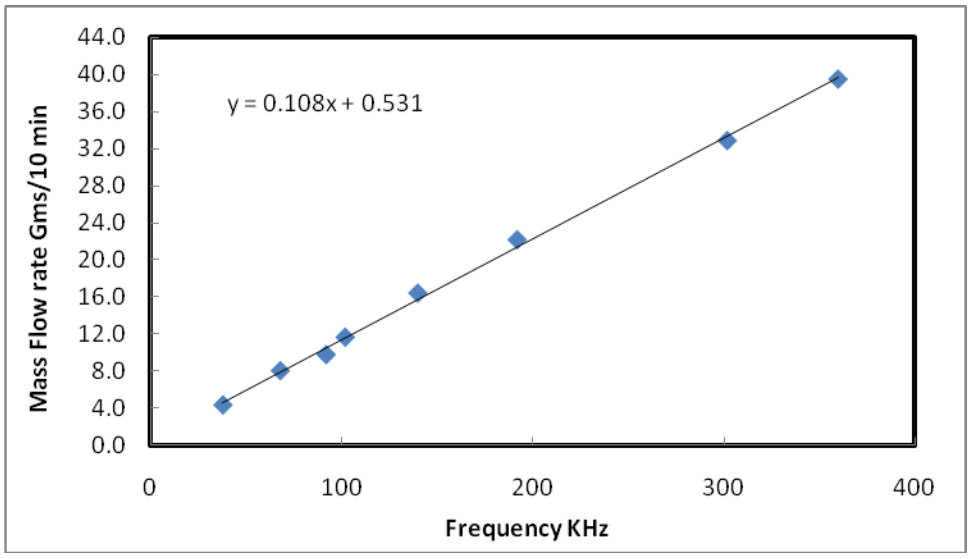

Figure 3.4. Calibration plot of feeder-II (LDPE).

After passing through the extruder the polymer then flows into the melt pump which is again being controlled by the same computer. The melt pump as shown in Figure 3.5 was set to a constant feeding rate of 10 rpm at 210 °C to pump the material to the film blowing die. A cylindrical film blowing die as shown in Figure 3.5 was used to blow the molten polymer. The die temperature with a diameter of 25 mm was set to 230 °C. This die had an inlet from the bottom for the compressed air line to inflate or deflate the bubble so as to produce films of different width. The bubble diameter was varied to obtain different BRs. A compressed air line was connected to the bottom of the die and the pressure inside the bubble was recorded using a pressure sensor. A cooling air ring was also placed on the top of the die to cool the film from outside. The material flowing out from this film blowing die was pulled up by the nip rolls of the take off unit. The speed of the nip rolls was varied and the DR was calculated using this speed of the nip roll over the speed of the film. The melt flow rate at the die exit was calculated by the

using the mass flow rate of the melt over the product of melt density at that temperature [21] and the area of cross-section at the die opening. The equation for the speed of the film and the area is given by

$$Melt\,Velocity\ m\ (m/\min) = \frac{Mass\,Velocity\ (g/\min)}{Density\ (g/cm^3) \times Area\ (cm^2)} \times (10^{-2}\, m/cm)$$

$$= \frac{m\ (g/\min)}{\rho (g/cm^3) A\ (cm^2)} \times (10^{-2}\, m/cm)$$

$$A = \frac{\Pi}{4}(D_o^{\,2} - D_i^{\,2})$$

Where D_o (2.50 cm) and D_i (2.30 cm) are the outer and inner diameters of the die.

$$DR = \frac{Film\,Velocity}{Melt\,Velocity}$$

Speed of the film = Speed of the nip rolls

$$BR = \frac{Bubble\ Diameter}{Average\ Die\ Diameter}$$

m = Melt Mass Flow Rate (g/min)

$\rho_{LLDPE} = 0.8674 - 6.313\times10^{-4}\times T + 0.367\times10^{-6}\times T^{\,2} - 0.055\times10^{-8}\times T^{\,3}$ according to [21]

$\rho_{LLDPE} = Melt\ Density\ (g/cm^3) = 0.7349\,(g/cm^3)$ at 230 °C

$\rho_{LDPE} = 0.868\exp(-6.73\times10^{-4}\times T)$ according to [21]

$\rho_{LDPE} = Melt\ Density\ (g/cm^3) = 0.7435\,(g/cm^3)$ at 230 °C

A = area (cm^2) = 0.7536 cm^2

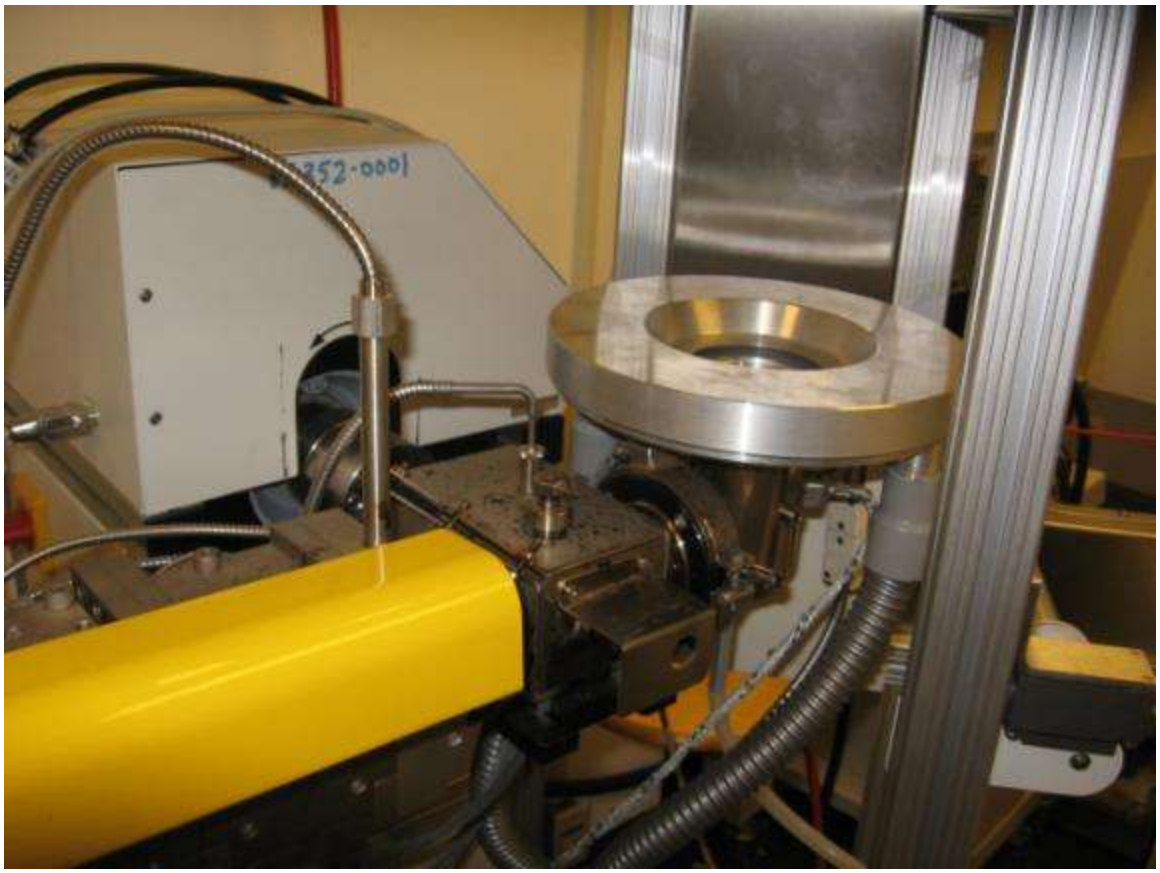

Figure 3.5. Film blowing die and cooling air ring connected inline with melt pump.

3.2 Crystallinity - Differential Scanning Calorimetry (DSC)

Differential Scanning calorimetry thermograms were used to measure the percent crystallinity. Mettler DSC 882 as shown in Figure 3.6 was used in the present study for thermal analysis. Temperature calibration of the instrument was done with indium sample. Samples were prepared by cutting circular discs from the film to fit into the aluminum pans. These discs were stacked until the weight was in the range of 3 mg to 5 mg. The crucibles were then covered with an aluminum lid and sealed. An empty sealed aluminum pan was used as a reference.

Samples were scanned on Mettler DSC 882 unit from 20 °C to 180 °C for all the prepared samples at a rate of 10 °C/min. The enthalpy value used for h-LLDPE was 293.6 J/g [22, 23]. Three samples at each condition were tested and its average value has been reported.

Figure 3.6. Mettler DSC 882.

3.3 Orientation

An optical microscope along with a compensator as shown in Figure 3.7 was used to measure the degree of orientation in the films in both machine direction (MD) and transverse direction (TD). The microscope was set in dark field transmission mode with the lens axis appearing on the screen. A glass plate was kept between the polarizer and the analyzer with a compensator placed between the sample and the analyzer. The first dial reading of the compensator at this position was recorded. A rectangular sample of

8cm X 2.5cm was prepared and placed between two glass plates. This assembly was then placed between the polarizer and the analyzer. The base was turned to an angle of +45° or -45° so as to observe the orientation in the MD direction of the film. The multi-cross was aligned with the axis of the lens and the compensator reading recorded. The orientation was measured as the retardation wavelength with respect to the dial increment of the compensator. The thickness of the film was also an important factor in deriving the degree of orientation in the film. The difference in retardation wavelength with the film and without the film was then divided upon its thickness to obtain the birefringence in the plane.

Figure 3.7. Optical Microscope.

3.4 Tensile Test

A Instron tensile testing machine as shown in Figure 3.8 was used for testing films in tension. The films were tested in accordance to the ASTM D 882 standard [24] in both MD and TD directions. Specimens of rectangular type were cut using a die in both MD and TD with a gauge length of 15mm and width 3.14mm as shown in Figure 3.9. The thickness was measured for different films using a high precision micrometer with an accuracy of 0.001mm and then clamped between the jaws with a cardboard padding. The films were stretched at a controlled rate of 50mm/min. A plot of tensile stress against tensile strain was obtained. The tensile properties such as the yield stress, ultimate tensile strength, stress at break and the toughness were determined from the graph. The toughness was calculated as the area under the curve of the stress strain graph. Five samples at each condition have been tested and its average value has been reported.

Figure 3.8. Instron tensile testing machine.

Figure 3.9. Tensile test rectangular specimen.

3.5 Dart Impact Test

This test can be carried out using one of these standards, i.e., ASTM D 1709 [25], ISO 7765-1 [26], ISO 7765-2 [27] or ASTM D3798 [28]. The test procedures mentioned in ASTM D 1709 and ISO 7765-1 are technically equivalent and according to this test the energy that causes plastic film to fail under specified conditions of impact of a free falling dart is evaluated. A freely falling dart impact tester was developed at our lab using the specifications as mentioned in the ASTM D1709. The tester was designed and manufactured as shown in Figure 3.10. In this test, the energy is expressed in terms of the weight (mass) of the dart (missile) falling from a specified height resulting in 50% failure of the specimens which are being tested. This failure is the puncture of the film due to impact. Impact strength results by one test method vary from the other due to varying conditions of missile velocity, impinging surface diameter, effective specimen diameter and the thickness. These test variables are highly dependent on the method of film fabrication.

Figure 3.10. Dart Impact Tester as per ASTM D 1709 and ISO 7765-1 specifications.

The ASTM D 1709 or ISO 7765-1 standard consists of two test methods, test method A employs a dart with a 38.10 mm diameter hemispherical head dropped from a height of 0.66 m. The test method A may be used for films whose impact resistances require masses of 0.05 Kg to about 2 kg to fracture them. Test method B employs a dart with a 50.80 mm diameter hemispherical head dropped from a height of 1.50 m. Its range of applicability is from 0.3 kg to about 2 kg.

One drawback of the ASTM D 1709 or ISO 7765-1 standard is the requirement of wide films because of the large film holder diameter. The ring clamp of the dart impact tester has an inner diameter of 127mm, same is the case with ASTM D 3798, and where in a fixture of clamping diameter of 76 mm is to be used. However, for the films processed at low BR's, the total width of the film was not large enough to be clamped within the 127mm and 76 mm ring clamp. This would limit our study to the impact testing of films processed at medium and high BRs only. Hence the most appropriate standard for testing all the specimens processed at different BR can only be achieved using ISO 7765-2 standard. Thus, an instrumented dart impact tester (Instron 9250G) was used and the films were tested using ISO 7765-2 standard. The Instron Dynatup 9250G is connected to a computer with impulse data acquisition and analysis system. The equipment comprises of gravity based drop weight system with pneumatic brakes as shown in the Figure 3.11. A fixture of 40 mm inner diameter ring clamp was designed and manufactured in our lab. The fixture (Figure 3.12) was manufactured as per the specifications mentioned in the ISO 7765-2 standard. The fixture was designed in such a way that the circular specimen was clamped flat and held securely during the test. A ring of emery paper was placed on the clamping faces to avoid any slippage. A dart of 0.78 inch in diameter as shown in Figure 3.13 was used for impact testing.

Samples of 80 mm diameter were cut in circular disc form and were piled over one another to make up a thickness of around 0.8 mm. A dart with 0.78 inch diameter was used for the impact test. The dart along with the tup weighed around 9.4 kg. The velocity of the dart striking the film clamped perpendicular to it was maintained at a constant value of 2 m/s. A method file designed for testing films as per ISO 7765 standard was

used for the impact tests. Five samples with same processing conditions were tested and its average impact resistance value was taken.

Figure 3.11. Instron Dynatup 9250G impact testing machine.

Figure 3.12 Fixture for Impact test as per ISO 7765-2

Figure 3.13. Dart of 0.78 inch diameter used for impact testing.

The principle for the instrumented dart impact test is that the test specimen is penetrated normal to its plane by a striker at a nominally uniform velocity. The resulting force deformation or force – time diagram is electronically recorded. The test specimen is firmly clamped during the test. The force deformation diagram obtained in these tests show several features of the material's behavior under impact as shown in Figure 3.14. For example, the fracture may be "brittle", "ductile", "tough" or characterized by initial damage or by crack initiation and propagation. In addition, dynamic effects may be present, such as load-cell/indentor resonance, specimen resonance and initial contact/inertia peaks [27]. These resonance effects observed during the tests has been eliminated by the use of an algorithm to smoothen the curve.

The force deformation diagram as shown in Figure 3.14 explains the various terms used in impact testing such as the peak force 'F_M', energy to peak force 'W_M', peak deformation 'S_M', failure force 'F_F', failure deformation 'S_F', failure energy 'W_F' and total penetration energy 'W_T'. Peak force 'F_M', is the maximum force exerted by the striker in the direction of impact. Energy to peak force 'W_M' is the area under the force deformation curve bounded by the origin, the peak force and the deformation at peak force. The force exerted by the striker in the direction of impact and measured at failure point is known as failure force 'F_F'. The deformation in the direction of impact at the centre of test specimen, measured at failure point is known as failure deformation 'S_F'. Failure energy 'W_F' is the area under the force deformation curve bounded by the origin, the failure force and the failure deformation. Total penetration energy 'W_T' is the total energy expended in penetrating the test specimen [27]. The normalized values are for unit thickness of the film. The force deformation diagrams of h-LLDPE and LDPE used in the

present study shows a clear point of first failure (failure point) indicated by a sharp drop in force. This failure point is of great significance to us as it would represent the total resistance (failure energy) the film would offer before giving away. Thus, we would consider the failure energy to be the deciding factor in selecting the optimum DR and BR.

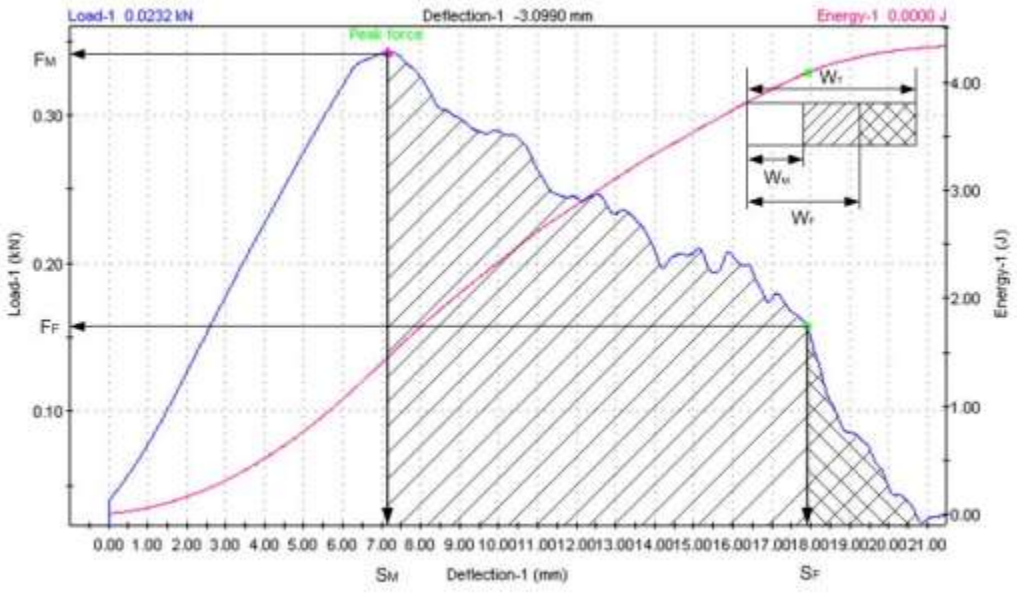

Figure 3.14. Force deformation diagram for impact tested specimen.

3.6 Elmendorf Tear Test

This test was carried out according to the ASTM D 1922 standard [29] on an Elmendorf tear tester (Figure 3.15). In this test method the average force required to propagate tearing through a specified length of plastic film after the tear has been initiated was determined. The force in grams was measured using a precisely calibrated pendulum device. The sample was mounted in the pneumatic jaws of the tear testing machine. The specimen is held on one side by the pendulum and on the other side by a stationary member. The cut is initiated using a sharp blade provided in the machine. When the

pendulum is released, acting by gravity, the pendulum swings through an arc, tearing the specimen from a precut slit. Since some energy will be consumed in tearing the film, the pendulum has less energy than if it had fallen freely. The loss in energy by the pendulum is indicated on the digital display. The displayed value is a function of the force required to tear the specimen. Normalized tear resistance of the film was calculated by dividing the tear resistance over the thickness of the film. This method is widely used as an index of the tearing resistance in packaging applications. Tear strength of packaging films was expressed in grams/mm. Ten samples in each direction for the same processing conditions have been tested and its average value has been reported.

Figure 3.15. Elmendorf tear tester.

3.7 Work Plan

The work plan is summarized in Figure 3.16. The processability window of h-LLDPE was evaluated in terms of the broadness of BR and DR range at specific temperatures. The temperature which had the widest window was selected. We also looked at the effect of degradation in the temperature range of 210°C to 270°C with an interval of 20°C, and concluded in future section that 230°C is the optimum temperature having the widest window. After selecting this temperature we varied the DR from 7 to 86 and according to mechanical testing which is described in next section we selected 21 as the DR in terms of better impact resistance value. The next step was the selection of BR and we tried three BR's varying from 1.12 to 1.78 (3 values) which is limited by the bubble stability and we reach to the conclusion that BR 1.6 is a suitable value which gives maximum impact resistance of the film. The above values were set constant for the following studies of blend ratios. In this regard we have studied five different blends with two virgin materials LDPE and h-LLDPE.

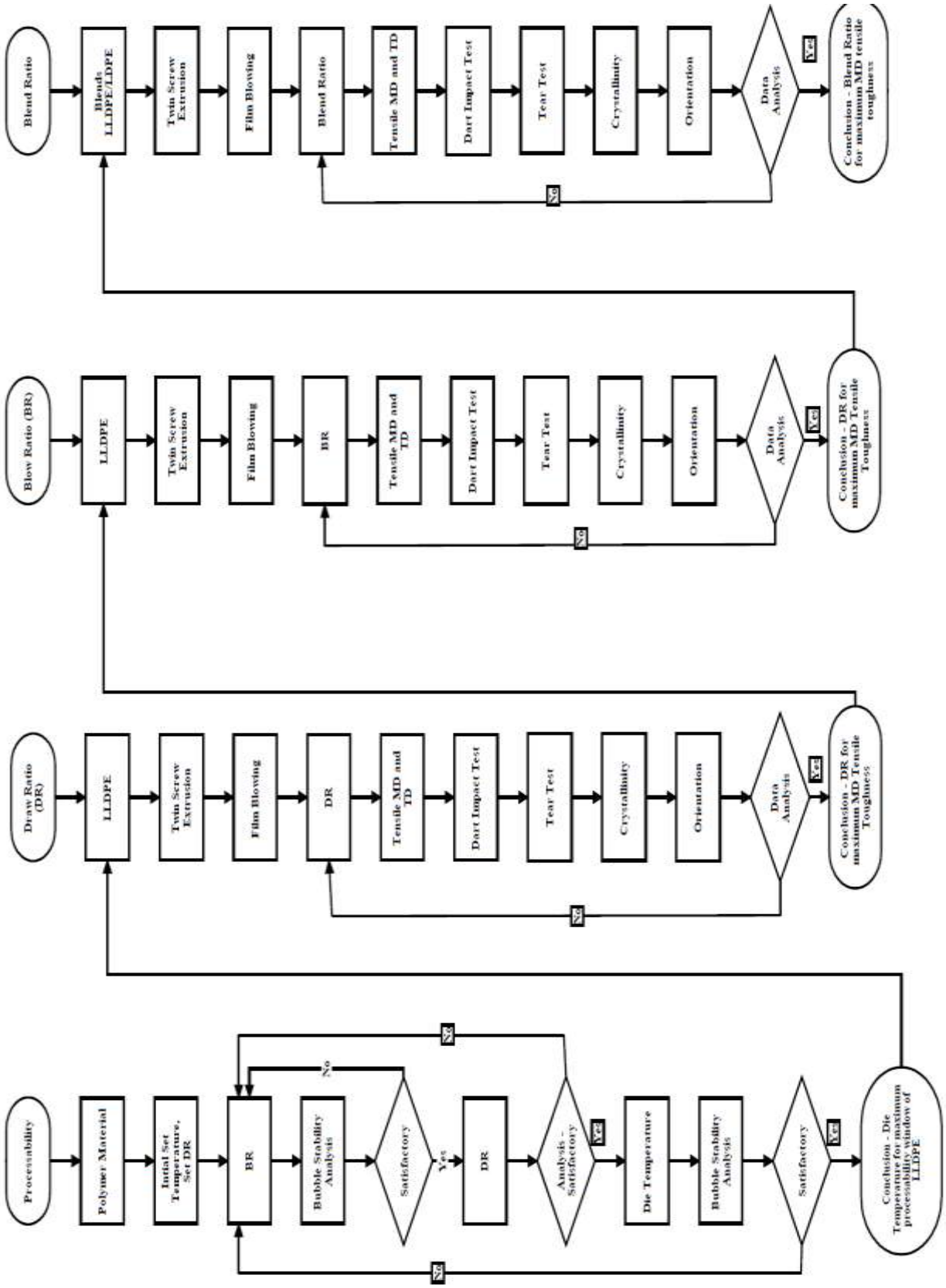

Figure 3.16. Work plan.

CHAPTER 4

RESULTS

4.1 Effect of Die Temperature on the Bubble Stability of LDPE and h-LLDPE Blown Films

This section is briefly describing the selection of temperature without degradation and easy processability. A temperature profile of 120/150/180/200/200/200/200 °C was maintained in the extruder. An extruder screw speed of 12 rpm was used and a constant pressure of 14 to 16 bar was maintained at the extruder die exit. Thus the melt pump speed was set to a constant feeding rate of 10 rpm at 230 °C to pump the material to the film blowing die. The maximum mass flow rate at these feed rates was around 8 g/min. The die temperature was varied from 210 °C to 270 °C and its effect on the operating window of h-LLDPE and LDPE polymer was determined. The bubble stability window for h-LLDPE and LDPE was evaluated by varying the BR and DR while keeping the mass flow rate and the extruder temperature profile constant. At this extruder temperature profile and the mass flow rate the BR was limited to a maximum of 1.78. The Bubble stability was defined as the region where in the bubble remained stable for the corresponding values of BR and DR. The various bubble instabilities observed during the process were the draw resonance, helicoidal instability and the bubble rupture as shown in Figure 4.1. The DR could be varied upto the maximum limit of the instrument (Take off unit) and the BR was varied from a minimum to the maximum limit where the bubble either ruptures or touches the cooling air ring or when there is some kind of instability

induced in the bubble. The axis range of BR and DR was kept constant for all the films produced at different temperatures. The BR axis was set to a range of 0 to 3 and the DR was set to a range of 0 to 90. These ranges were selected as it would include all the data points generated for the different materials and the temperatures studied. This way the total area of the plot was maintained constant and then the operating window area was evaluated and its percentage value was calculated over the total area to give the relative percentage of operating window. This relative percentage area of the operating window was then compared to select the optimum die temperature which gave the maximum bubble stability window without any degradation effect at that temperature. The operating windows of h-LLDPE and LDPE evaluated at different temperatures have been listed in Figure 4.2-Figure 4.9. Films produced at these temperatures were tested on the DSC to determine the effect of degradation at these elevated temperatures. The plots of DSC for the films tested at different temperatures for h-LLDPE and LDPE has been listed in the Figure 4.10-Figure 4.13.

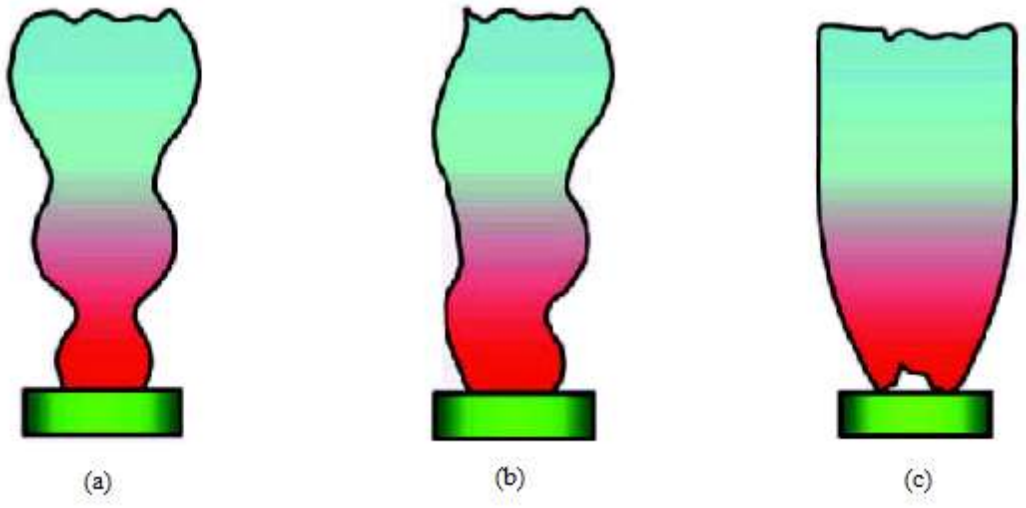

Figure 4.1. (a) Draw Resonance (b) Helicoidal Instability (c) Bubble rupture.

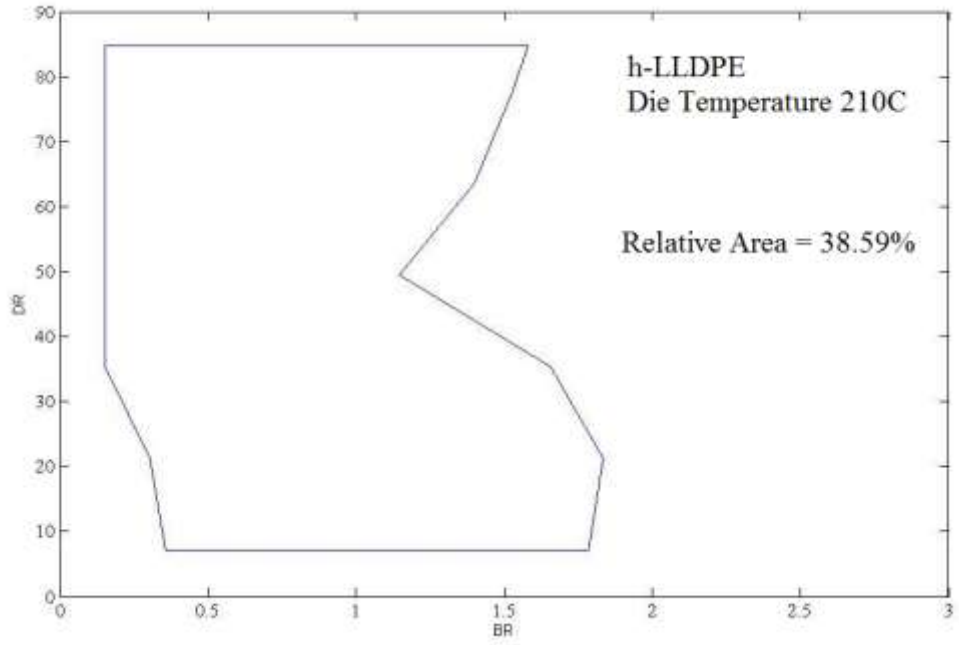

Figure 4.2. Bubble Stability Window for h-LLDPE at 210 °C.

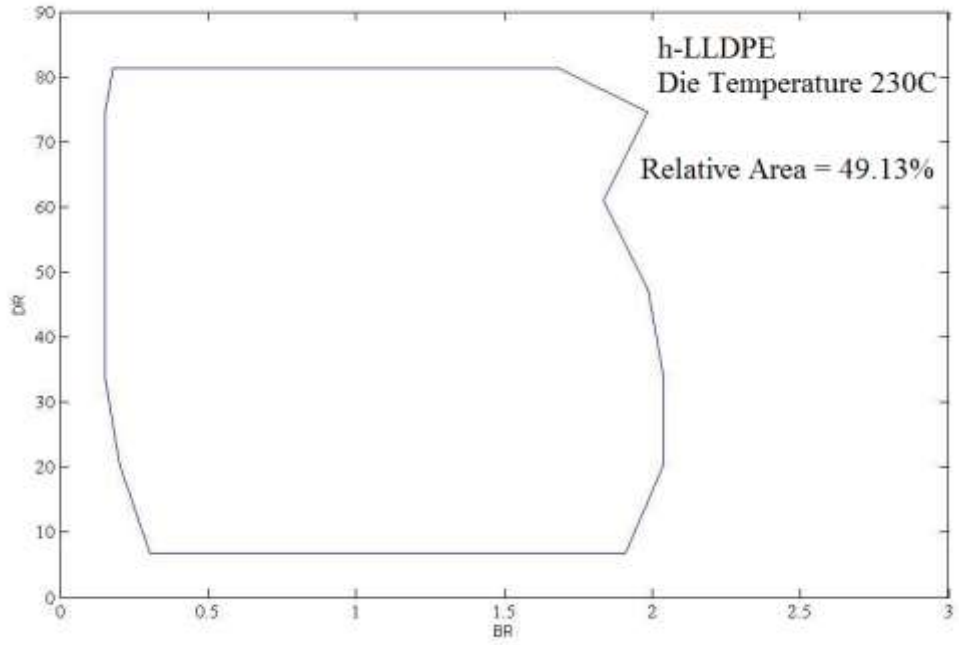

Figure 4.3. Bubble Stability Window for h-LLDPE at 230 °C.

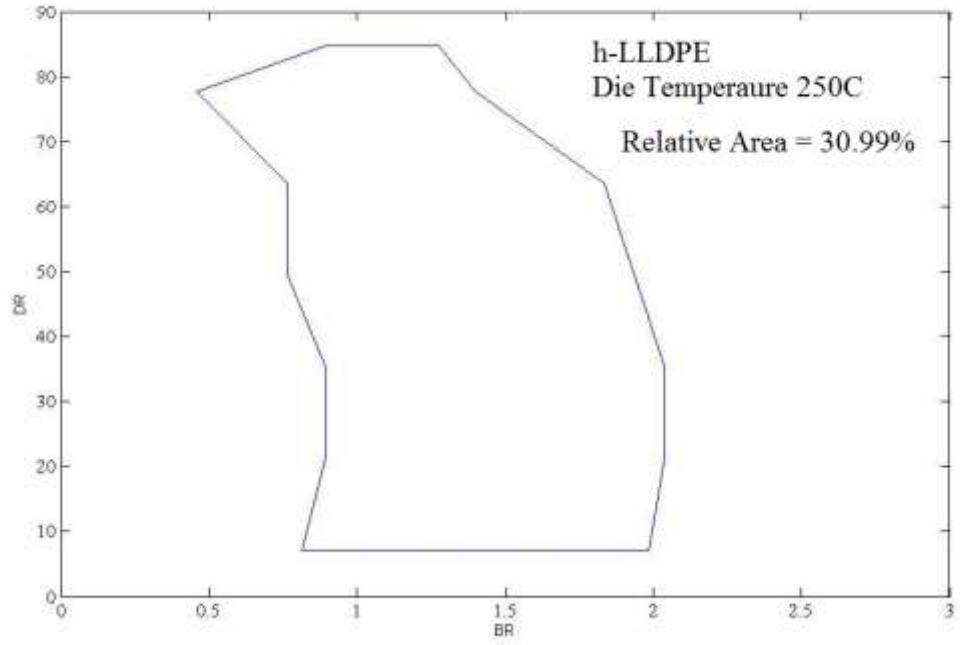

Figure 4.4. Bubble Stability Window for h-LLDPE at 250 °C.

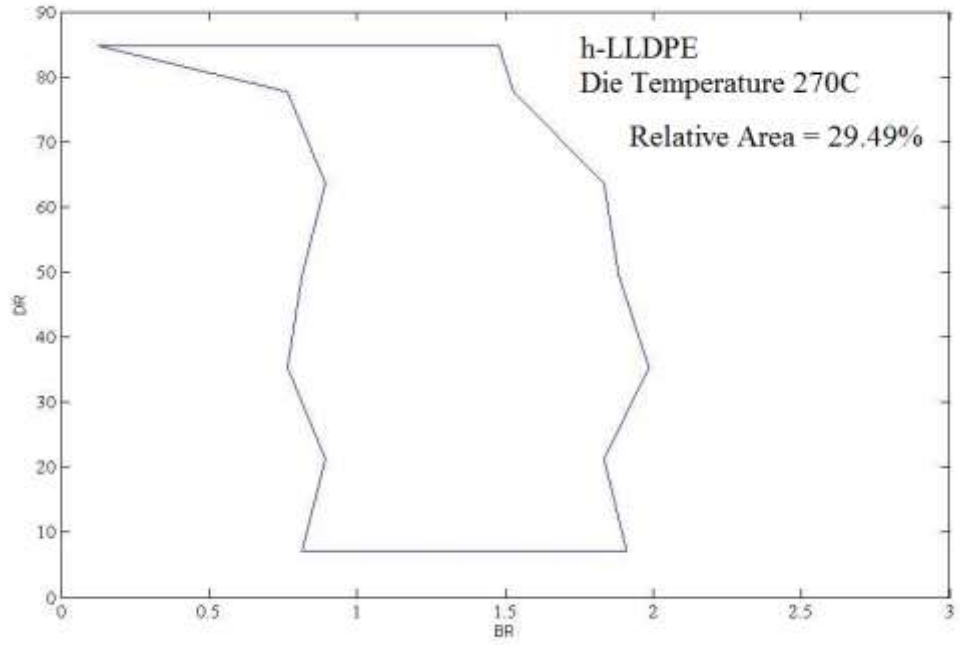

Figure 4.5. Bubble Stability Window for h-LLDPE at 270 °C.

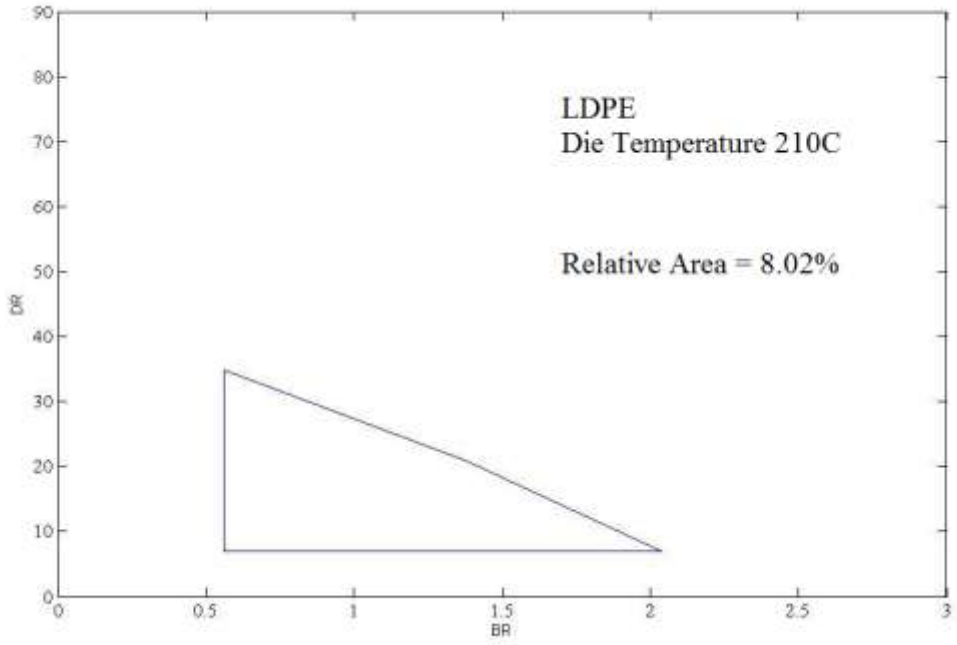

Figure 4.6. Bubble Stability Window for LDPE at 210 °C.

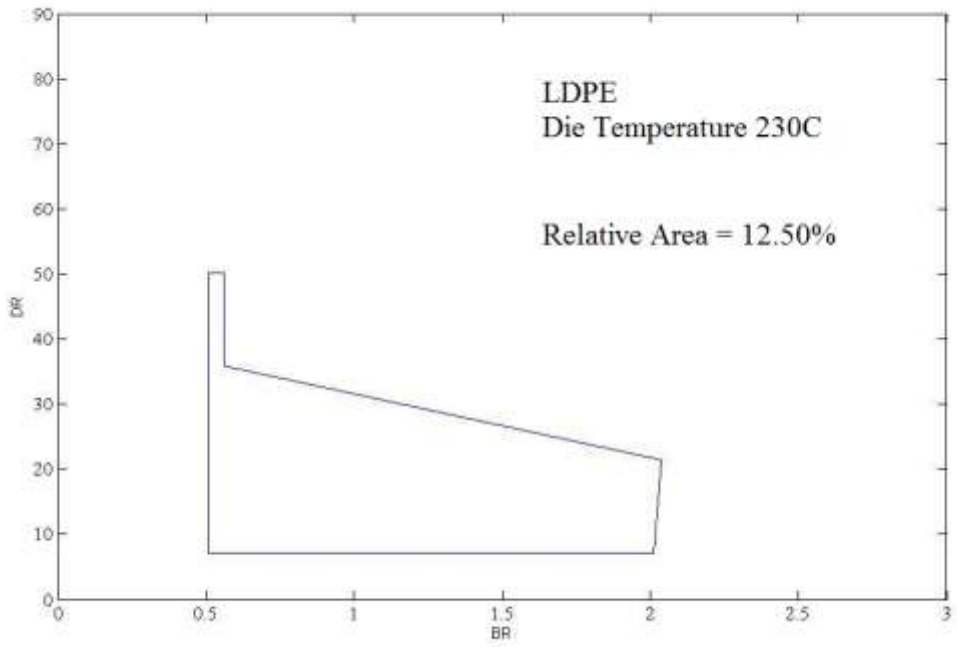

Figure 4.7. Bubble Stability Window for LDPE at 230 °C.

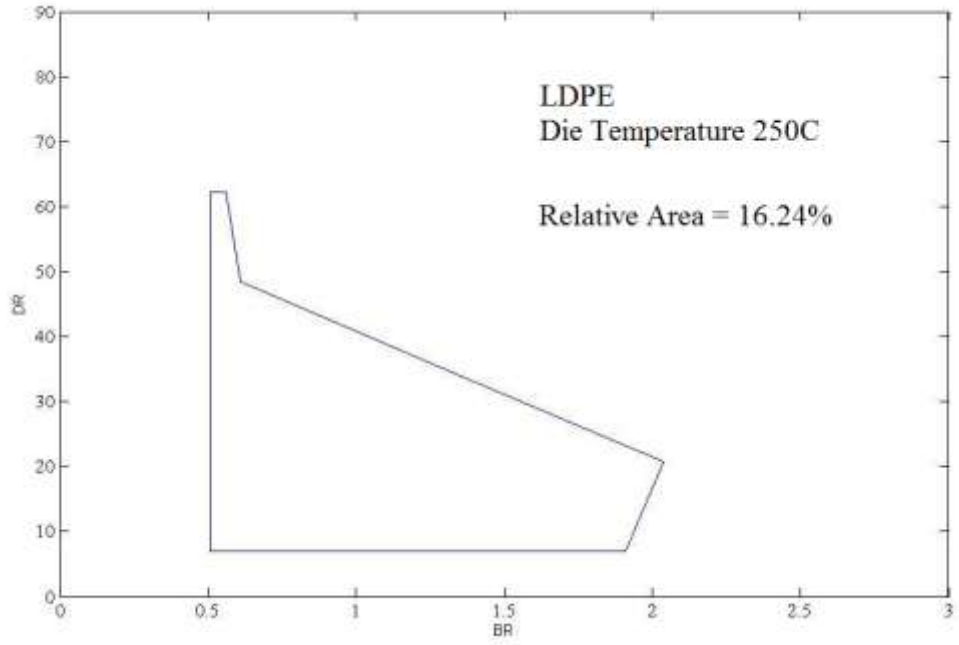

Figure 4.8. Bubble Stability Window for LDPE at 250 °C.

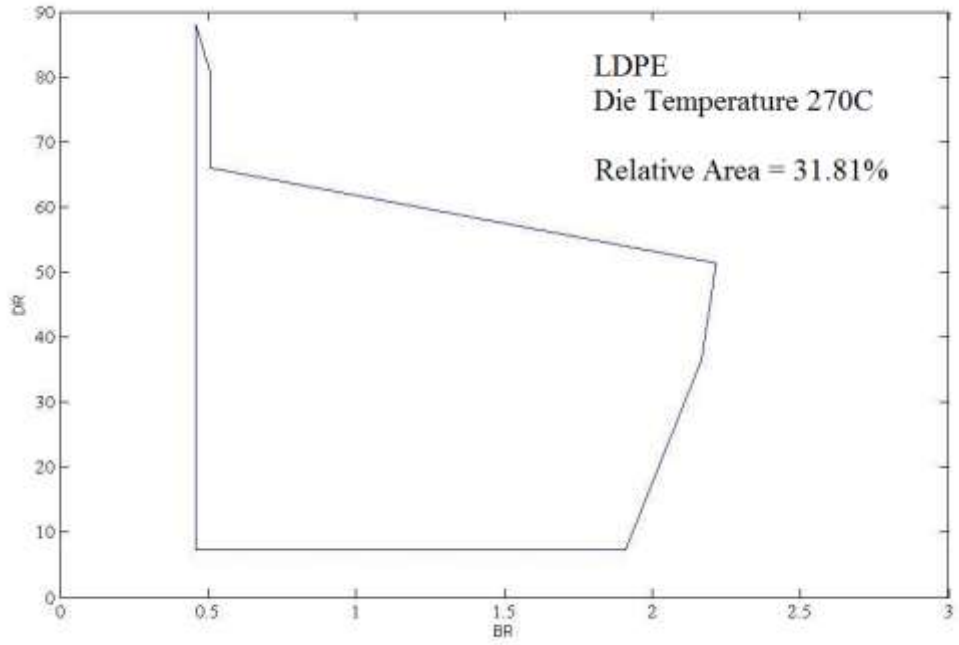

Figure 4.9. Bubble Stability Window for LDPE at 270 °C.

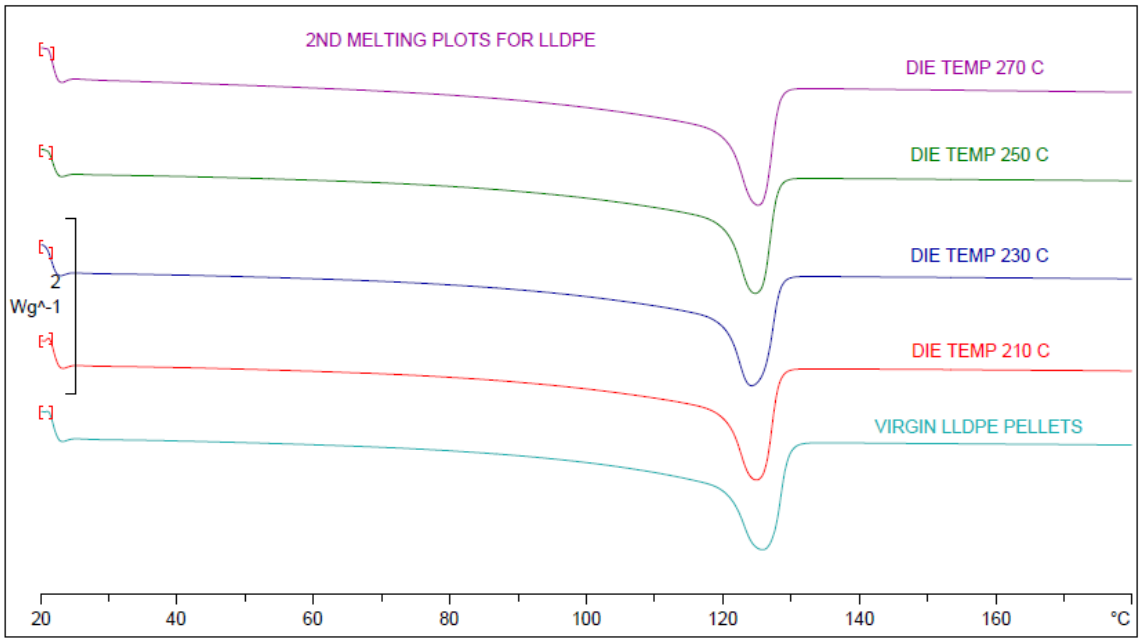

Figure 4.10. DSC 2nd melting curves of h-LLDPE processed at different die temperatures.

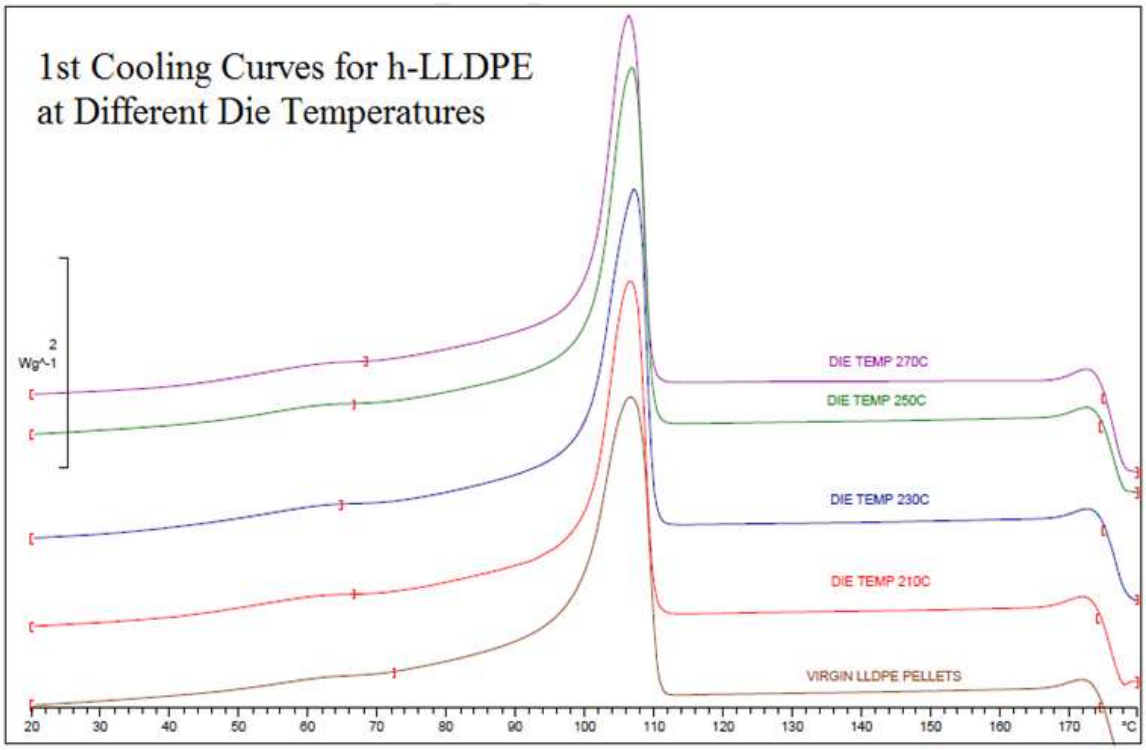

Figure 4.11. DSC 1st cooling curves of h-LLDPE processed at different die temperature.

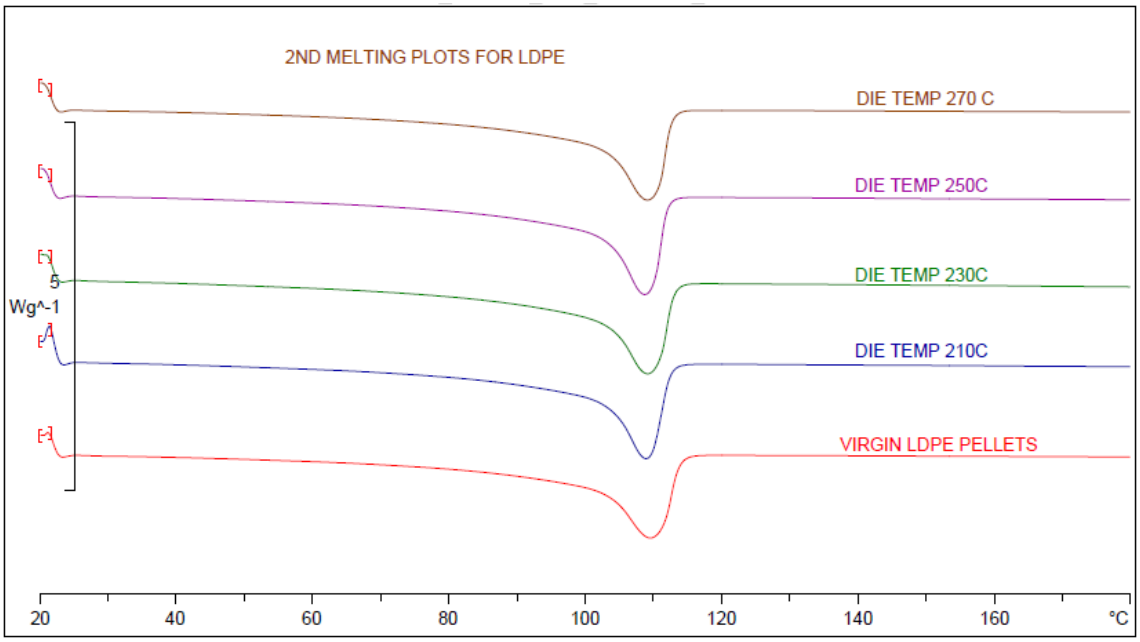

Figure 4.12. DSC 2nd melting curves of LDPE processed at different die temperatures.

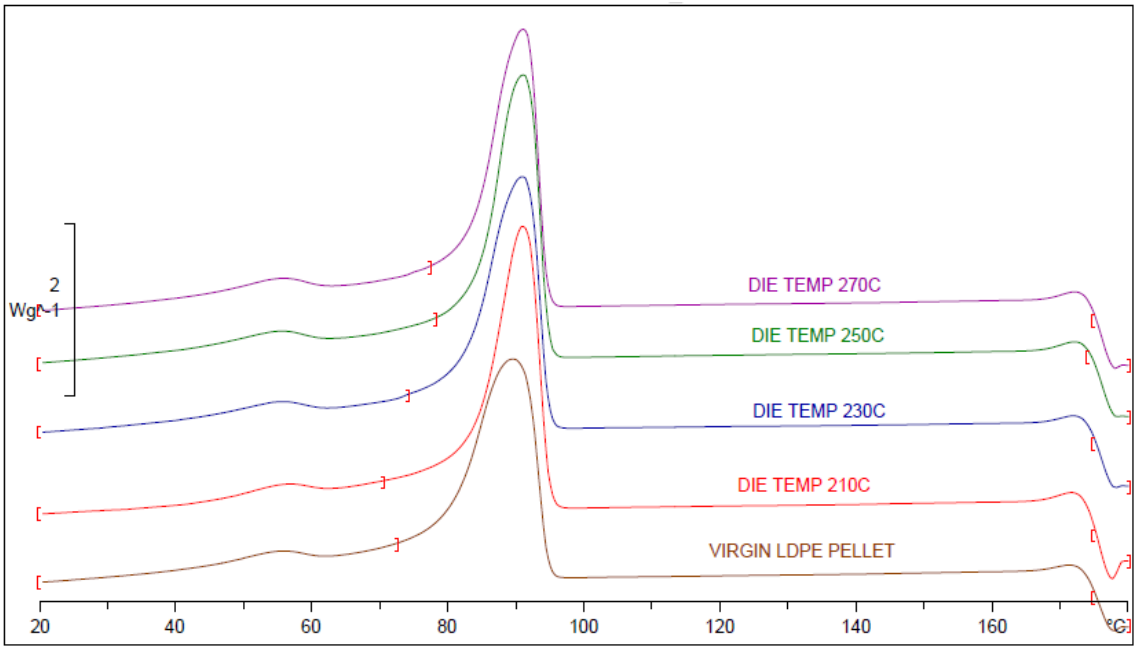

Figure 4.13. DSC 1st cooling curves of LDPE processed at different die temperature.

From these DSC plots we conclude that there is not much degradation. DSC is not the best technique for determining the degradation; however, we go by these results as the other instruments are not available in our lab. A better technique is the gel permeation chromatography (GPC) and we do not have an access to this. As an alternative we are using the DSC to give an indication. If there is an appreciable degradation it will be visible. If there is degradation, it will show in the thermal behavior from DSC profile as a shift in the curve, change of shape (broader or narrower) or change in crystalline content. For example, if there is molecular weight degradation we have smaller or larger molecular weight. When material crystallizes at lower temperature we have smaller molecular weight. If the material crystallizes at higher temperature it implies that the molecules are less mobile and therefore larger molecules exists indicating that cross linking has occurred The experimental DSC results show that there is not much deviation in the thermal history of the films when compared to virgin history of polymer.

4.2 Effect of DR on Thermal and Mechanical Properties of h-LLDPE Blown Films

The results of thermal and mechanical tests conducted on the h-LLDPE films processed at different DRs (7, 21, 36, 49, 64 and 86) are presented in this section.

4.2.1 Crystallinity

The samples processed at different DRs were analyzed and their 1st heating curves are shown in Figure 4.14. The melting range of h-LLDPE is observed to be in the range of 115°C to 124°C.

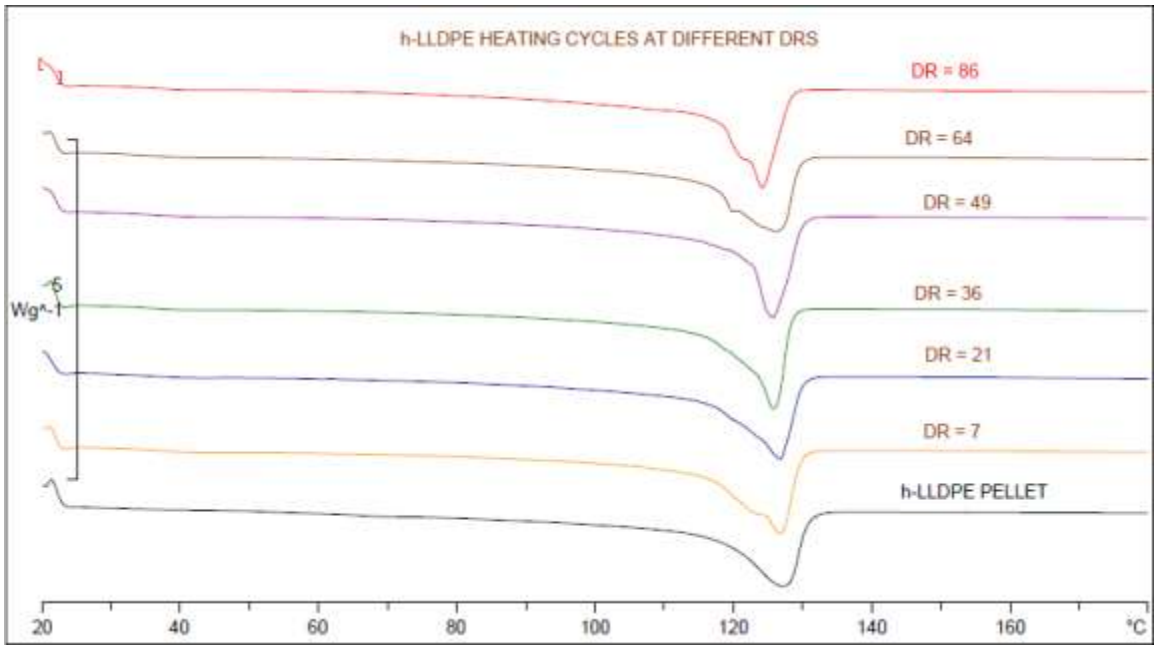

Figure 4.14. DSC heating plots of h-LLDPE films processed at different DRs.

4.2.2 Orientation

The birefringence (Δn) when viewed from MD in the plane of the film is calculated and listed in Table 4.1 for different DR. The Figure 4.15 shows the average thickness variation for h-LLDPE film at different DRs.

Table 4.1 Birefingence at different DRs

DR	Birefringence x 1000 MD direction
7	0.73
21	-2.11
36	-4.24
49	-2.12
64	3.82
86	4.8

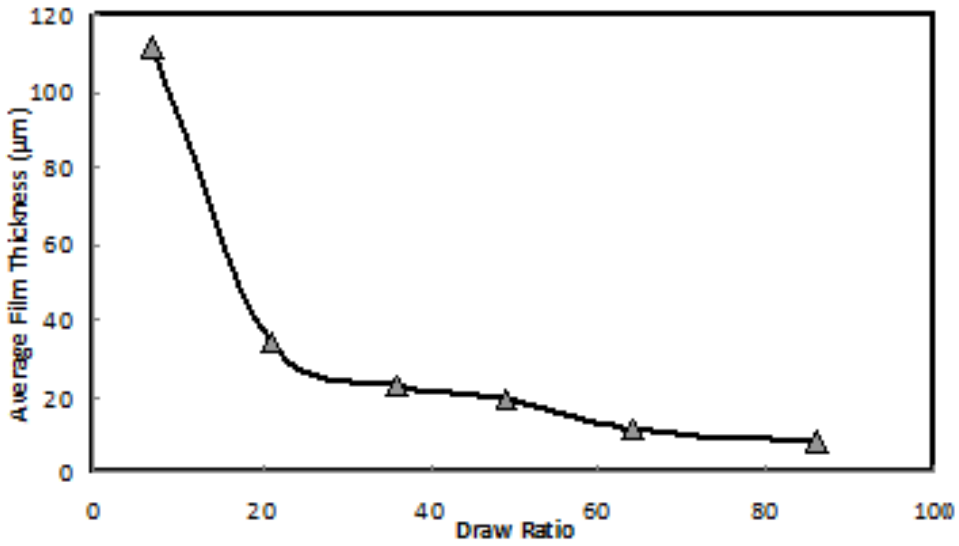

Figure 4.15. Average film thickness of h-LLDPE at different DRs.

4.2.3 Tensile Test

Tensile tests were carried out in accordance with ASTM D882 standard in both MD and TD directions. Five samples were tested in both the directions for each processing condition. The stress strain plots of h-LLDPE films at DR 7 in machine direction (MD) are shown in Figure 4.16. The tensile properties of h-LLDPE at different DRs in MD are listed in

Table 4.2. The stress strain plots of h-LLDPE films at DRs 7 in transverse direction (TD) are shown in Figure 4.17. The tensile properties of h-LLDPE at different DRs in TD are listed in Table 4.3.

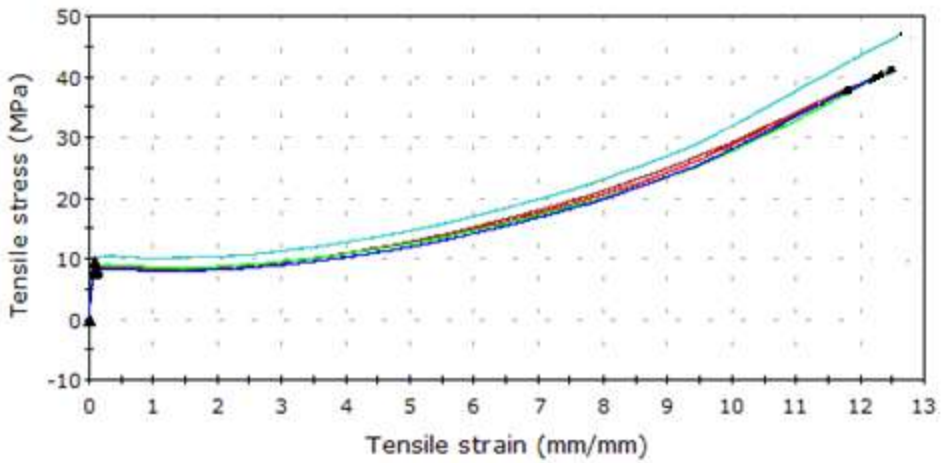

Figure 4.16. Machine Direction (MD) tensile stress-strain curves for DR 7.

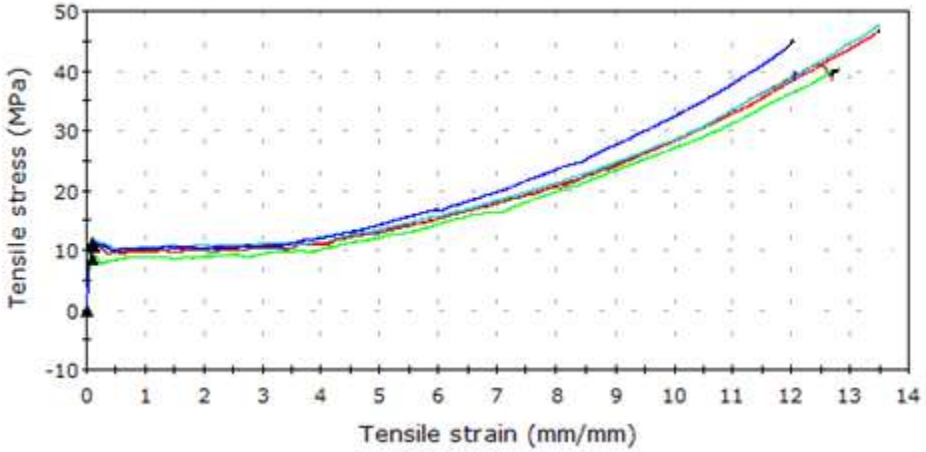

Figure 4.17. Transverse Direction (TD) tensile stress-strain curves for DR 7.

Table 4.2 Machine Direction (MD) tensile properties of h-LLDPE at different DRs

DR	UTS	STD	σ_y	STD	ϵ_F	STD	T_E	STD
set	(MPa)		(MPa)		(%)		(Mpa)	
7	41.52	3.4	8.22	0.6	1231	33	229.78	25.1

21	39.68	7.9	7.06	1.8	772.5	35.8	129.38	32.6
36	41.95	8.4	8.05	1.2	616.8	54.1	115.31	25.1
49	27.67	3.6	4.68	0.5	493.2	49.3	61.98	11.3
64	64.51	15.1	12.86	1.8	385.3	43.8	126.62	27.5
86	44.78	6.9	10.09	1.3	293.2	43.4	75.79	16.4

Table 4.3 Transverse Direction (TD) tensile properties of h-LLDPE at different DRs

DR	Ultimate Tensile Stress	Std Dev	Tensile Stress at Yield	Std Dev	Tensile Strain at Break - Ductility	Std Dev	Toughness - Energy at Break	Std Dev
set	(MPa)		(MPa)		(%)		(Mpa)	
7	44.27	3.69	10.28	0.96	1294	66.4	260.1	0
21	43.44	2.78	9.98	0.99	1179	40.5	227.6	15.1
36	23.89	5.84	6.25	1.39	992.5	93.7	111.1	30.5
49	24.75	2.95	10.04	0.87	917	91.1	64.1	10.5
64	24.06	7.75	9.64	1.26	1004	142	126.6	37.3
86	23.22	3.71	11.32	1.62	950.5	104	124.9	27.7

4.2.4 Dart Impact Test

Impact tests were carried out in accordance with ISO 7765-2 standard. Five samples were tested at each processing condition (DR) and an average impact energy value has been reported. The force-deformation diagrams for five samples tested at DRs 7 are shown in Figure 4.18 for h-LLDPE films. The normalized peak force, peak energy, failure force, failure deformation and failure energy values for the five films tested at different DRs have been listed in the Table 4.4.

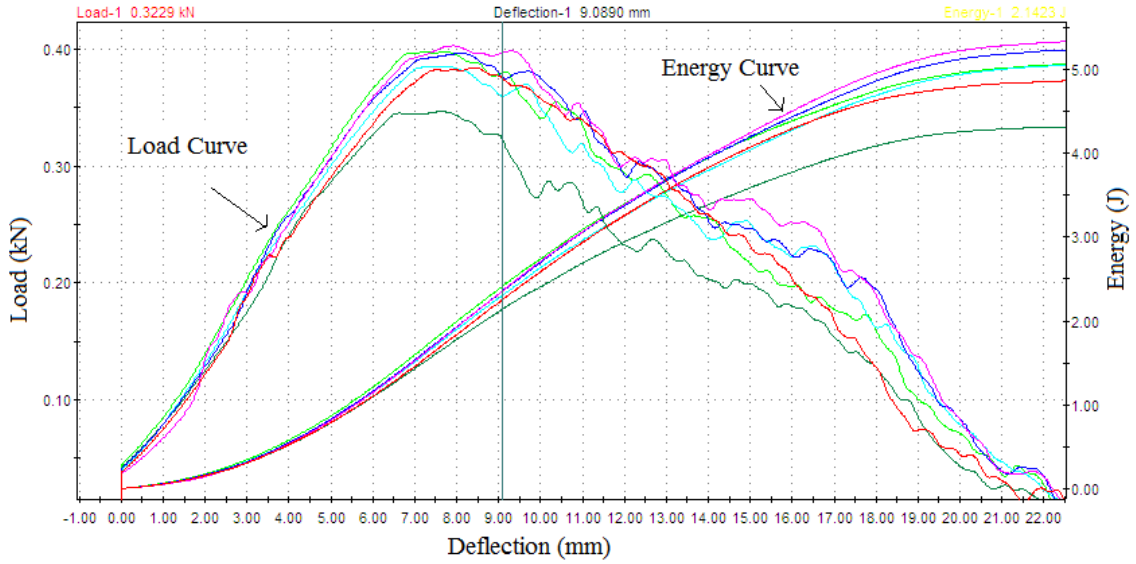

Figure 4.18. Force deformation plots of h-LLDPE at DR 7.

Table 4.4 Impact test results at different DRs

Draw Ratio (DR)	F_{PN} (N)	STD	E_{PN} (J)	STD	F_{FN} (N)	STD	ΔL_{FN} (mm)	STD	E_{FN} (J)	STD
7	455.3	23	2.17	0.15	235.4	35.5	20.35	0.66	5.34	0.36
21	479.2	4	2.42	0.06	216.4	29.2	22.24	0.79	5.44	0.08
36	404.2	14	1.95	0.19	207.3	7.5	22.65	1.01	4.99	0.25
49	259	7	1.09	0.05	107.5	10.6	19.8	2.2	2.67	0.30
64	274.8	10	1.15	0.05	55.4	4.5	16.09	1.81	2.36	0.28

4.2.5 Elmendorf Tear Test

The tear resistance tests were carried out in accordance with ASTM D1922 standard. Ten samples in both directions and at each processing condition were tested and an average tear resistance value has been reported. The normalized tear resistance in MD and TD directions for h-LLDPE are listed in Table 4.5 and Table 4.6 respectively.

Table 4.5 MD tear resistance of h-LLDPE films at different DRs

DR	TR	STD	TR_N	STD
	g	g	KN/m	KN/m
7	1346.5	136.2	113.4	11.4
21	136.7	18.3	34.8	4.6
36	92.2	24.8	44.7	12
49	48.5	44.1	27.7	25.2
64	21.5	6.7	16.8	5.3

Table 4.6 TD tear resistance of h-LLDPE films at different DRs

DR	TR	STD	TR_N	STD
	g	g	KN/m	KN/m
7	3338.2	570.2	281.3	48
21	988.8	89.7	98.8	21.9
36	584.5	35.8	304.3	18.7
49	607.4	35	364.7	20.9
64	550.4	58.5	443.6	47.2

4.3 Effect of BR on Thermal and Mechanical Properties of h-LLDPE Blown Films

The results of thermal and mechanical tests conducted on the h-LLDPE films processed at different BRs (1.12, 1.4 and 1.78) are presented in this section.

4.3.1 Crystallinity

The heating curves of the samples processed at different BRs are shown in Figure 4.19. The melting range of h-LLDPE is observed to be in the range of 115°C to 124°C.

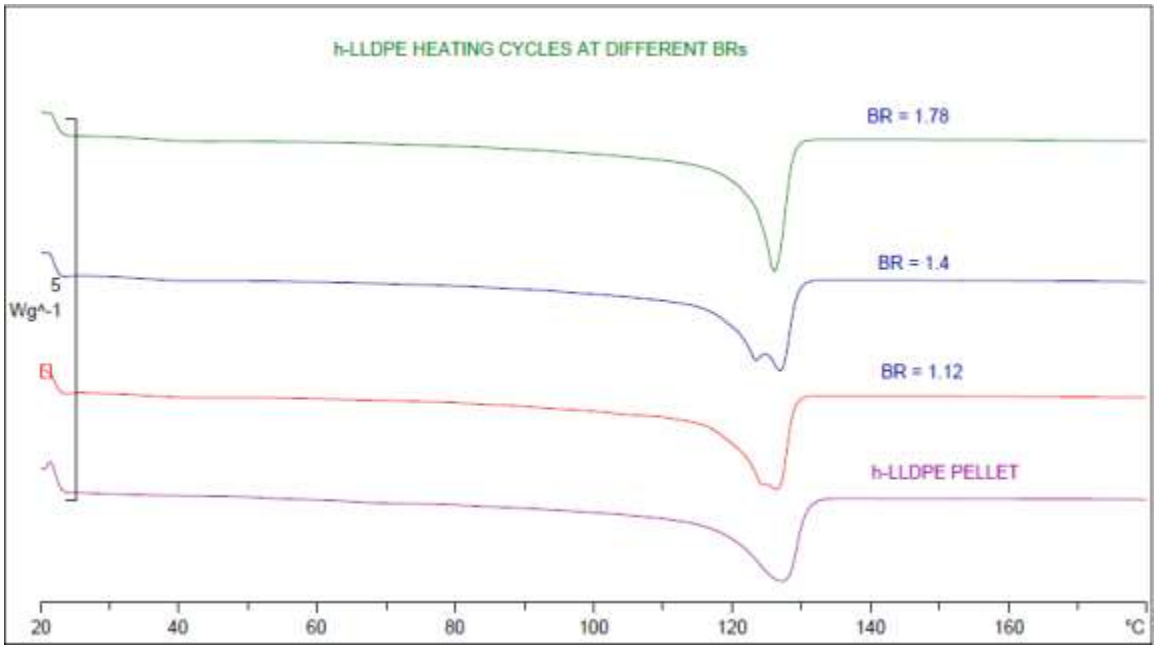

Figure 4.19 Heating cycles of h-LLDPE films processed at different BRs.

4.3.2 Orientation

The birefringence (Δn) when viewed from machine direction (MD) in the plane of the film is calculated and listed in Table 4.7 for different BR values at a constant DR value of

21 and a constant die temperature of 230 °C. Three readings were recorded and an average value has been reported.

Table 4.7 Birefringence at different BRs, DR = 21, and die temperature of 230°C

BR	Birefringence x 1000 MD direction
1.12	-1.28
1.4	-3.46
1.78	-3.52

4.3.3 Tensile Test

Tensile tests were carried out in accordance with ASTM D882 standard in both MD and TD directions. Five samples were tested in both the directions for each processing condition. The stress strain plots of h-LLDPE films, obtained from five samples, were tested at different BRs (1.12, 1.4 and 1.78) in MD and TD directions. The tensile properties of h-LLDPE at different BRs in machine direction (MD) are listed in Table 4.8. The tensile properties of h-LLDPE at different BRs in transverse direction (TD) direction are listed in Table 4.9.

Table 4.8 MD tensile properties for h-LLDPE at different BRs

BR set	UTS (MPa)	STD	σ_y (MPa)	STD	ϵ_F (%)	STD	T_E (Mpa)	STD
1.12	42.86	4.56	9.84	0.67	813.61	82.24	159.35	25.24
1.4	20.27	3.79	7.72	1.14	599.72	42.51	71.06	16.20
1.78	39.99	6.99	9.06	1.06	726.00	49.46	131.38	23.00

Table 4.9 TD tensile properties for h-LLDPE at different BRs

BR	Ultimate Tensile Stress	Std Dev	Tensile Stress at Yield	Std Dev	Tensile Strain at Break - Ductility	Std Dev	Toughness - Energy at Break	Std Dev
	(MPa)		(MPa)		(%)		(Mpa)	
1.12	36.98	3.91	10.75	0.35	1170.28	45.94	206.27	0.00
1.4	28.28	3.36	8.05	1.06	1089.89	85.33	145.39	25.03
1.78	21.26	5.54	8.30	0.31	877.50	148.27	105.43	30.23

4.3.4 Dart Impact Test

Impact tests were carried out in accordance with ISO 7765-2 standard. Five samples were tested at each processing condition and an average impact energy value has been reported. The force-deformation diagrams for five h-LLDPE films were tested at BR values of (1.12, 1.4 and 1.78). The normalized peak force, peak energy, failure force, failure deformation and failure energy values for the five films tested at different BRs are shown in the Table 4.10.

Table 4.10 Impact test results at different BRs

Blow Ratio (BR)	F_{PN} (N)	STD	E_{PN} (J)	STD	F_{FN} (N)	STD	ΔL_{FN} (mm)	STD	E_{FN} (J)	STD
1.12	430.1	8.8	1.8522	0.03	203.4	0.01	22.5	0.2	5.11	0.14
1.4	453.8	4.7	1.9436	0.03	254.8	0.05	21.1	0.9	5.23	0.07
1.78	435.9	25.2	1.8869	0.15	260.6	0.04	20.7	0.6	4.91	0.5

4.3.5 Elmendorf Tear Test

The tear resistance tests were carried out in accordance with ASTM D1922 standard. Ten samples in both directions and at each processing condition were tested and an average tear resistance value has been reported. The normalized tear resistance in MD and TD directions for h-LLDPE are listed in Table 4.11-Table 4.12.

Table 4.11 MD tear properties of h-LLDPE at different BRs

BR	TR	STD	TR_N	STD
	g	g	KN/m	KN/m
1.12	450.56	147.33	113.88	37.24
1.4	374.4	150.69	107.36	43.21
1.78	242.67	99.77	87.6	36.02

Table 4.12 TD tear properties of h-LLDPE at different BRs

BR	TR	STD	TR_N	STD
	g	g	KN/m	KN/m
1.12	963.2	113.14	268.6	31.55
1.4	1044.8	66.63	301.35	19.22
1.78	664.53	32.11	239.88	11.59

4.4 Effect of Blend Ratio on the Thermal and Mechanical Properties of h-LLDPE and LDPE Blended Blown Films

The results of thermal and mechanical tests conducted on the h-LLDPE films processed at different blend ratios are presented in this section. A die temperature of 230 °C, blow ratio (BR) of around 1.6 and draw ratio (DR) of 21 was kept constant while the blend ratios were varied.

4.4.1 Crystallinity

The 1st heating cycles of virgin h-LLDPE and LDPE samples are shown in Figure 4.20. The samples processed at different blend ratios were analyzed and their 1st heating curves are shown in Figure 4.21. The melting range of h-LLDPE is observed to be in the range of 115°C to 124°C.

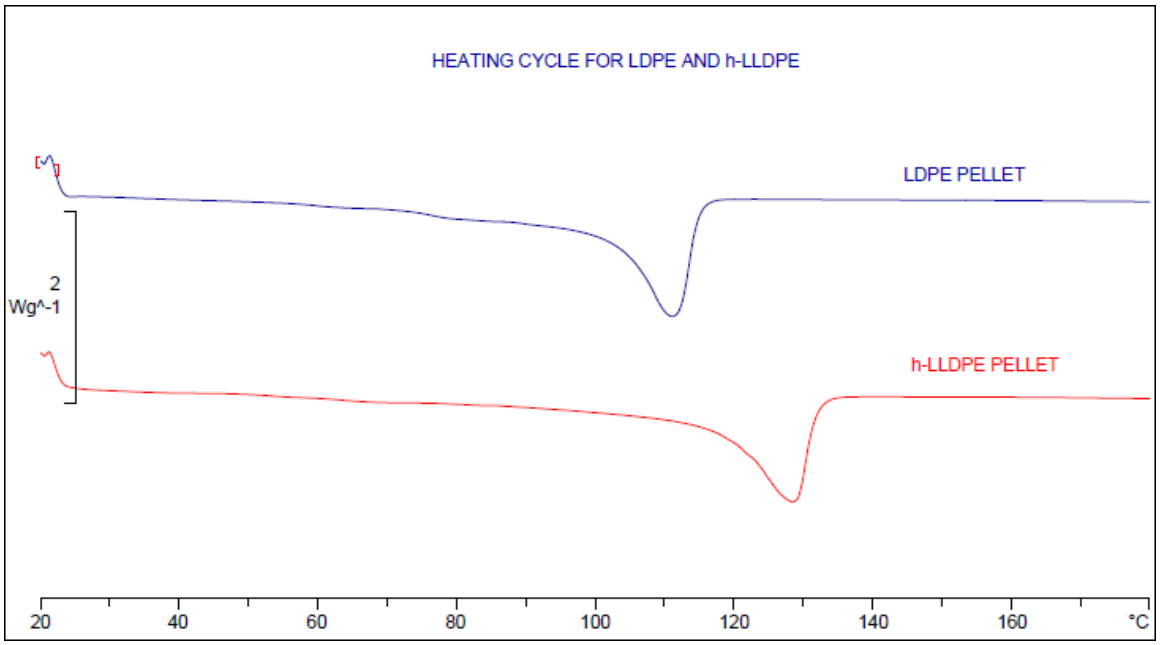

Figure 4.20. Heating cycles of h-LLDPE and LDPE pellets.

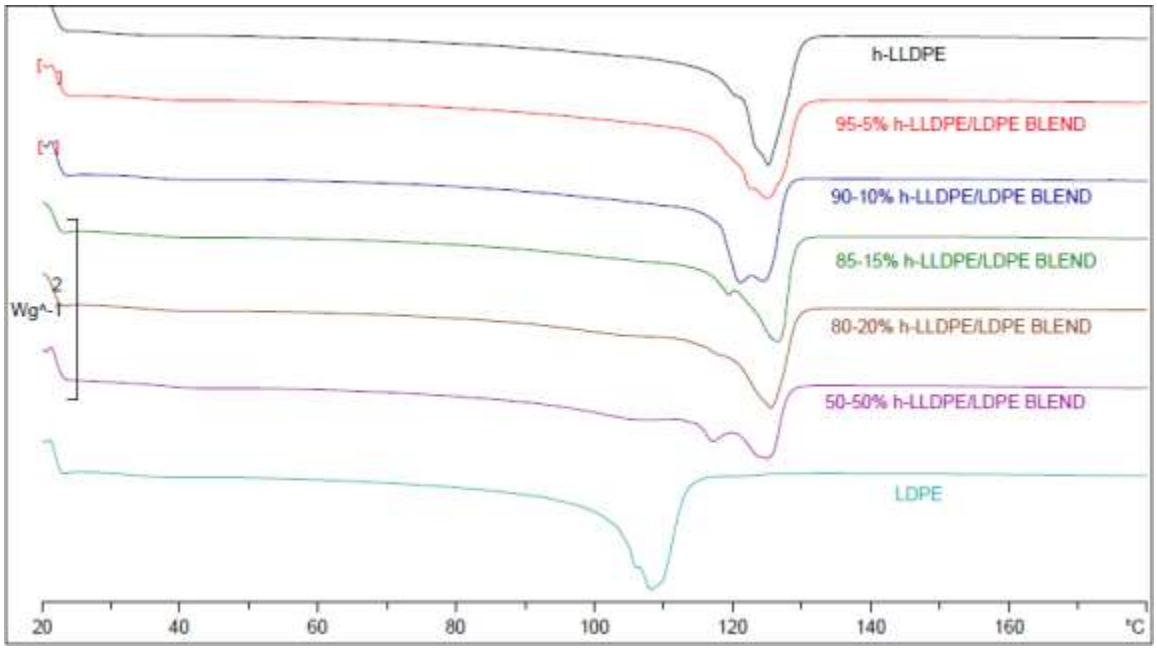

Figure 4.21. Heating cycles of h-LLDPE /LDPE blended films.

4.4.2 Orientation

The birefringence (Δn) when viewed from MD direction in the plane of the film is calculated and listed in Table 4.13 at different blend ratios by weight percentage.

Table 4.13 Birefringence at different blend ratios

LDPE content in h-LLDPE/LDPE blend (%)	Birefringence x 1000 MD direction
0	-3.01
5	-1.79
10	1.35
15	1.94
20	2.42
50	5.49
100	2.96

4.4.3 Tensile Test

Tensile tests were carried out in accordance with ASTM D882 standard in both MD and TD directions. Five samples were tested in both the directions for each processing condition. The tensile properties of h-LLDPE / LDPE films at different blend ratios in MD are listed in Table 4.14. The 15% LDPE blend ratio gives the maximum tensile strength, elongation and toughness in MD direction. The tensile properties of h-LLDPE / LDPE films at different blend ratios in TD are listed in Table 4.15. The 10% LDPE blend ratio is the best performing blend based on strength, elongation and toughness in TD direction.

Table 4.14 Machine Direction (MD) tensile properties of h-LLDPE /LDPE blends

LDPE Content (%)	UTS	STD	σ_y	STD	ϵ_F	STD	T_E	STD
set	(MPa)		(MPa)		(%)		(Mpa)	
0	43.64	7.19	8.16	0.93	760.11	25.89	137.63	19.21
5	43.64	4.10	8.77	1.01	776.17	13.31	159.25	14.52
10	42.17	7.99	9.24	1.78	767.67	38.75	170.07	40.32
15	43.88	10.83	9.61	2.12	783.83	50.74	194.85	58.49
20	39.33	4.37	9.79	1.18	735.61	25.58	184.30	21.17
50	27.57	1.74	7.14	0.87	222.72	24.10	51.18	5.62
100	28.79	2.77	7.18	1.08	163.33	17.50	33.17	6.76

Table 4.15 Transverse Direction (TD) tensile properties of h-LLDPE /LDPE blends

LDPE Content (%)	UTS	STD	σ_y	STD	ϵ_F	STD	T_E	STD
set	(MPa)		(MPa)		(%)		(Mpa)	
0	38.67	34.67	8.36	1.14	1085.78	36.79	174.02	26.65
5	34.67	3.62	8.66	1.05	1105.00	66.13	172.01	24.65
10	37.06	2.91	10.18	0.99	1177.11	47.87	203.99	20.11
15	29.12	2.34	8.38	1.38	1099.72	58.90	153.09	14.19
20	26.29	4.99	7.02	1.79	1091.44	120.63	137.40	32.76
50	24.74	2.81	8.07	1.48	1039.33	108.28	136.60	28.14
100	11.92	0.92	5.91	0.62	699.44	50.75	54.44	7.74

4.4.4 Dart Impact Test

Impact tests were carried out in accordance with ISO 7765-2 standard. Five samples were tested at each processing condition and an average impact energy value has been reported. The force-deformation diagrams for pure h-LLDPE, blends with (5%, 10%, 15%, 20% and 50% and 100% LDPE) were obtained. The normalized peak force, peak energy, failure force, failure deformation and failure energy values for the five films tested at different blend ratios have been listed in the Table 4.16. The 5% LDPE blend ratio is the best blend based on both impact peak force and toughness, whereas 50% LDPE blend ratio has the strongest impact failure force.

Table 4.16 Impact test results for different blend ratios

Blend Ratio h-LLDPE/LDPE	F_{PN} (N)	STD	E_{PN} (J)	STD	F_{FN} (N)	STD	ΔL_{FN} (mm)	STD	E_{FN} (J)	STD
100-0	702.4	37.7	6.59	0.53	432.3	0.0499	31.75	2.09	12.59	0.99
95-5	880.8	14.2	7.92	0.55	323.1	0.0839	33.09	1.95	15.25	0.44
90-10	799.9	34.8	5.65	0.66	234.1	0.0667	27.8	2.44	11.36	1.40
85-15	812	26.6	5.54	0.34	339.5	0.1206	23.63	0.85	10.42	0.35
80-20	623	19.6	4.10	0.38	152.8	0.0538	21.44	1.25	7.14	0.33
50-50	629.2	19.3	3.42	0.54	671.7	0.0437	26.95	0.97	9.82	0.97
0-100	615.5	29.3	2.94	0.43	505.4	0.0422	27.77	1.72	8.73	0.99

4.4.5 Elmendorf Tear Test

The tear resistance tests were carried out in accordance with ASTM D1922 standard. Ten samples in both directions and at each processing condition were tested and an average tear resistance value has been reported. The normalized tear resistance in MD and TD direction for h-LLDPE is listed in Table 4.17-Table 4.18. The 5% LDPE blend has the best blend properties based on the tear properties in MD direction, whereas 10% LDPE blend has optimum tear properties in TD direction.

Table 4.17 MD tear properties of h-LLDPE /LDPE blends

Blend Ratio	**TR**	**STD**	**TR_N**	**STD**	**TR_N**	**STD**
%	**g**	**g**	**g/mm**	**g/mm**	**KN/m**	**KN/m**
100-0	324.11	129.11	10752.61	4283.32	105.45	42.01
95-5	219.73	17.34	7406.74	584.53	72.64	5.73
90-10	128	21.8	3801.98	647.45	37.28	6.35
85-15	61.73	13.32	2329.56	502.5	22.85	4.96
80-20	50.93	24.39	1787.14	856.01	17.52	8.39
50-50	136.23	22.22	4040.68	659.01	39.62	6.46
0-100	410.13	90.02	12062.75	2647.64	118.29	25.96

Table 4.18 TD tear properties of h-LLDPE/LDPE blends

Blend Ratio	**TR**	**STD**	**TR_N**	**STD**	**TR_N**	**STD**
%	**g**	**g**	**g/mm**	**g/mm**	**KN/m**	**KN/m**
100-0	613.94	77.72	19713.76	2495.44	193.32	24.47
95-5	979.73	176.99	33590.86	6068.07	329.41	59.50
90-10	1161.6	166.49	38936.31	5580.54	381.83	54.72
85-15	1141.76	123.63	39157.89	4066.89	384.01	39.88
80-20	1094.93	77.10	39815.76	2803.78	390.46	27.5
50-50	538.83	45.86	13875.36	1180.88	136.07	11.58
0-100	136.88	10.54	4049.70	311.92	39.714	3.05

CHAPTER 5

DISCUSSION

The objective is to see the effect of blend ratio and all the films are to be processed at same processing conditions of DR, BR, and mass flow rate. These process parameters are set to the optimum values such that they lead to best film properties. Therefore we have to appropriately select the die temperature. So the following discussion will be for die temperature selection, then for the DR selection, then for the BR selection. Our selection will be based on the mechanical characteristics. Meanwhile we try to explain the effect of these factors on the product and on the crystallinity and orientation which develop during the process.

5.1 Effect of Die Temperature on the Bubble Stability of LDPE and h-LLDPE Blown Films

The plots of DSC as shown in Figure 5.1-Figure 5.6 indicate that there isn't much effect of degradation at these elevated temperatures. An average of three data points at the same die temperature has been reported. It is observed that the 2^{nd} melting peak temperatures are almost the same at different die temperatures. Also, the onset and peak crystallization temperatures for the 1^{st} cooling cycle are almost similar over different die temperature range. There is a slight increasing trend in the onset crystallization temperature during the first cooling profile. Thus, it now depends on the relative bubble stability area to decide

the die temperature to be used for processing these films. The relative area of the operating window was calculated against the constant base area of DR and BR. The size of operating window at different die temperatures is listed in the Table 5.1. It was observed that the BR range was largest at a die temperature of 230 °C as shown in Figure 5.8, whereas the DR range is almost constant over the temperature range studied. The relative area percentage in terms of the size of the operating window was observed to be the largest at the die temperature of 230 °C as shown in Figure 5.9. Thus the die temperature was fixed to 230 °C while the other variables will be optimized as discussed in the next sections.

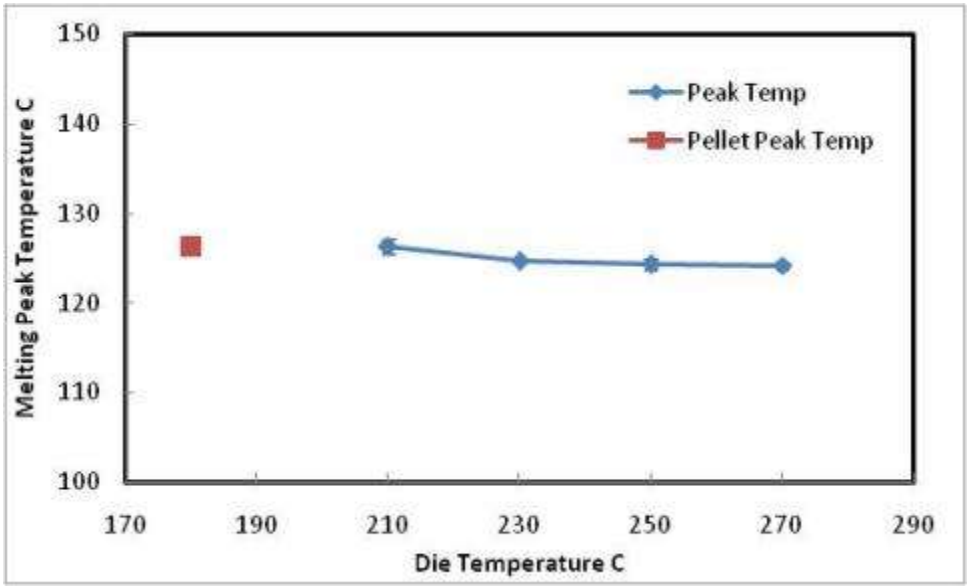

Figure 5.1. Melting Peak Temperature from the 2nd DSC heating profile for h-LLDPE at different die temperatures.

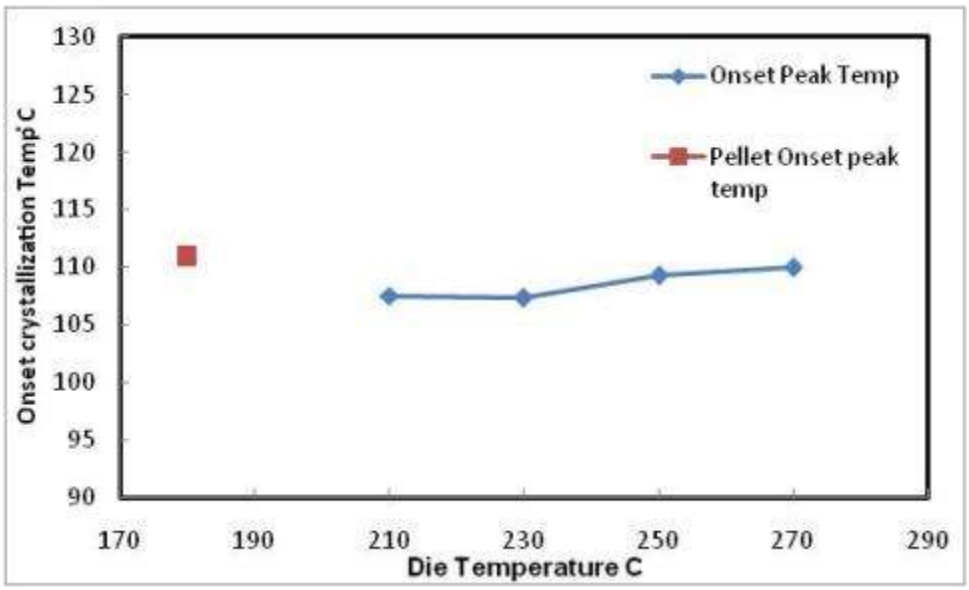

Figure 5.2. Onset crystallization temperature for the 1st cooling profile of the h-LLDPE at different die temperatures.

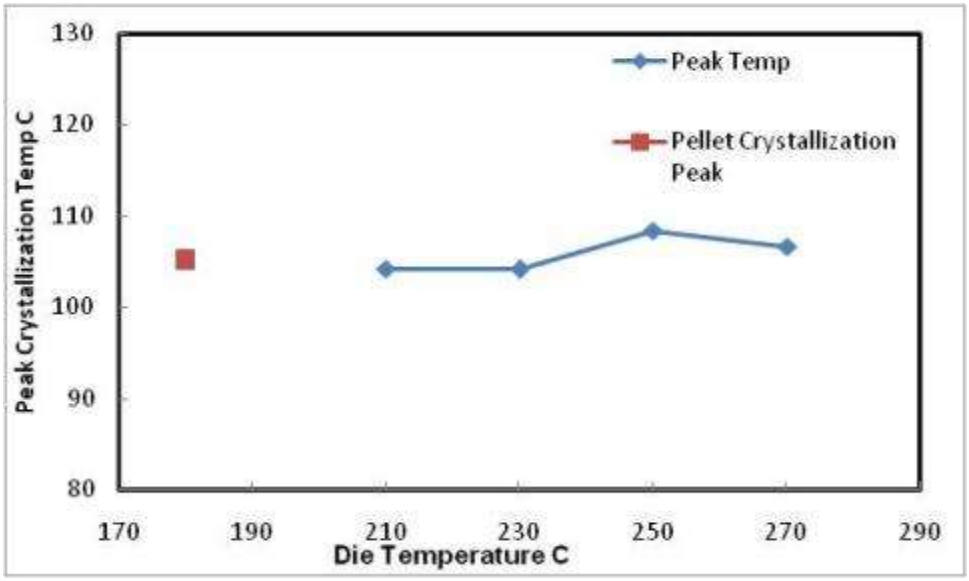

Figure 5.3. 1st Cooling Peak crystallization temperature for 1st DSC cooling profiles of the h-LLDPE at different die temperatures.

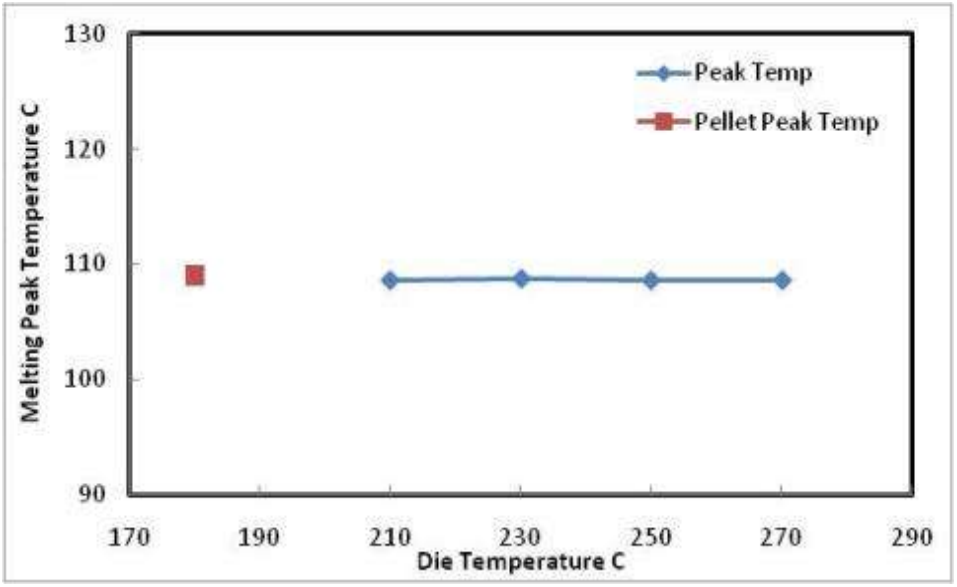

Figure 5.4. Melting Peak Temperature for 2nd DSC melting profiles of LDPE at different die temperatures.

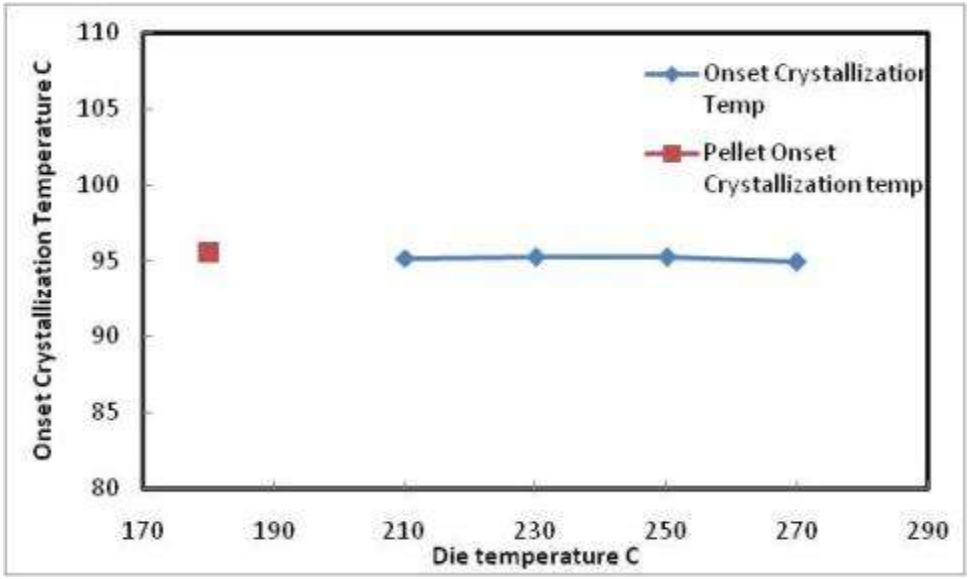

Figure 5.5. Onset crystallization temperature for 1st DSC cooling profiles of the LDPE at different die temperatures.

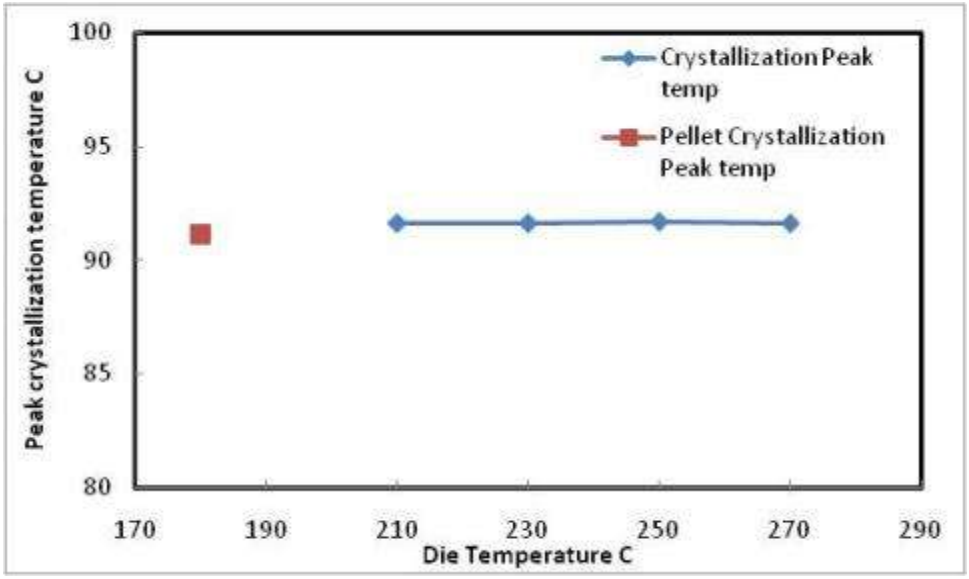

Figure 5.6. Peak crystallization temperature for 1st cooling DSC profiles of the LDPE at different die temperatures.

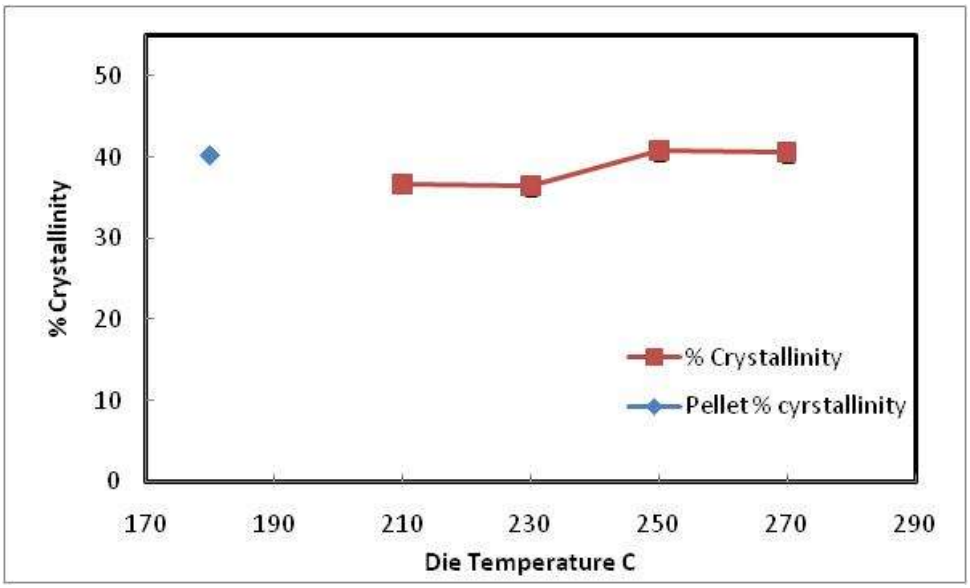

Figure 5.7. Crystallinity % of 1st cooling DSC profile of h-LLDPE at different die temperatures.

Table 5.1. Size of operating window at different die temperatures

S.No	Temperature	BR		DR		Size of Operating Window
	°C	min	max	min	max	%
1	210	0.2	1.6	7.06	84.76	38.6
2	230	0.2	2	6.78	81.30	49.1
3	250	0.8	2	6.77	81.33	30.9
4	270	0.8	1.9	6.75	81.01	29.5

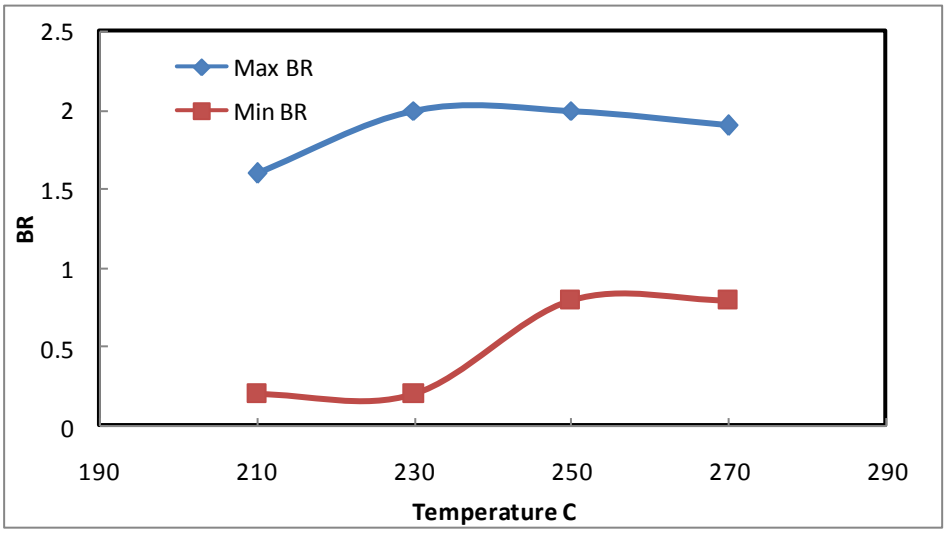

Figure 5.8. BR range for h-LLDPE at different die temperatures.

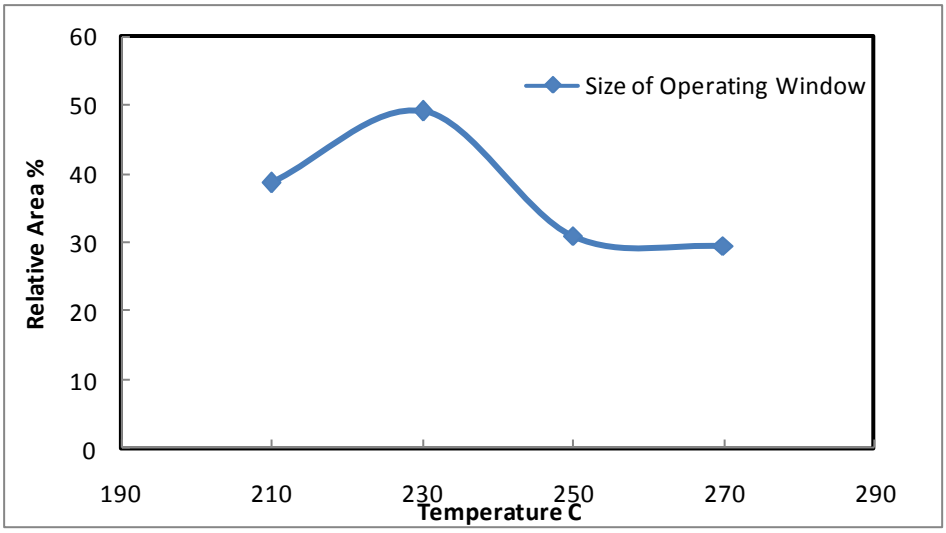

Figure 5.9. Percentage size of operating window of h-LLDPE at different die temperatures.

5.2 Effect of DR on Thermal and Mechanical Properties of h-LLDPE Blown Films

The results of thermal and mechanical tests conducted on the h-LLDPE films processed at different DRs (7, 21, 36, 49, 64 and 86) are discussed in this section. The effect of DR was studied by keeping the die temperature constant at 230 and with a constant mass flow rate of around 8 g/min. This was the maximum possible mass flow rate at the given processing conditions of the instrument used. A slightly higher mass flow rate led to the automatic shutting down of the instrument.

5.2.1 Crystallinity

The average percent crystallinity, melting peak temperatures and the end of the melting temperature range of the samples tested at different DRs have been listed in Table 5.2. The percentage crystallinity at different DRs for h-LLDPE is shown in Figure 5.10.

Table 5.2. DSC results for h-LLDPE at different DRs

DR	1st Heating			
	% Crystallinity	Stdev	Melting Peak °C	Endset of Melting °C
7	41.8	1.3	124.8	129.3
21	40.7	2.3	124.9	130.0
36	39.1	0.5	125.4	128.5
49	39.4	0.5	124.7	129.1
64	39.2	0.6	126.2	129.4

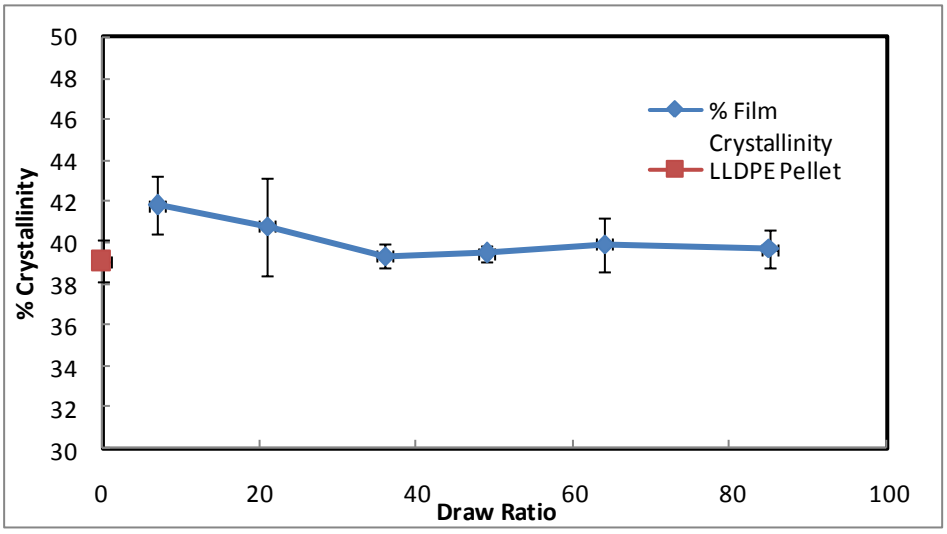

Figure 5.10. Percentage crystallinity of h-LLDPE from the 1st melting profiles of DSC at different DRs.

5.2.2 Orientation

A plot of birefringence orientation when viewed from MD direction is shown in Figure 5.11. The birefringence goes to negative with increase in DR upto a DR of 36 and then increases with increase in DR.

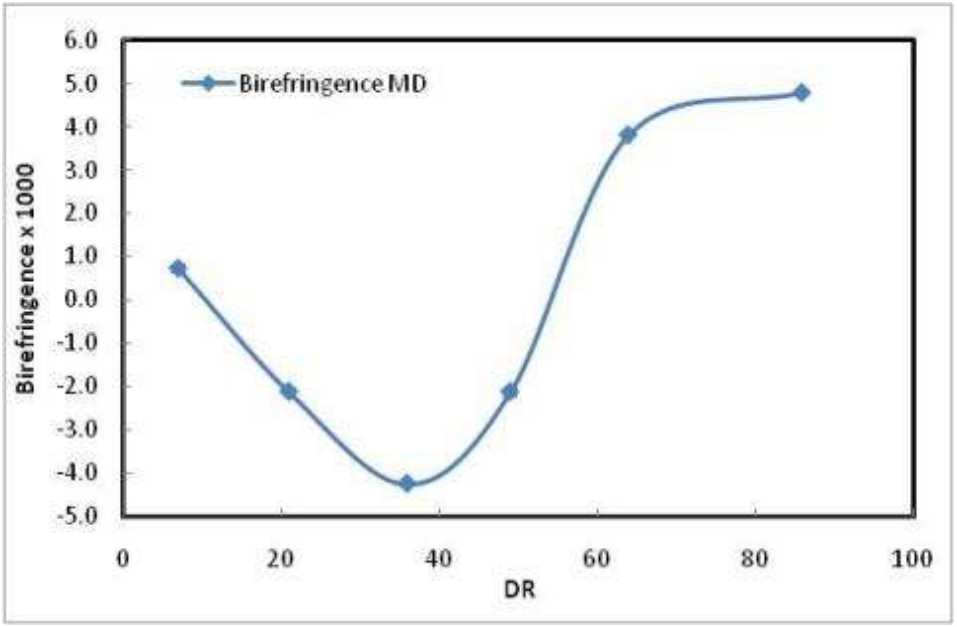

Figure 5.11. Orientation results for 1st order birefringence at different DRs.

5.2.3 Tensile Test

The profile of stress strain plots of h-LLDPE at different DRs in MD is shown in Figure 5.12. The MD tensile strength and yield stress of h-LLDPE films remained almost constant for initial DRs of 7, 21 and 36; it then slightly dropped at DR 49 followed by an increase in tensile properties upto DR 64 and then decreased with further increase in DR. The plots of MD tensile strength and yield stress are shown in Figure 5.13-Figure 5.14. The percentage ductility in MD decreased with increase in DR as shown in Figure 5.15. The MD toughness decreased with increase in DR as shown in Figure 5.16.

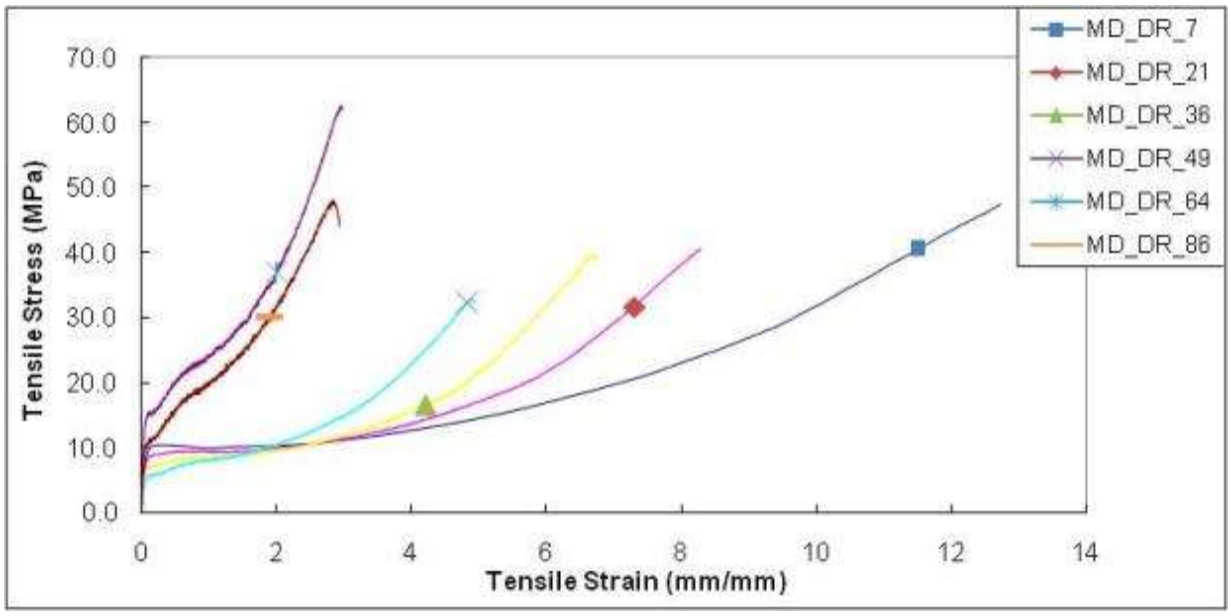

Figure 5.12. MD tensile stress-strain curves at different DRs.

From the tensile strength results (Figure 5.13) in MD direction it seems as though there are two types of morphologies which are developed in the process and which requires detailed structure development morphological investigation using SEM and TEM. These are more time consuming and could be done as the future work of the present study. However, Bobovitch et al [30] from their study (films produced from double bubble process, density = 0.920 g/cm^3) have found an increase in MD tensile strength of LLDPE from 107 MPa to 118 MPa with increase in DR value from 4.9 to 5.8. They also concluded that the tensile strength no longer depended on the c-axis orientation after a certain value for orientation of the crystalline chain segments as the tensile strength leveled off from DR=5.8 to DR=6. In our study which is concerned with high draw ratio, beyond DR=6, showed a constant MD tensile strength of 40 MPa up to DR=36. However, from our results, scattering data was observed against different DRs above the value of 36. This could be due to the presence of one or more crystallites at higher DR of 64 and 86 as observed from the DSC endotherms. Thus, the present study highlights the

importance of DR for the MD tensile strength of the blown films over a wide range of values.

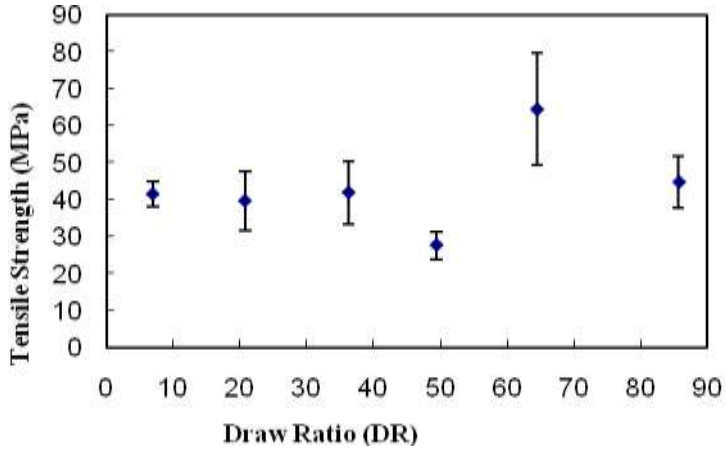

Figure 5.13. MD tensile strength of h-LLDPE at different DRs.

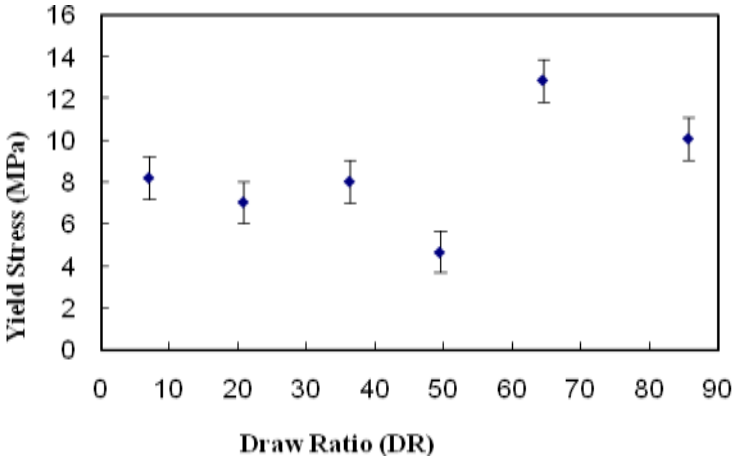

Figure 5.14. MD yield stress of h-LLDPE at different DRs.

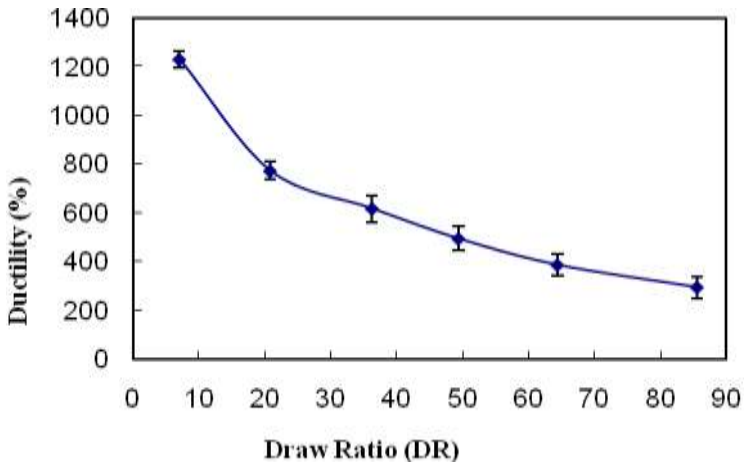

Figure 5.15. MD ductility of h-LLDPE at different DRs.

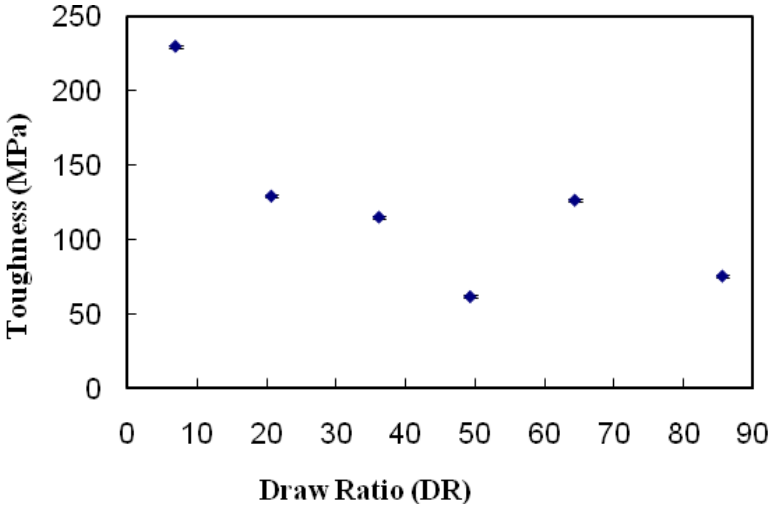

Figure 5.16. MD toughness of h-LLDPE at different DRs.

The profile of stress strain plots of h-LLDPE at different DRs in TD is shown in Figure 5.17. The TD tensile strength of h-LLDPE films remained at a higher constant value for DR up to 21 and then remained constant at a lower strength value with increase in DR as shown in Figure 5.18. This could be attributed to relatively higher crystalline content at DR 7 and 21, as shown in Table 5.2. Moreover, Bobovitch et al [30] from their study (film blowing using double bubble process, density=0.920 g/cm^3) have found a decrease in TD

tensile strength of LLDPE with increase in DR values ranging from 4.8 to 6. In our study the DRs above DR=6 were studied and the TD tensile strength had two different constant values with a higher strength of 45 MPa value for DRs ranging between 7 to 21 and a lower strength of 25 MPa value for DRs between 36 to 86. The TD yield stress also remained almost constant with increase in DR except at a DR of 36 where a drop was observed in its value as shown in Figure 5.19. The TD percentage ductility decreased with increase in DR as shown in Figure 5.20. Also, it has been observed for TD toughness the is trend similar to that of strength, there are two sets of toughness values, one around 240 MPa for the DR 7 and 21 and a lower set of toughness in the range of 100 MPa for the DRs above 36 as shown in Figure 5.21.

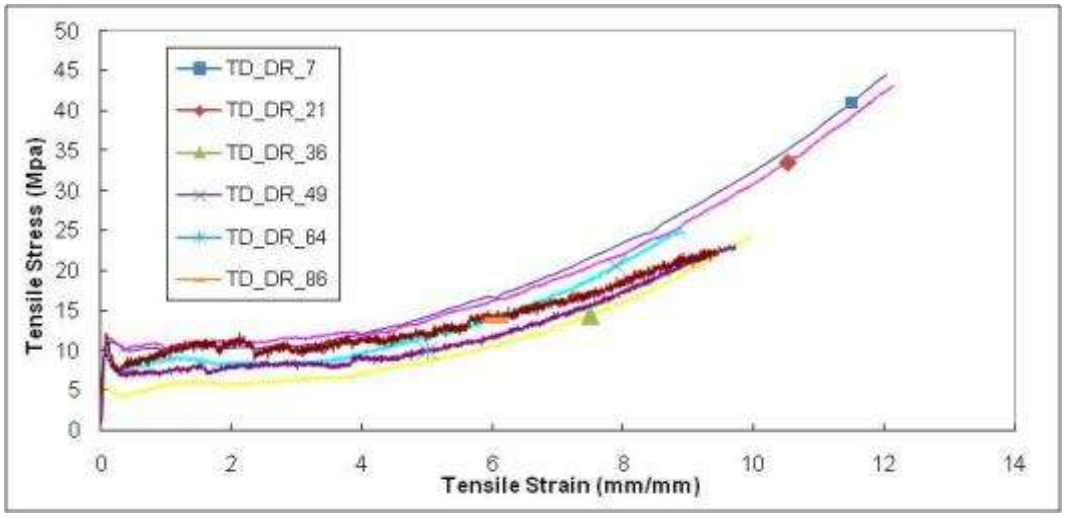

Figure 5.17. TD tensile stress-strain curves at different DRs.

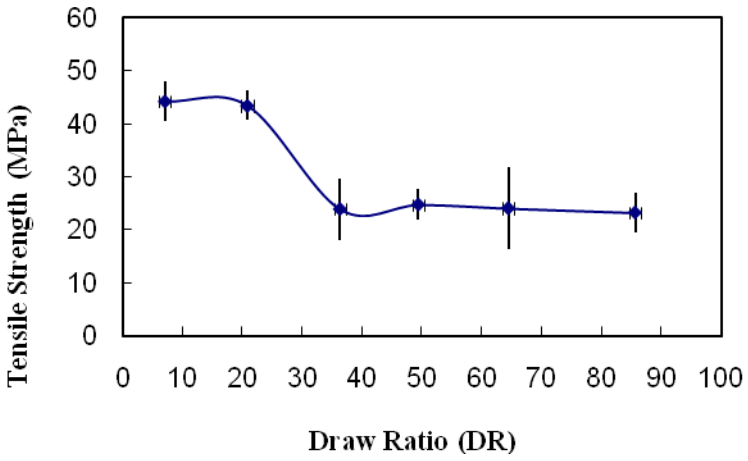

Figure 5.18. TD tensile strength of h-LLDPE at different DRs.

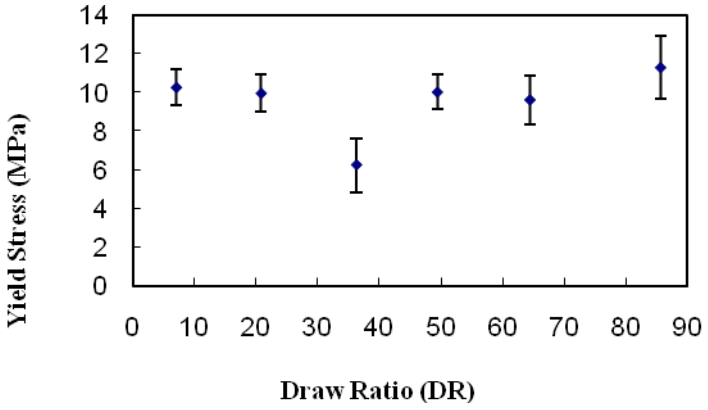

Figure 5.19. TD yield stress of h-LLDPE at different DRs.

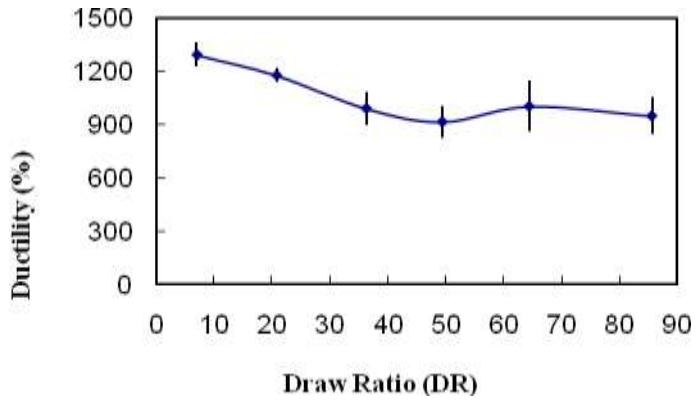

Figure 5.20. TD ductility of h-LLDPE at different DRs.

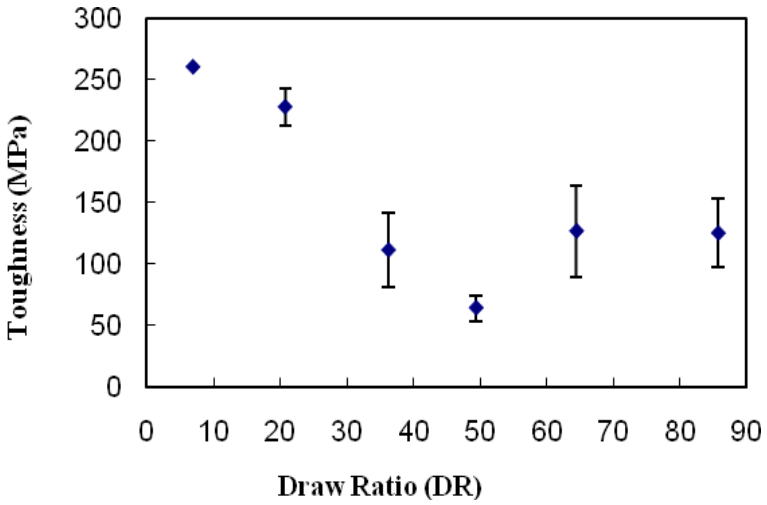

Figure 5.21. TD toughness of h-LLDPE at different DRs.

5.2.4 Dart Impact Test

The force deformation diagrams for different DRs are shown in Figure 5.22. The force deformation plots reveal that the films at DRs 7, 21, 36 seems to be quite tough which is evident from the wide plateau region observed in Figure 4.20 with relatively higher peak force values. The images of impact tested specimens as shown in Figure 5.23 suggest that all the films had deformed biaxially. Thus, these films offer relatively higher impact resistance. The toughness of the films at DR 7, 21 can be attributed to the marginally higher crystalline content (Figure 5.10) at these DRs as shown in Table 5.2; and due to

the biaxial deformation of the films as shown in Figure 5.23. However, this increase is marginal and is not the significant factor effecting it, as at all DRs the crystallinity value is almost in the same range. For the DR 49 and DR 64 the force deformation curve has slightly lesser plateau region as is shown in Figure 5.22 with a decreased load carrying capacity (peak load).

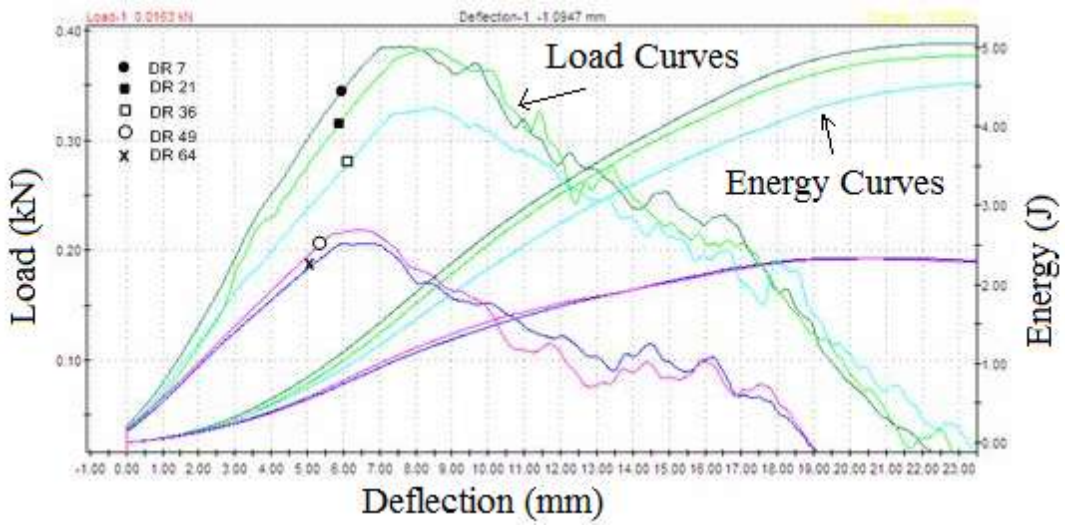

Figure 5.22. Force deformation plots of h-LLDPE at different DRs.

The trend of normalized peak force, peak energy and failure force was observed to be almost similar. For the first two DRs of 7 and 21 the plot remained almost constant and with a slight decrease at DR 36, it then decreased upto DR 49 and once again remained constant with higher DRs as shown in Figure 5.24-Figure 5.28. Normalized entities are calculated for unit thickness of the film. It can thus be concluded that the DR 7 and DR 21 result in higher impact properties of the h-LLDPE films. When comparing the two, DR 21 will yield a longer length of film with the same amount of material as that of DR

7. It implies that the DR 21 and 36 leads to higher productivity without compromising on the strength of the film. From the results of Figure 5.24-Figure 5.28 DR 21 and 36 seems to have better mechanical properties.

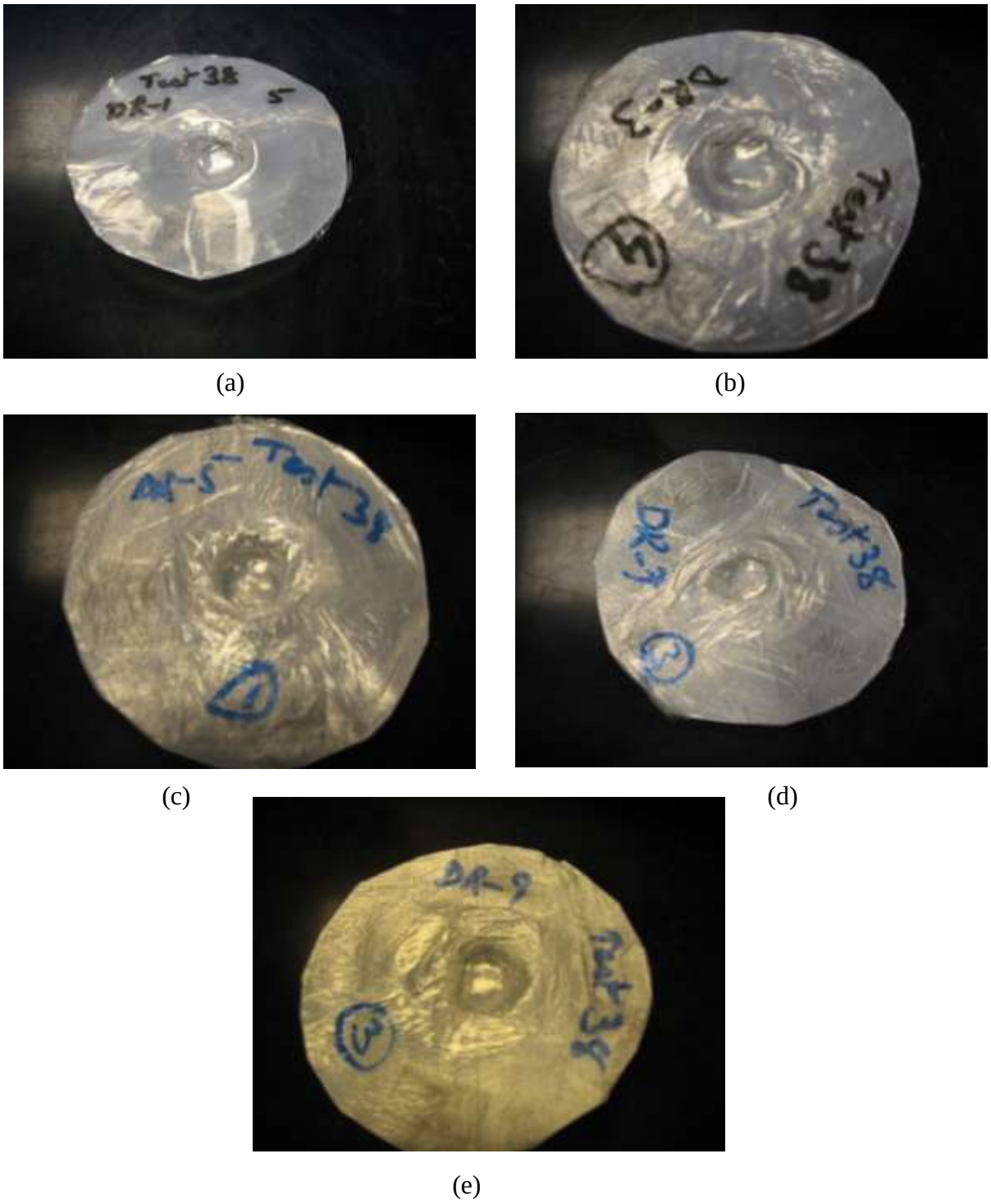

Figure 5.23. Impact tested specimens at different DRs, (a) DR =7 (b) DR = 21 (c) DR = 36 (d) DR = 49 (e) DR = 64.

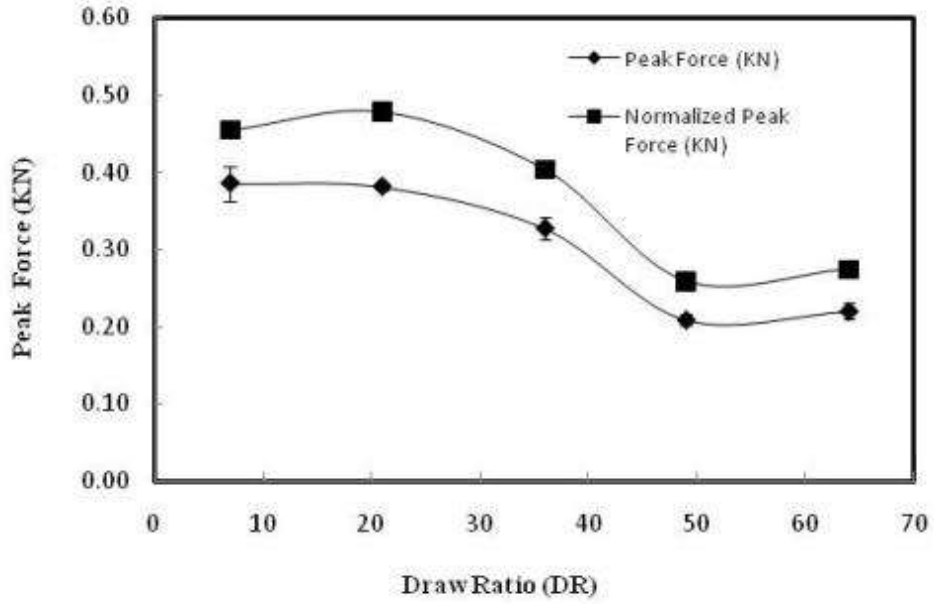

Figure 5.24 Peak Force at different Draw Ratios (DR)

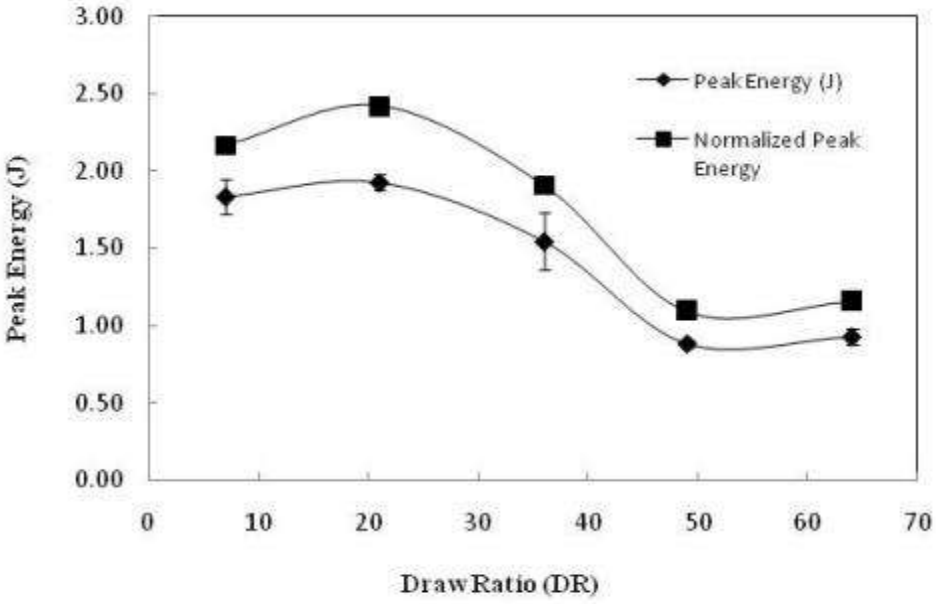

Figure 5.25 Peak Energy at different Draw Ratios (DR)

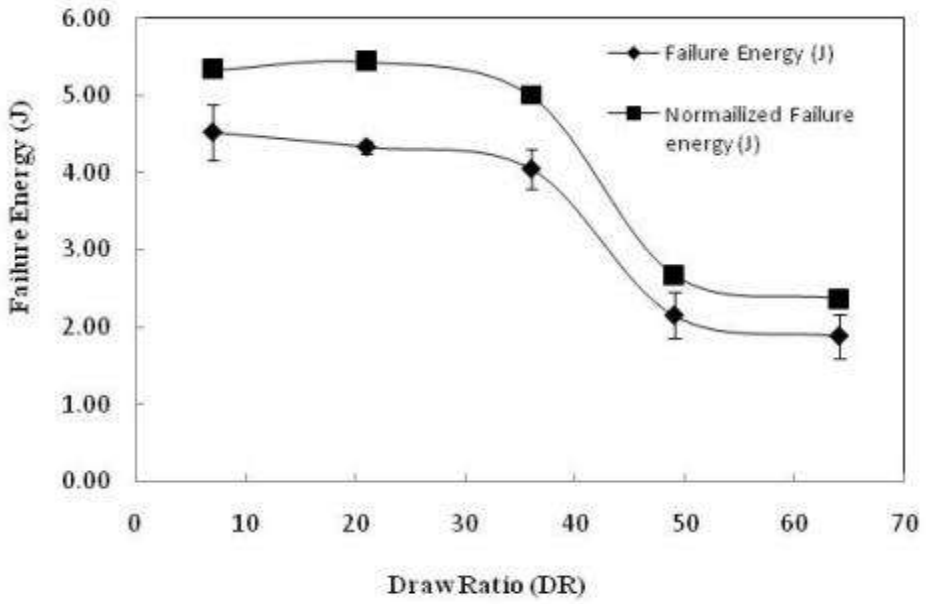

Figure 5.26 Failure Energy at different Draw Ratios (DR)

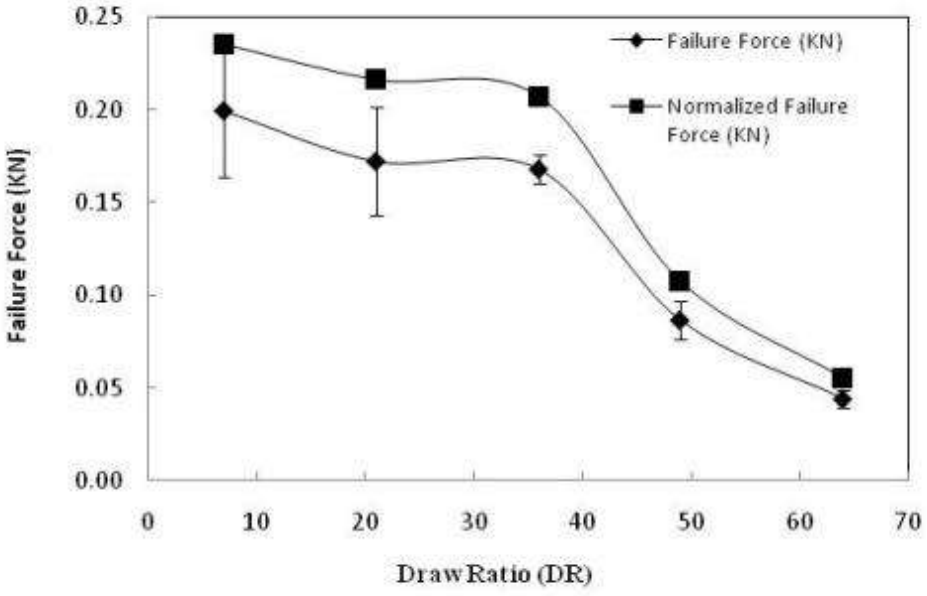

Figure 5.27 Failure Force at different Draw Ratios (DR)

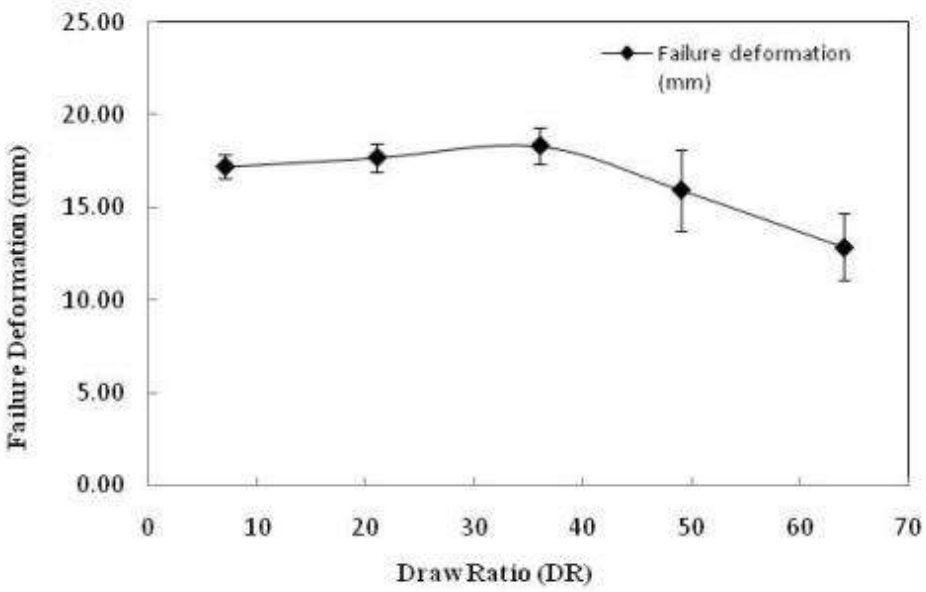

Figure 5.28 Failure Deformation at different Draw Ratios (DR)

5.2.5 Elmendorf Tear Test

It has been observed that the tear resistance shows a non linear decrease in MD direction. This decrease is observed from 120 KN/m to 20 KN/m. A large and rapid decrease of MD tear resistance is observed from a high value around 120 KN/m to about 40 KN/m from DR 7 to 21, and then, there is slight decrease from 40 KN/m to 20 KN/m for wide range of DR from 21 to 66 as shown in Figure 5.29. Bobovitch et al. [30] from their study (with double bubble film blowing of LLDPE and density=0.920 g/cm^3) have found that the MD tear strength decreases from 33 g/mil to 20 g/mil with increase in DR from 4.9 to 6. However, their study was only limited to DR values ranging from 4.9 to 6. They attributed the decrease in MD tear resistance to the lamellar organization as observed from their morphological studies. Their morphological studies revealed that below a

certain value of DR in MD direction the lamellar arrangement remained somewhat random. In contrast, above that DR, lamellae tend to align perpendicular to MD direction as observed from the microscopy and Fourier Transform Infra Red (FTIR) spectroscopy measurements. Consequently, the decrease in MD tear resistance was described using this lamellar organization induced by the deformation. From our study, the MD tear strength decreased non-linearly with increase in DR and this could be due to the lamellar arrangement. The orientation results as shown in Figure 5.11 indicate that the MD tear resistance is as high as 120 KN/m for relatively balanced orientation in MD and TD direction with DR=7. For higher DRs, with orientation values higher in either MD or TD direction, the MD tear resistance was observed to be in the low range of 20 KN/m to 40 KN/m. Two different trends were observed for TD tear resistance as shown in Figure 5.30. There was a decrease in TD tear resistance from 280 KN/m to 90 KN/m for DR from 7 to 21. For the DRs ranging between 36 to 66 an increase in TD tear resistance was observed from 280 KN/m to 450 KN/m indicating presence of two different types of morphologies. However, Bobovitch et al. [30] concluded from their study, that the TD tear strength almost remained constant with increase in DR up to a value of DR=6. Moreover, they were unclear as to why their TD tear strength remained unchanged to the change in DR. In our study, a wide range of DRs were studied and there is a further scope of investigation for the lamellar orientation using SEM and WAXD, as the orientation obtained from birefringence did not give a good correlation to the TD tear resistance trend.

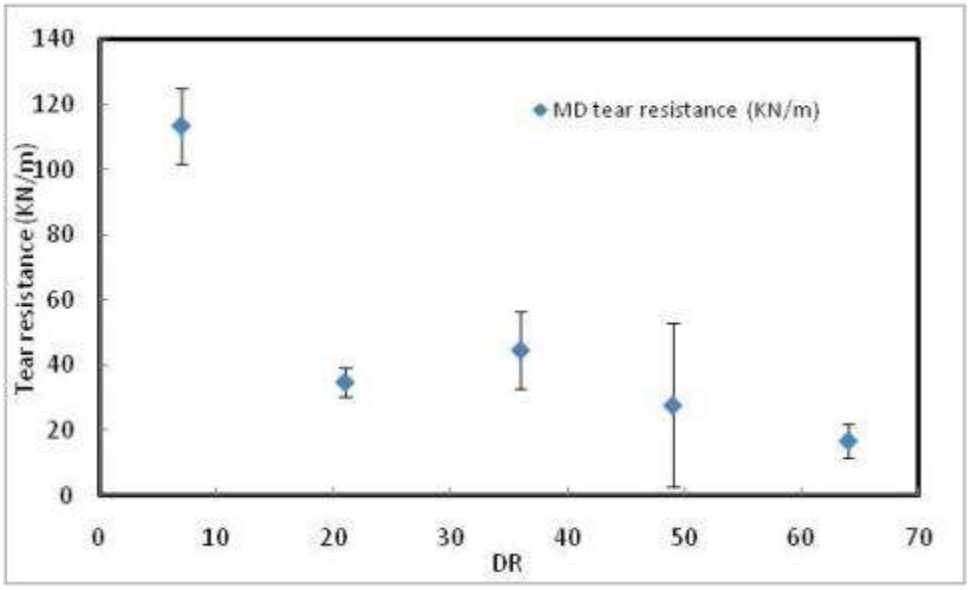

Figure 5.29. MD tear resistance of h-LLDPE at different DRs.

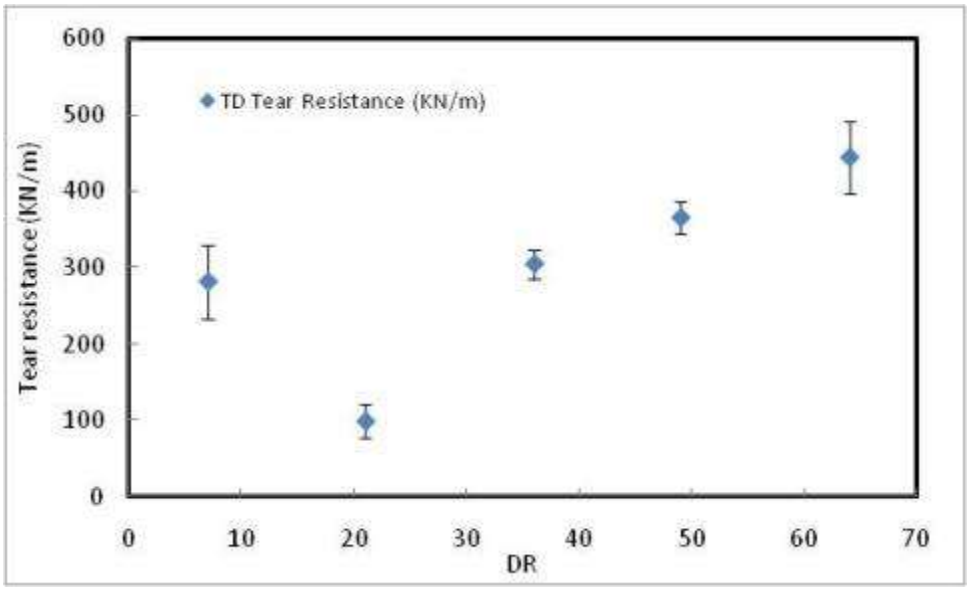

Figure 5.30. TD tear resistance of h-LLDPE at different DRs.

Impact test results take into consideration the effect of both MD and TD directions simultaneously, which is not the case with the other mechanical properties. Thus, impact test results were chosen for selecting the optimum DR. The DR 7 and 21 had the maximum impact energies for h-LLDPE films. Since DR 21 will give us a greater length of film with the same amount of material and equivalent impact properties as that obtained at DR 7, a DR value of 21 would be preferred. It can be summarized from tensile, tear and impact toughness of the films that DR 7, 21 and 36 give better mechanical properties. In terms of productivity, DR 21 and 36 are the most appropriate ones. Almost all the properties are slightly greater for DR 21 except for TD tear resistance where DR 36 is greater. As a conclusion, we fix our DR variable to a value of 21 to obtain the optimum results. The next step is to select a suitable BR.

5.3 Effect of BR on Thermal and Mechanical Properties of h-LLDPE Blown Films

The results of thermal and mechanical tests conducted on the h-LLDPE films processed at different BRs (1.12, 1.4 and 1.78) are presented and discussed in this section. The effect of BR was studied by keeping the die temperature and the DR constant with their optimized values of 230 °C and DR of 21. The extruder temperature profile selected limited our study to a BR range of 1.12 to 1.78 with a constant mass flow rate of around 8 g/min.

5.3.1 Crystallinity

The average percent crystallinity, melting peak temperatures and the end of the melting temperature range of the samples tested at different BRs have been listed in Table 5.3. It was observed from the Figure 5.31, that the crystallinity for the first heating cycle which

contained the processing history almost remained constant with increase in BR with a slight decrease at BR=1.4.

Table 5.3 DSC results for h-LLDPE films at different BRs

Blow Ratio (BR)	1st Heating				
	% Crystallinity	Stdev	Melting Peak°C	Stdev	Endset of Melting °C
1.12	39.61	0.56	125.49	1.19399	129.22
1.4	38.92	0.4	125.46	0.93	128.87
1.78	39.14	0.82	126.1	0.44	129.64

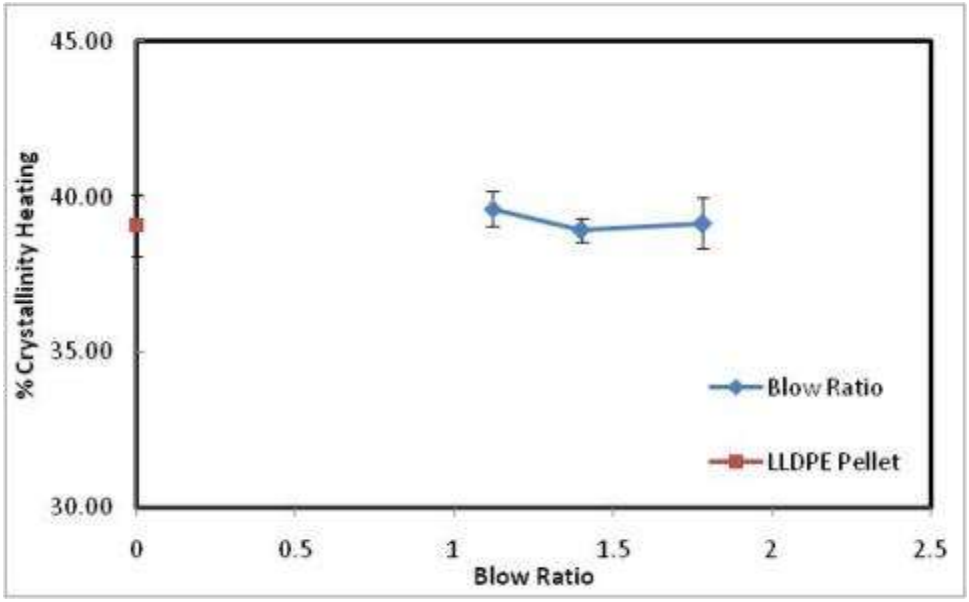

Figure 5.31. Percentage crystallinity of h-LLDPE at different BRs.

5.3.2 Orientation

A plot of birefringence orientation when viewed from MD direction is shown in Figure 5.32. The birefringence orientation index decreased with increase in BR and then remained almost constant at higher BRs. It means that there is more orientation along the TD direction which is the direction of BR.

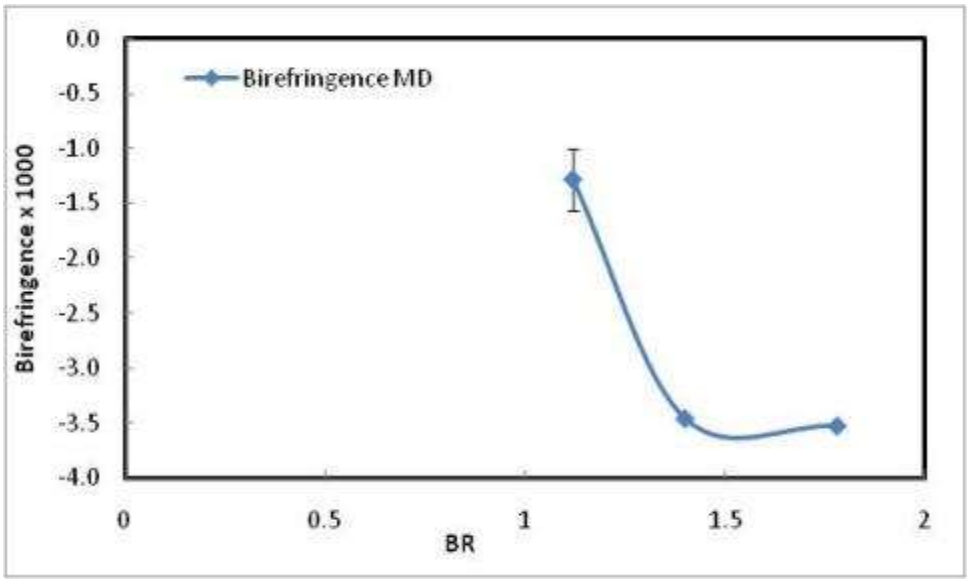

Figure 5.32. Birefringence at different BRs.

5.3.3 Tensile Test

The profile of stress strain plots of h-LLDPE at different BRs in MD is shown in Figure 5.33. The tensile strength, yield stress, ductility and toughness in MD direction of h-LLDPE processed at different BR are shown in Figure 5.34-Figure 5.37.

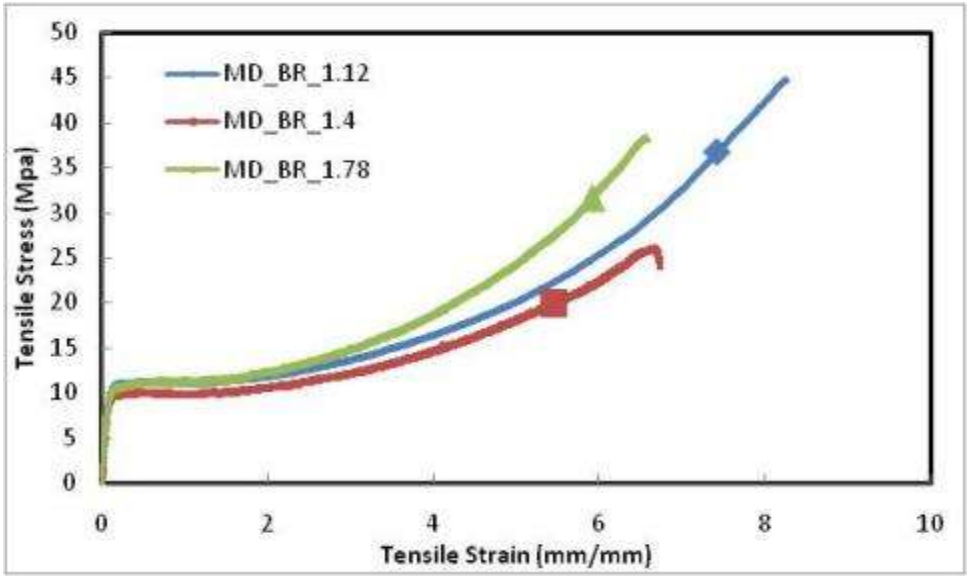

Figure 5.33. MD tensile stress-strain curves for different BRs.

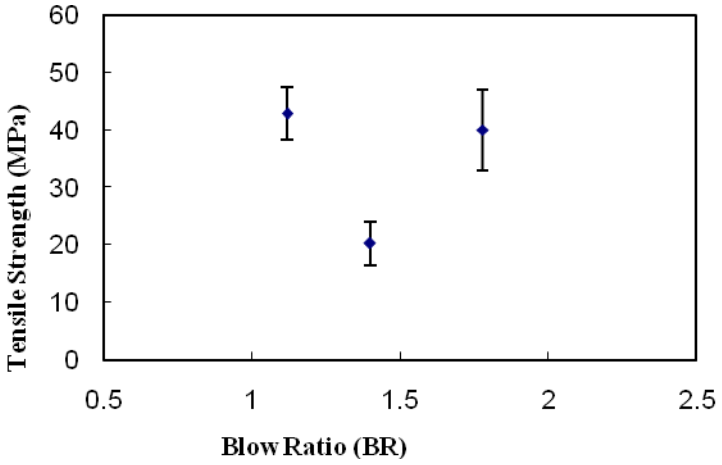

Figure 5.34. MD tensile strength of h-LLDPE at different BRs.

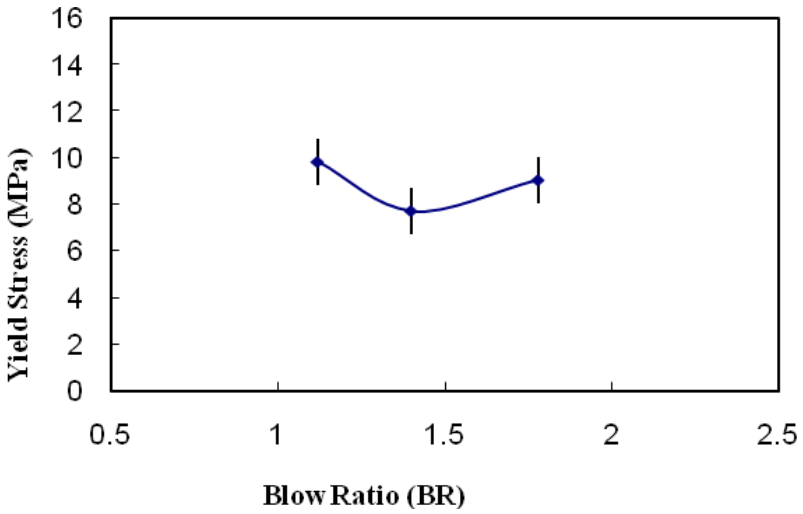

Figure 5.35. MD yield stress of h-LLDPE at different BRs.

The percentage ductility (elongation at break) in TD decreases with increase in BR as shown in Figure 5.41. Similar results were reported by M. Nouri et al. [31]. This may be due the increase in chain orientation for TD direction with increase in BR as shown in Figure 5.32.

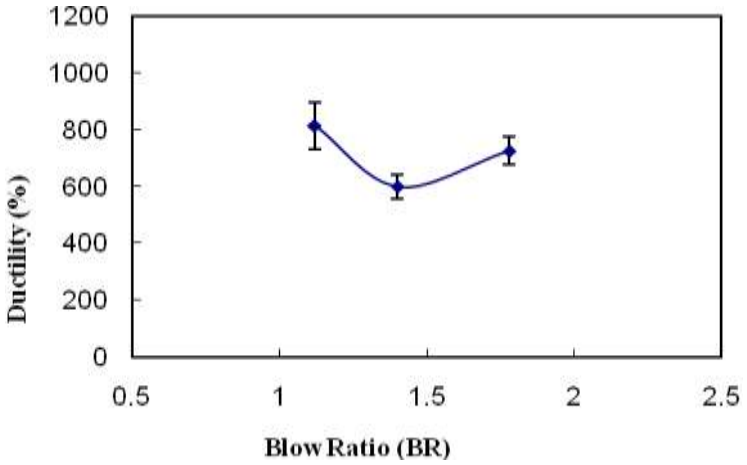

Figure 5.36. MD ductility of h-LLDPE at different BRs.

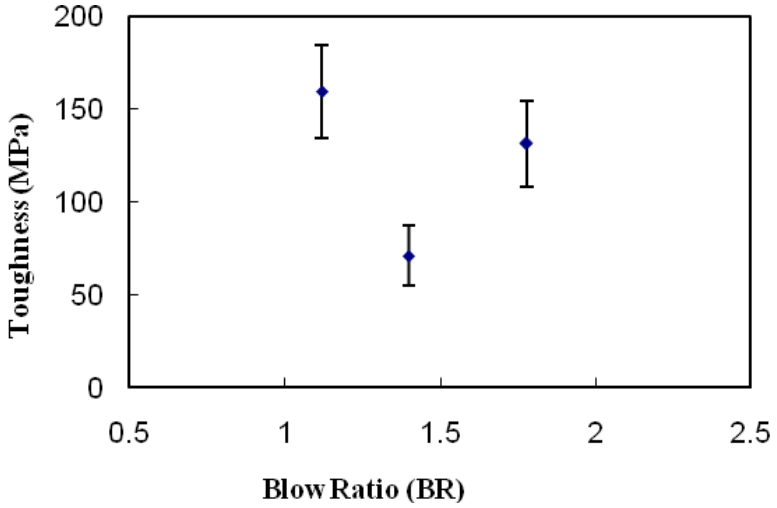

Figure 5.37. MD toughness of h-LLDPE at different BRs.

The profile of stress strain plots of h-LLDPE at different BRs in TD are shown in Figure 5.38. The tensile strength, yield stress, ductility and toughness in TD direction of h-LLDPE processed at different BR are shown in Figure 5.39-Figure 5.42. All of these properties decrease with increase in BR.

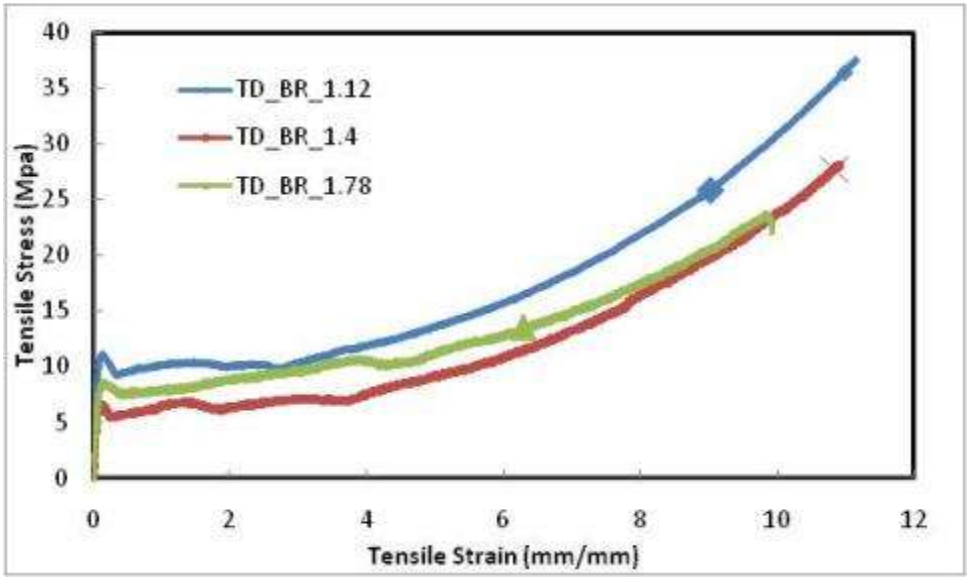

Figure 5.38. TD tensile stress-strain curves for different BRs.

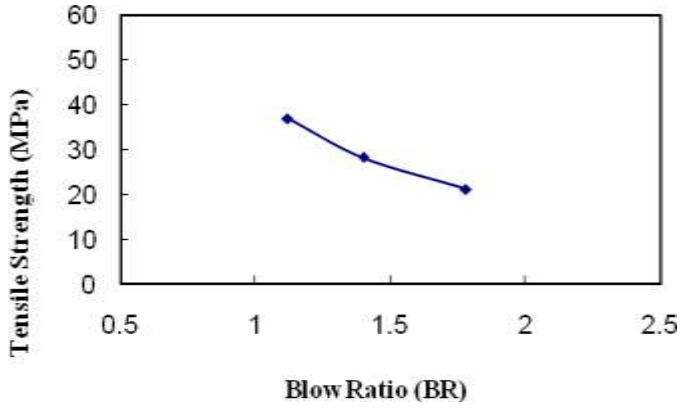

Figure 5.39. TD tensile strength of h-LLDPE at different BRs.

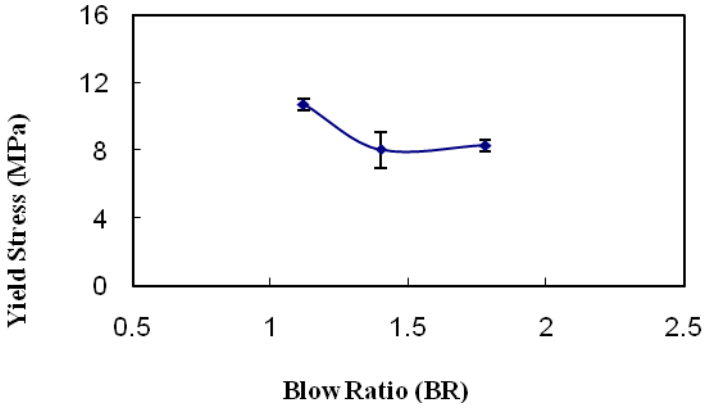

Figure 5.40. TD yield stress of h-LLDPE at different BRs.

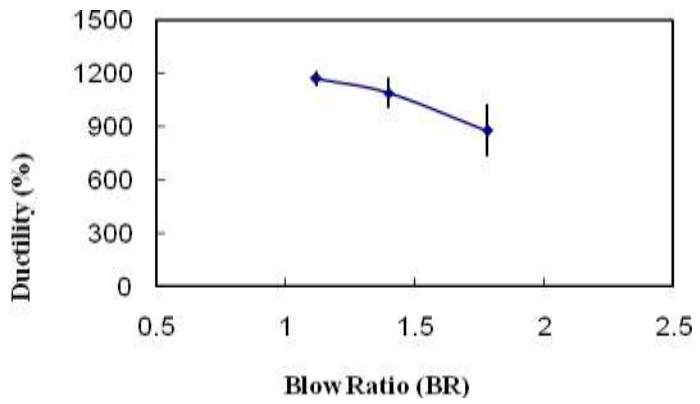

Figure 5.41. TD ductility of h-LLDPE at different BRs.

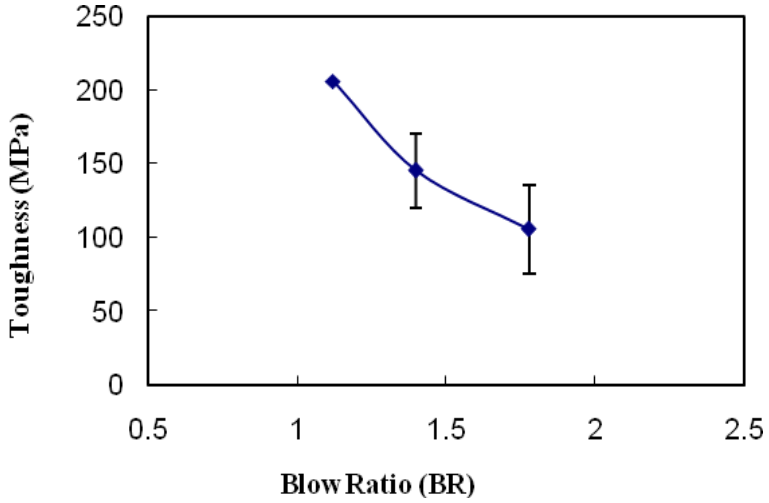

Figure 5.42. TD toughness of h-LLDPE at different BRs.

5.3.4 Dart Impact Test

The force deformation diagrams for different BRs are shown in Figure 5.43. The force deformation diagrams reveal that the curve has significantly wide plateau region after the peak indicating that the material is very tough. The normalized peak force, peak energy and the failure energy displayed a similar trend with increase in BR as shown in Figure 5.44-Figure 5.45 and Figure 5.48. The average impact failure energy values are slightly

higher at BR=1.4 and they seem to be constant at the different BR values studied. The failure deformation decreases with increase in BR as shown in Figure 5.47 thus indicating that the film should have lesser toughness as the plateau region is decreased. However there is an increase in failure force with increase in BR as shown in Figure 5.46 and this compensates for the lost energy due to shorter plateau to give an equivalent failure energy. The increase in failure force and decrease in failure deformation or in other words the plateau region would result in a less ductile film. Thus we would use a BR value between 1.4 to 1.78 as it would give us relatively higher toughness as well as the ductility. The average BR value of 1.6 would be selected to produce wider films with relatively better mechanical properties at a DR of 21. This would also eliminate the risk of working at extreme BR values, which otherwise would make the stable bubble more susceptible to instability. Also, this value would be closer to the BR value usually used in the industry.

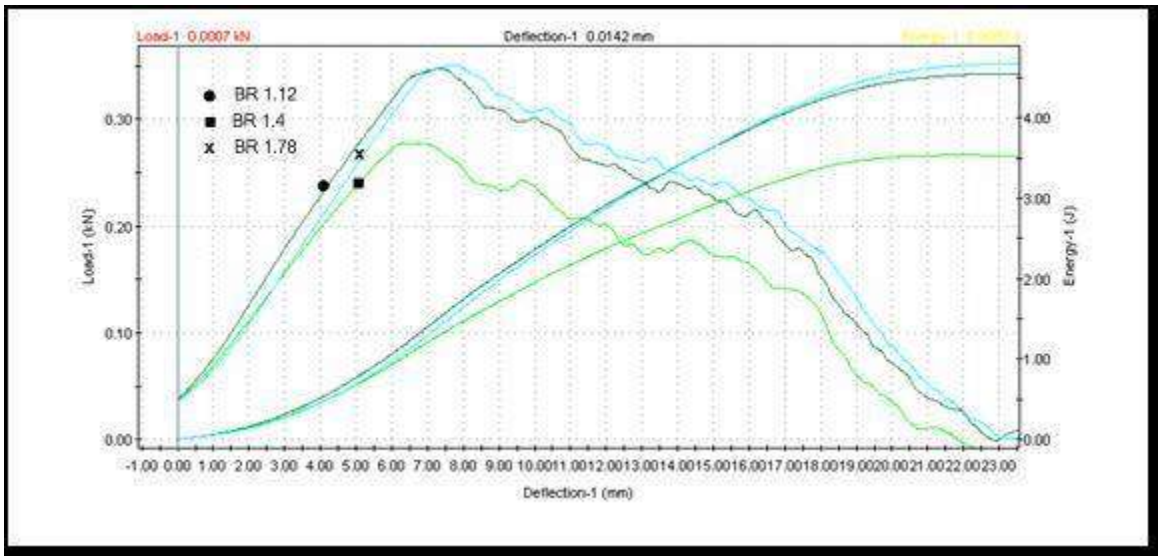

Figure 5.43. Force deformation plots of h-LLDPE at different BRs

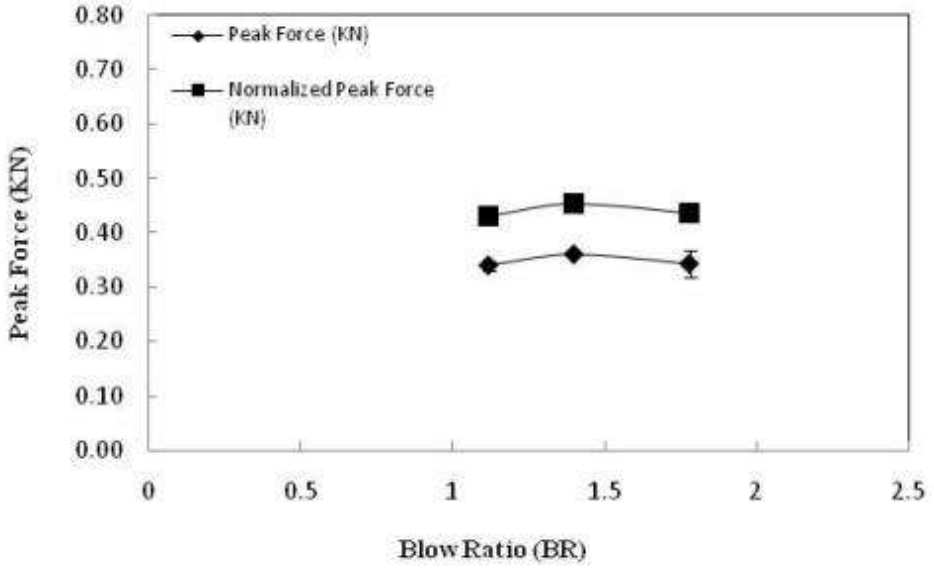

Figure 5.44 Peak Force at different Blow Ratios (BR)

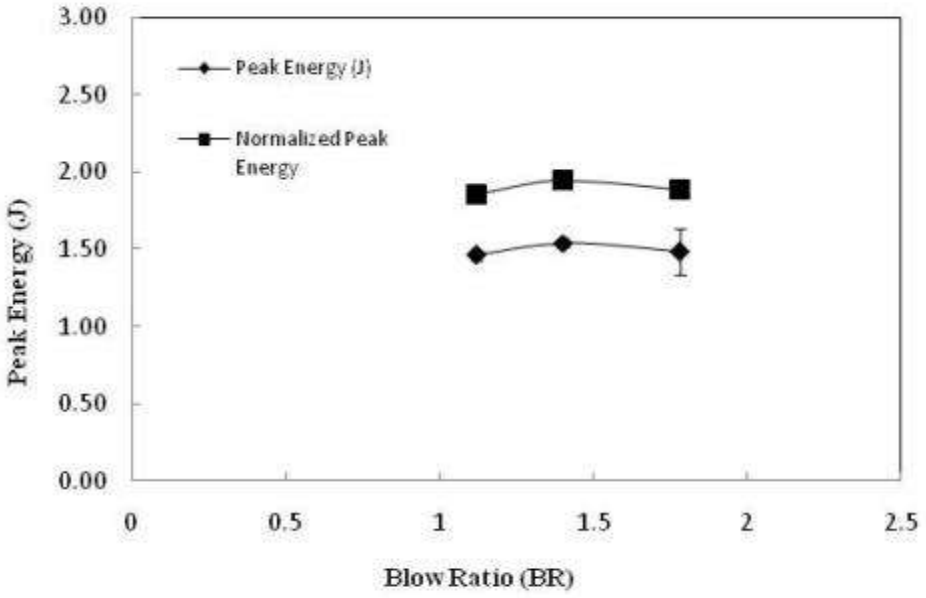

Figure 5.45 Peak Energy at different Blow Ratios (BR)

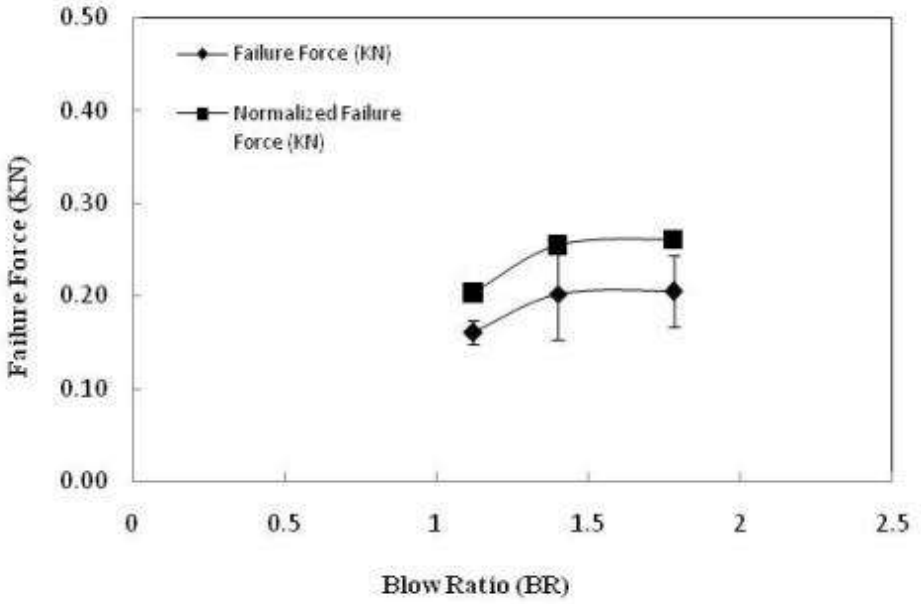

Figure 5.46 Failure Force at different Blow Ratios (BR)

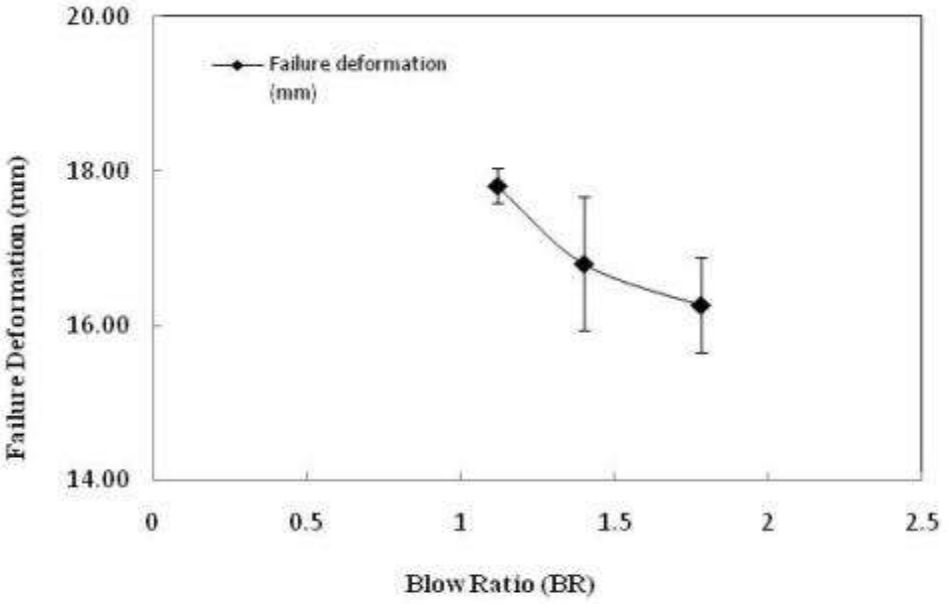

Figure 5.47 Failure Deformation at different Blow Ratios (BR)

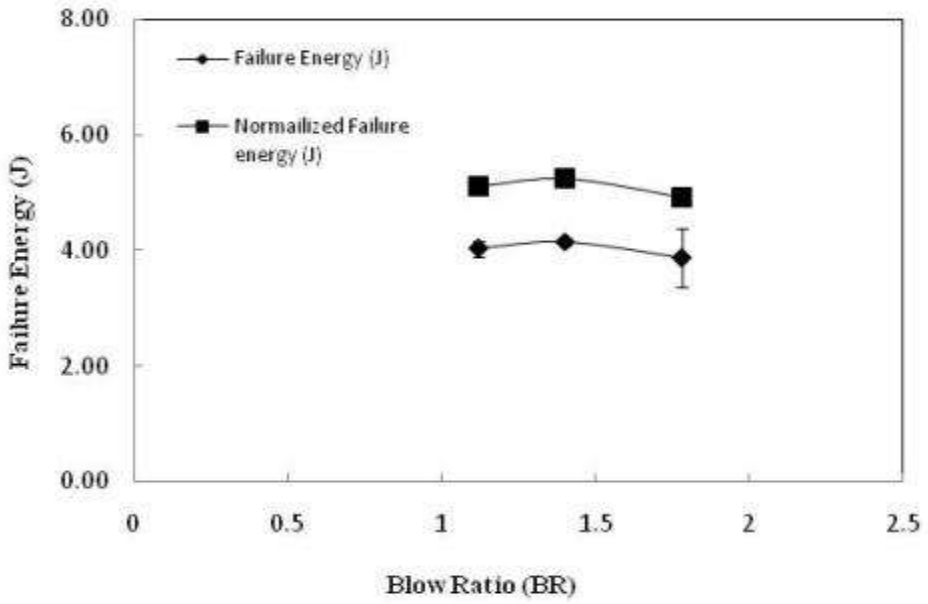

Figure 5.48 Failure Energy at different Blow Ratios (BR)

5.3.5 Elmendorf Tear Test

The MD Elmendorf tear resistance was observed to decrease with increase in BR as shown in Figure 5.49. The MD tear resistance trend correlate well with the birefringence results as shown in Figure 5.32. Both of these properties decrease with increase in BR. The TD Elmendorf tear resistance was observed to increase with increase in BR upto a BR of 1.4 and then decreased with increase in BR as shown in Figure 5.50. These results of TD tear resistance have an inverse relationship with the amount of crystalline content at these BRs.

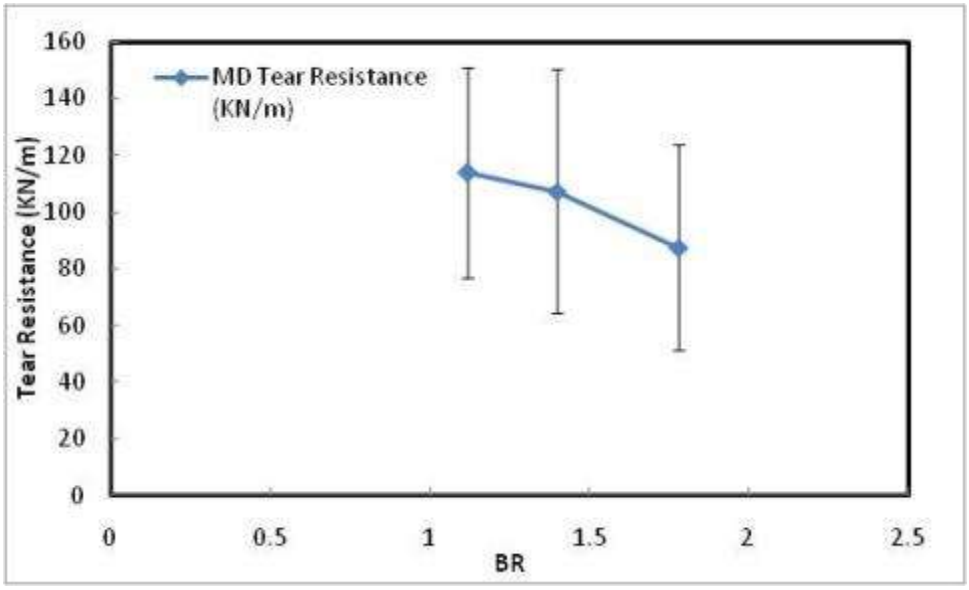

Figure 5.49. MD tear resistance of h-LLDPE at different BRs.

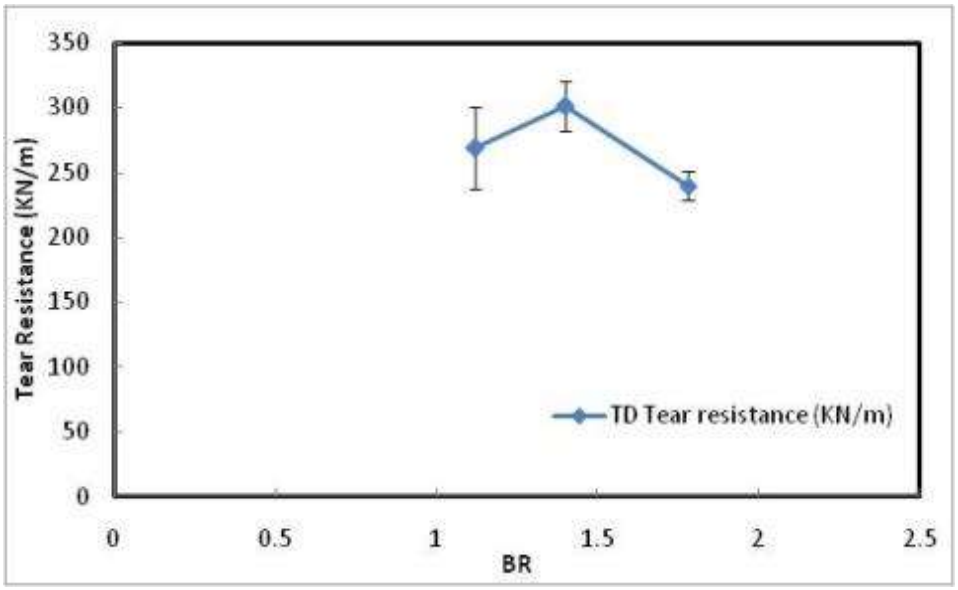

Figure 5.50. TD tear resistance of h-LLDPE at different BRs.

The effect of BR has been carried out on our laboratory instrument and it was limited to a BR range of 1.12 to 1.78. A BR of 2 to 2.5 is usually used in the industry and in some extreme cases it can be as high as 4. The material quality does not deteriorate for the reasonable BR range of 1.12 to 1.78, as it was observed that beyond a BR of 1.78 the bubble ruptures. This BR of 1.78 is limited due to the melt flow rate, and which in turn is dictated by the torque and the material characteristics. Therefore a BR 1.78 was found to be the maximum limit. The BR of 1.78, being at the extreme end, was not considered as it is more susceptible to rupture. Thus, based on the results of impact failure energy a value between 1.4 to 1.78 could be considered for carrying out mechanical tests and blending.

It can be summarized from tensile test results that the MD properties increase with an increase in BR from 1.4 to 1.78 and most of the TD tensile properties decrease with an increase in BR from 1.4 to 1.78. The Elmendorf tear properties in both MD and TD direction seem to decrease with an increase in BR from 1.4 to 1.78. Thus, it is not appropriate to select the BR from the above two results obtained in two individual directions MD and TD. It can be noted here that the impact test results take into consideration the cumulative effect of MD and TD directions. Hence, the impact resistance of the film was selected as the criteria for the selection of optimum BR.

The impact energy was observed to be highest for the BR value lying in the range of 1.4 to 1.78. As BR value of 1.78 is at the extreme end and when selected could lead to fluctuations and rupture of the bubble upon blending. For BR value of 1.4, though it has a higher impact energy values but is away from the BR value generally used in industry. Thus an average BR value of 1.6 was selected as the optimum BR. Therefore, we fix the

BR variable to a value around 1.6 to obtain the optimum results. The next step is to select a suitable blend ratio.

5.4 Effect of Blend Ratio (h-LDPE/LDPE) on the Thermal and Mechanical Properties of h-LLDPE and LDPE Blended Blown Films

The processing variables such as the die temperature, DR, BR, mass flow rate and extrusion temperature profile were now to be kept constant and the effect of blend ratio is to be studied. The die temperature with maximum operating window for h-LLDPE was set to 230 °C with a DR of 21 and a BR of 1.6. A constant mass flow rate of around 8 g/min was maintained for the blends by controlling the feed rate of the two different materials. Pure h-LLDPE material was processed and then small percentages of LDPE were added to it. Pure LDPE was also processed with the same processing conditions.

5.4.1 Crystallinity

The average percent crystallinity, melting peak temperatures and the end of the melting temperature range of the samples tested at different blend ratios have been listed in Table 5.4. In general, the crystallinity (Figure 5.31), for the first heating cycle containing the processing history almost remained constant with increase in BR. There is slight increase in crystallinity with the increase of blend ratio changing from about 37.9% to around 39%, when the blend has increased from 0 to 50% and then a decrease from 39% to 34% for LDPE material.

Table 5.4 DSC results of h-LLDPE /LDPE blended films

Blend Ratio	1st Heating				
	% Crystallinity	Stdev	Melting Peak °C	Stdev	Endset of Melting °C
Virgin h-LLDPE Pellets	39.09	1.01	127.78	0.76	131.44
0	37.90	0.71	124.29	0.35	129.84
5	37.85	1.42	124.35	0.36	129.02
10	39.37	1.00	123.64	2.78	128.85
15	38.87	0.53	125.74	0.69	129.73
20	39.19	0.89	125.05	1.11	129.51
50	39.11	0.72	121.78	4.35	128.48
100	34.52	2.32	109.01	1.26	113.53
Virgin LDPE Pellets	41.34	0.73	110.60	0.31	115.04

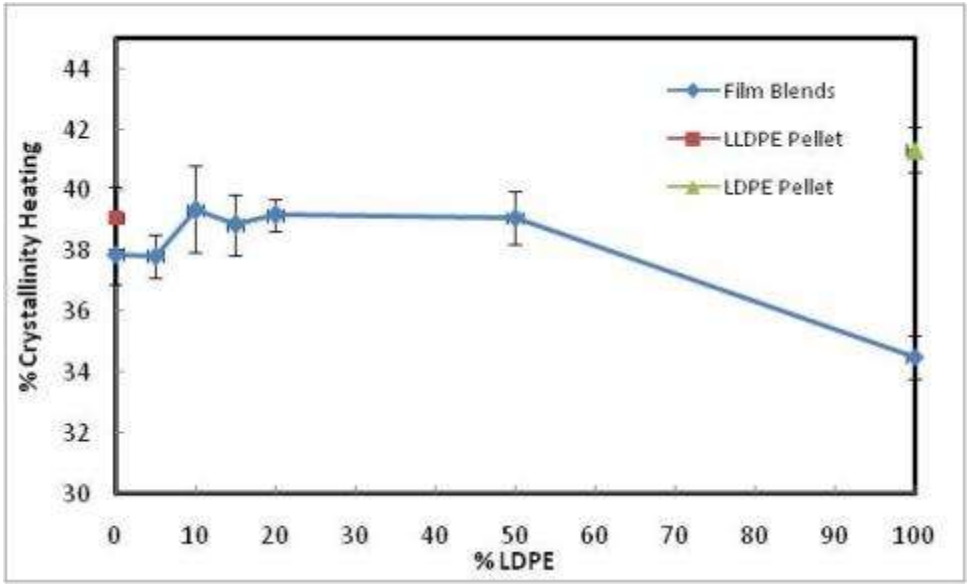

Figure 5.51. Percentage crystallinity of h-LLDPE/LDPE at different Blend ratio.

5.4.2 Orientation

A plot of birefringence orientation when viewed from MD direction is shown in Figure 5.52. There is an increase from $-3x10^{-3}$ to $5x10^{-3}$ when the blend ratio increases from 0 to 50%, and then the birefringence decreases to $3x10^{-3}$ for the pure LDPE. The birefringence index increased with an increase in blend ratio upto 50-50% and then decreased with an increase in blend ratio.

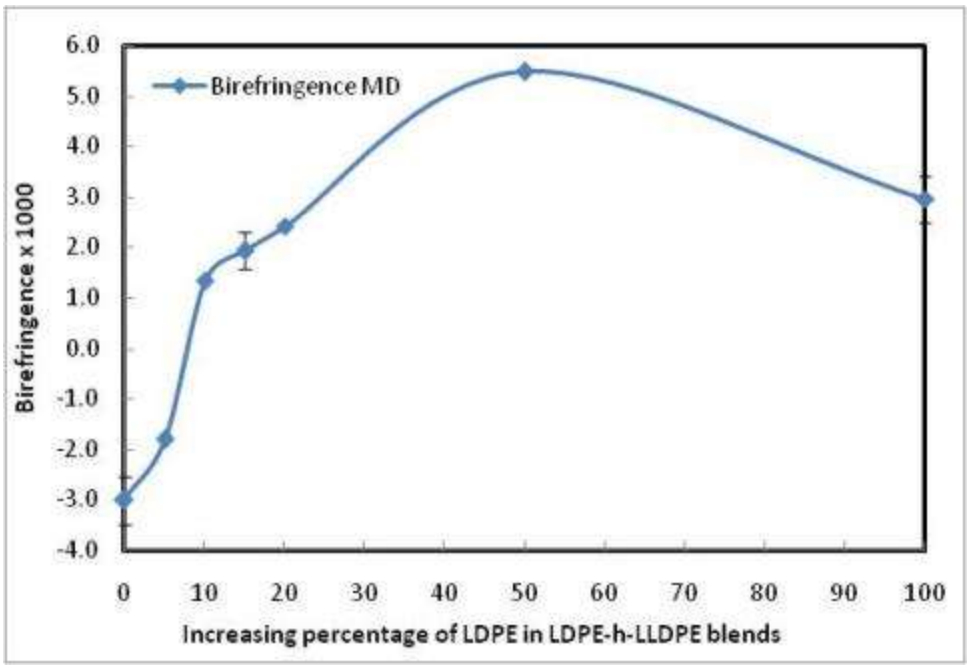

Figure 5.52. Birefringence at different Blend ratios.

5.4.3 Tensile Test

The profile of stress strain plots of h-LLDPE / LDPE films at different blend ratios in MD are shown in Figure 5.53. As shown in Figure 5.13 and Figure 5.18 the MD and TD tensile strength of h-LLDPE /LDPE blends decreases with increase in LDPE content. However some synergistical effects are seen at very low percentage of blends. The yield strength of the film blends of h-LLDPE with LDPE increases with the addition of LDPE upto the blends with 10% to 20% LDPE and then later decreases. That is around 20% enhancement in the yield strength of the film in MD for the low ratio blends in MD direction. There is not much loss of ductility in MD direction for the low blend ratios. Ductility of h-LLDPE is four times higher than that of LDPE. The addition of LDPE upto 80-20% blend ratio did not have any decrement in the ductility. This is of great

importance as the processability is improved with the addition of LDPE (in terms of reduction in torque) and without losing its tensile properties.

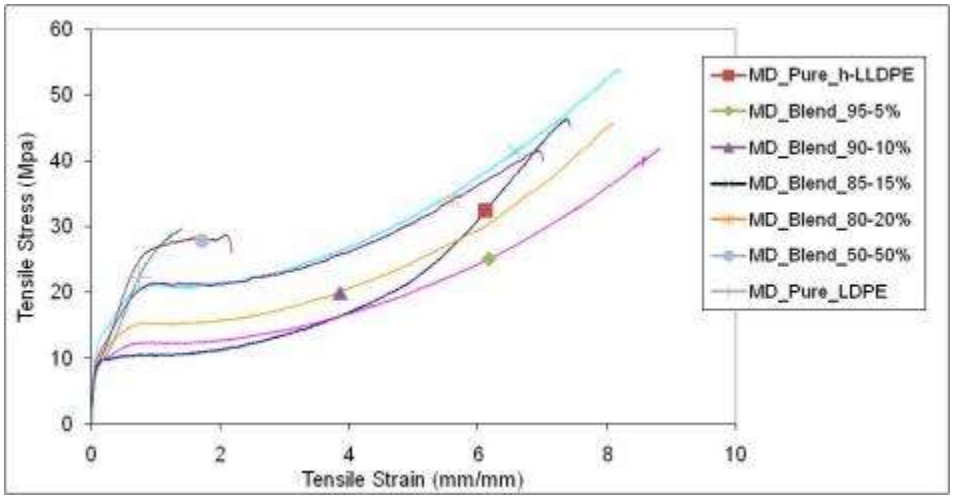

Figure 5.53. MD tensile stress-strain plots of different h-LLDPE /LDPE blends.

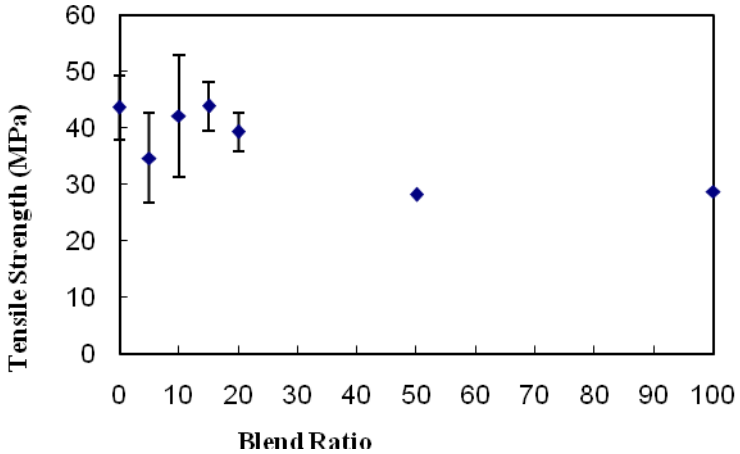

Figure 5.54. MD tensile strength of h-LLDPE /LDPE blends.

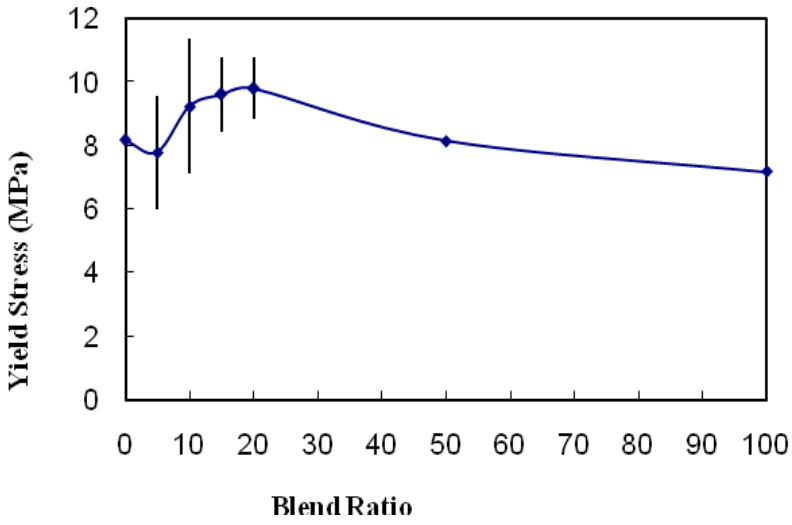

Figure 5.55. MD yield stress of h-LLDPE /LDPE blends.

The MD percentage ductility (elongation at break) almost remains constant up to 15% LDPE and then decreases non-linearly with increase in LDPE content as shown in

Figure 5.56. M. Nouri et al [31] from their study with 25%, 50% and 75% LDPE content reported that the percentage ductility in the MD direction decreased with increase in LDPE content. In the present study there is not much change in the ductility up to addition of 20% LDPE content. The percentage ductility is higher at higher percentages of h-LLDPE since h-LLDPE with relatively linear molecules has much more unfailing entanglements during elongation process. The tests for 80-20% and 50-50% blend ratio were repeated with emery paper padding and the results obtained were observed to be the same. The area of clamping also remained constant before and after the test, indicating that there was no slipping during the tests. The MD toughness for pure h-LLDPE is 140 MPa and for pure LDPE it is around 30 MPa. With small addition of LDPE content upto 80-20 % of blend ratio, the toughness increased to a value of 200 MPa. Thus there is

approximately 43% increment in MD toughness with the addition of LDPE in small quantity.

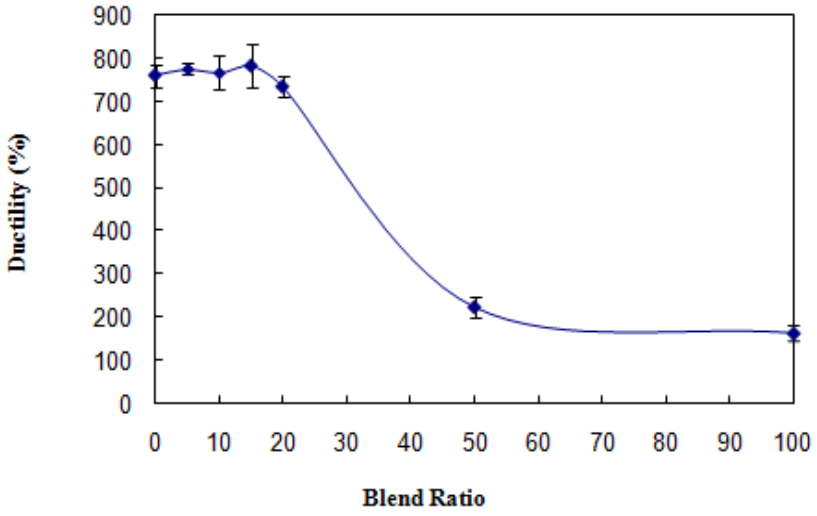

Figure 5.56. MD ductility of h-LLDPE /LDPE blends.

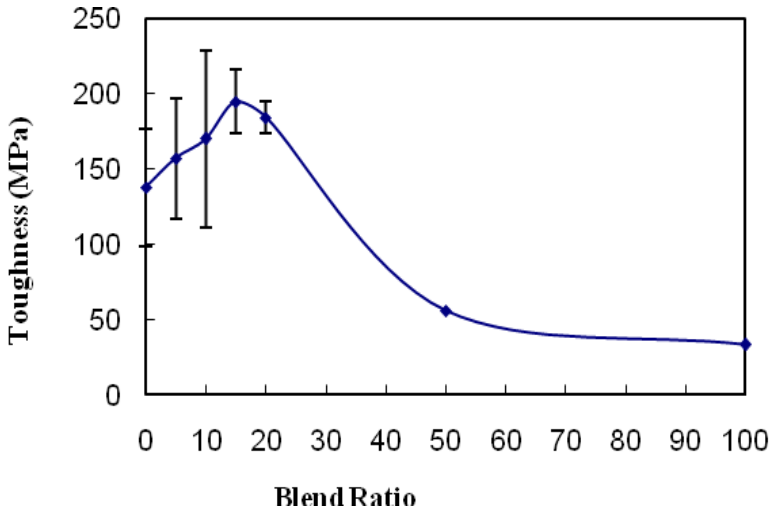

Figure 5.57. MD toughness of h-LLDPE /LDPE blends.

The profile of stress strain plots of h-LLDPE / LDPE films at different Blend ratios in TD are shown in Figure 5.58. The TD tensile strength increased more than 75% with addition of LDPE in 90-10 % of blend ratio. In TD direction the ductility of the blend increased by 30% when compared to pure h-LLDPE just by small addition of LDPE. The ductility is not reduced by the addition of LDPE content. As also shown in the orientation, this might be due to the alignment of molecules during the tension process. With blend ratio up to 50%, the toughness in the TD direction has shown small increase in its properties.

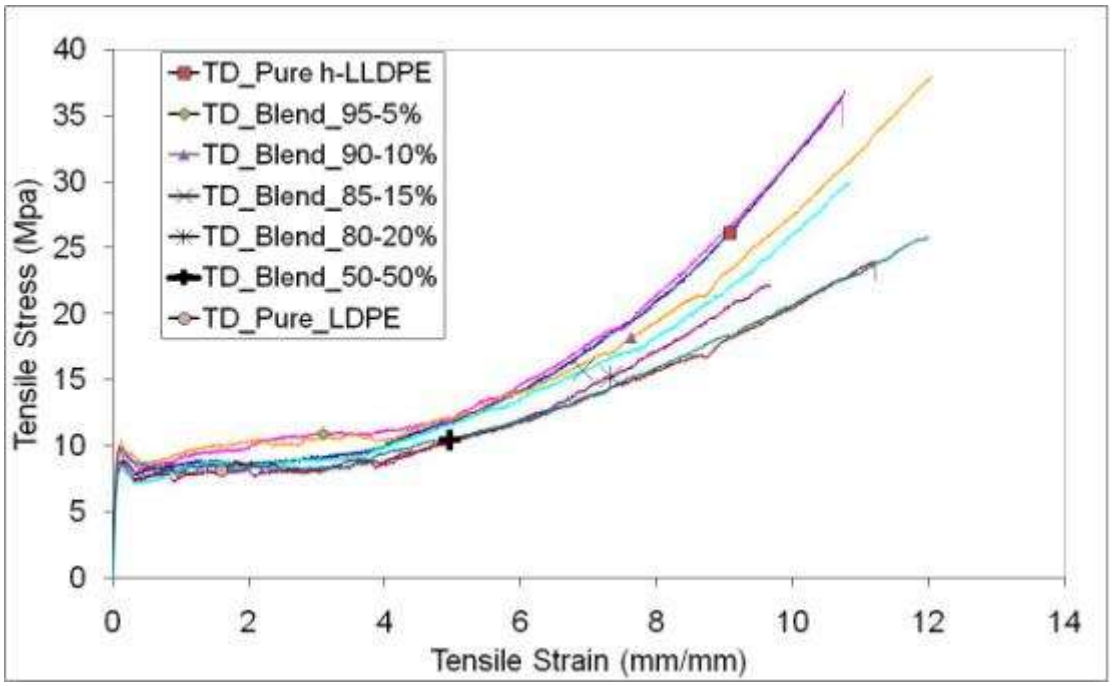

Figure 5.58. TD tensile stress-strain plots of different h-LLDPE /LDPE blends

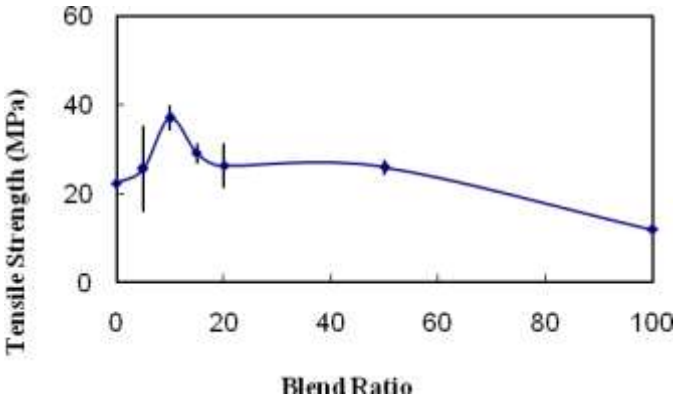

Figure 5.59. TD tensile strength of h-LLDPE /LDPE blends.

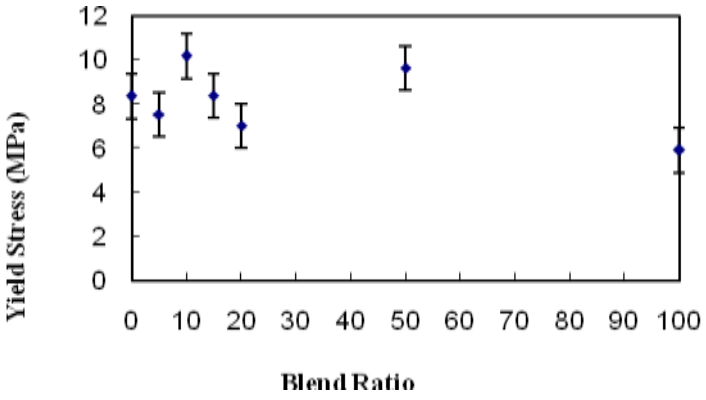

Figure 5.60. TD yield stress of h-LLDPE /LDPE blends.

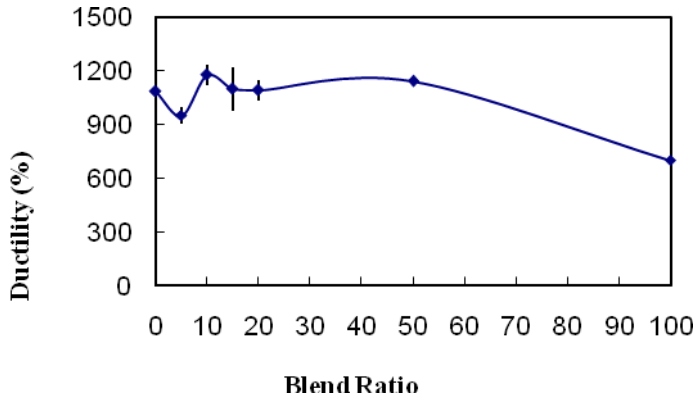

Figure 5.61. TD ductility of h-LLDPE/LDPE blends.

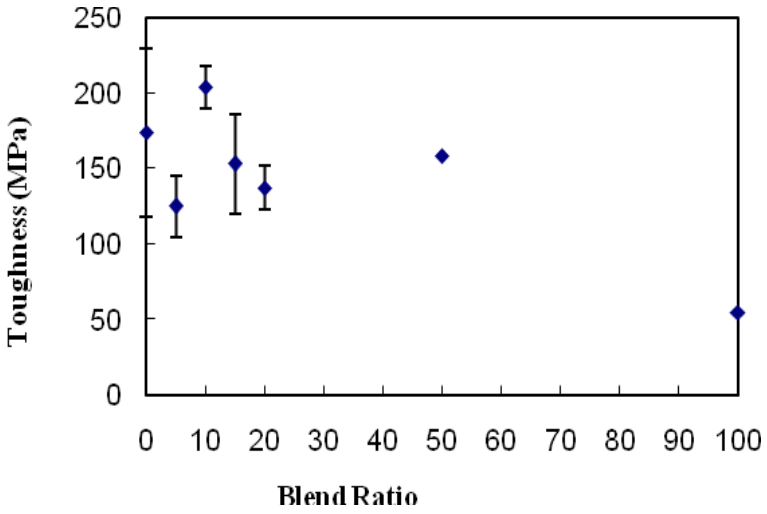

Figure 5.62. TD toughness of h-LLDPE/LDPE blends.

5.4.4 Dart Impact Test

The force deformation diagrams for different blend ratios are shown in Figure 5.63. The normalized peak force, peak energy, failure force, failure deformation and failure energy for different blend ratios are shown in Figure 5.64-Figure 5.68. There was around 20% improvement in impact peak force with the addition of LDPE to h-LLDPE. There is some

20% enhancement in impact failure energy due to 5% blend followed by a decrease of about 40% for higher blend ratios. The maximum normalized failure energy was observed at 5% blend ratio. The tear resistance also shows some kind of deterioration in MD direction, but there is a huge improvement for tear resistance in TD direction. It is that the structure in tensile is quite sensitive to the strain rate. The tear is sudden and the other molecules in the film which were not aligned did not offer any resistance nor were getting pulled. Whereas, in tensile the strain rate is slow and the other molecules which were not aligned start to align themselves when pulled and thus offer more resistance. However, in TD tear resistance where most of the structure is oriented perpendicular to MD and the unaligned molecules are now holding to give a higher TD tear resistance.

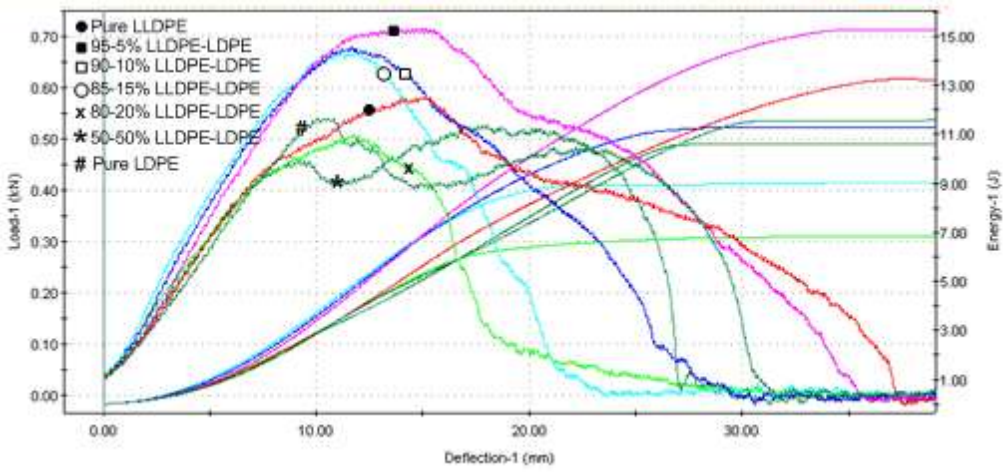

Figure 5.63. Force-deformation diagram at different blend ratios for h-LLDPE /LDPE films

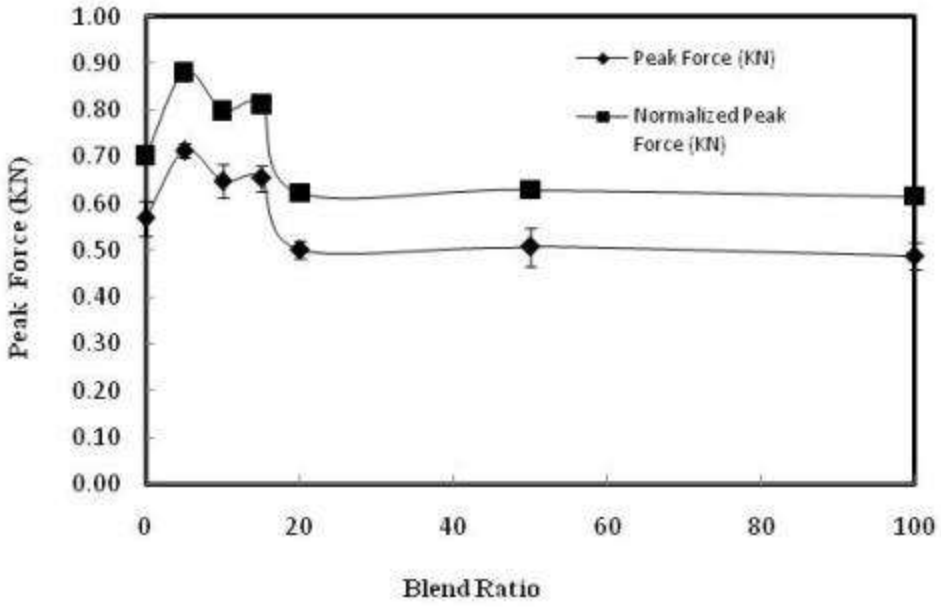

Figure 5.64. Peak Force at different blend ratios.

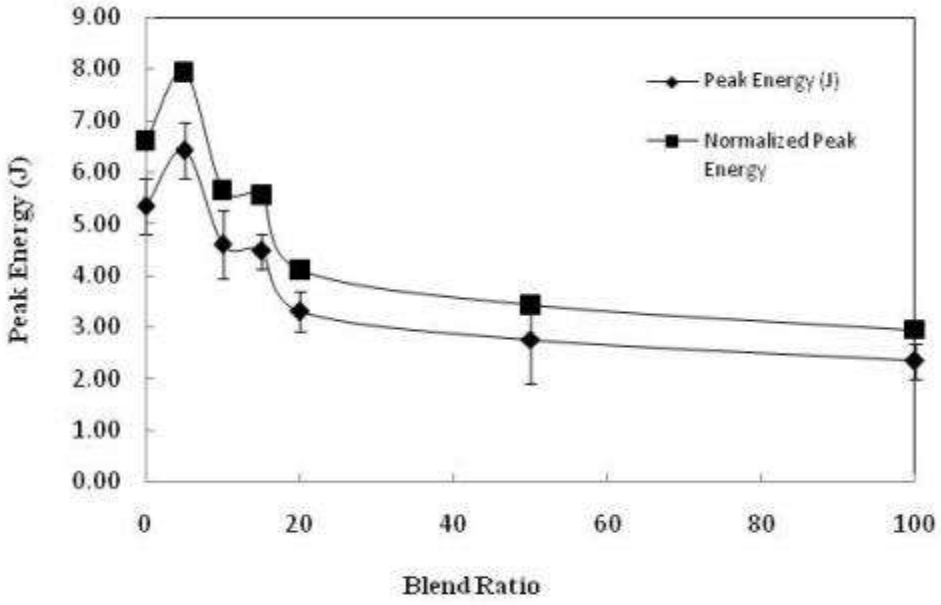

Figure 5.65. Peak Energy at different blend ratios.

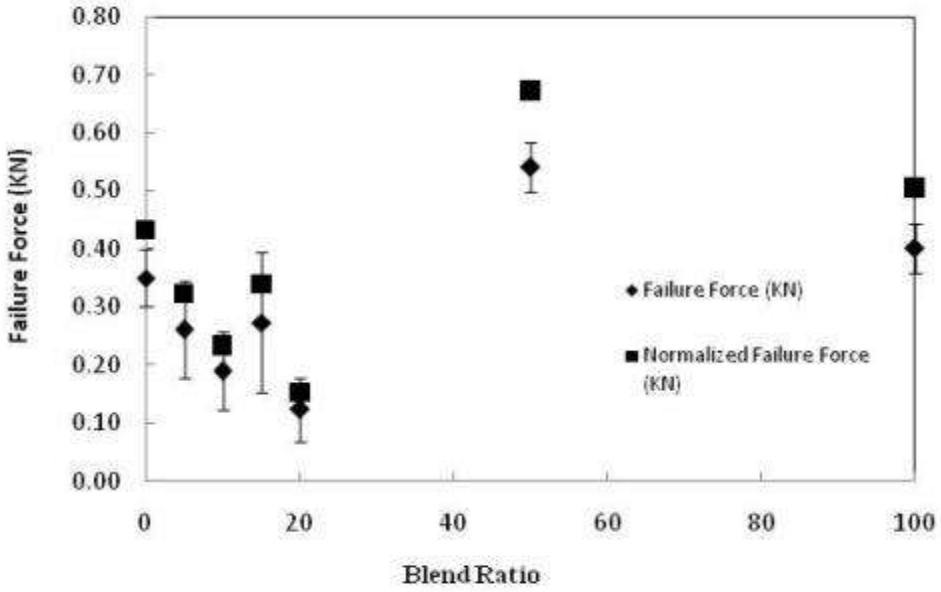

Figure 5.66. Failure Force at different blend ratios.

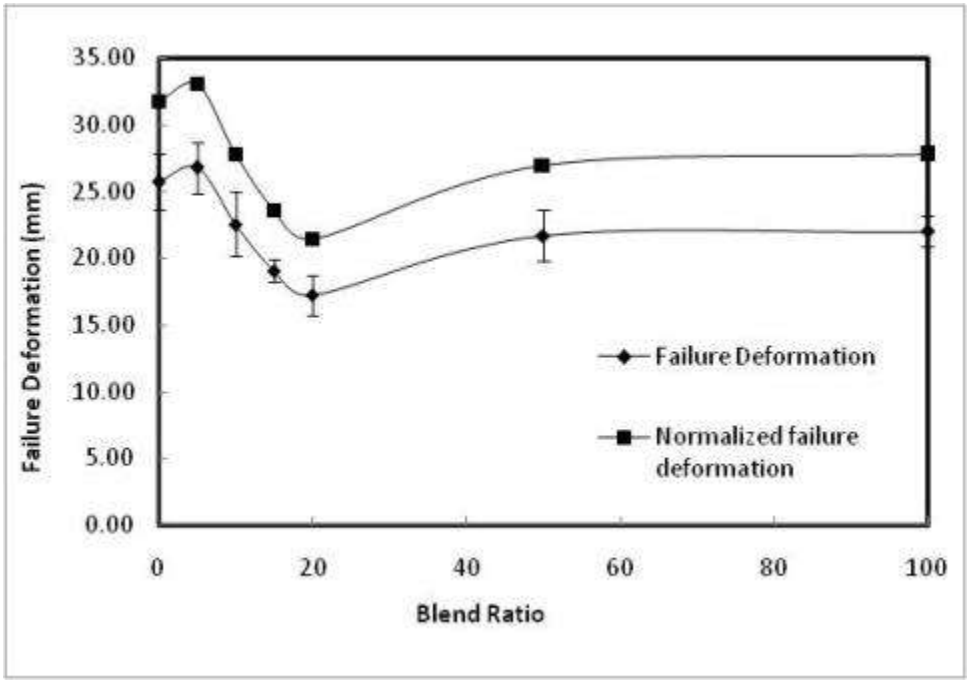

Figure 5.67. Failure Deformation at different blend ratios.

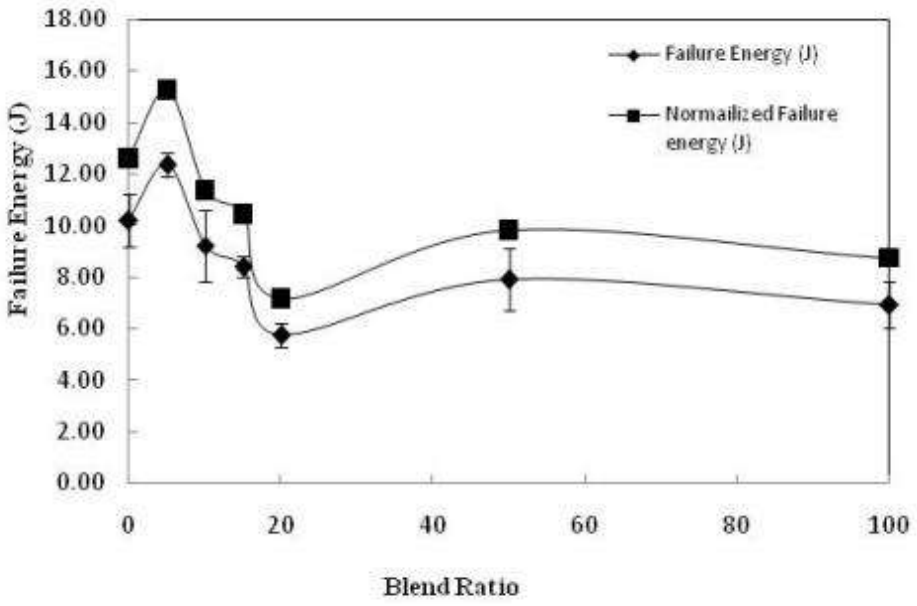

Figure 5.68. Failure Energy at different blend ratios.

5.4.5 Elmendorf Tear Test

The MD Elmendorf tear resistance was observed to decrease with increase in blend ratio up to 80-20% blend and then increased with further increase in blend ratio as shown Figure 5.69. It is observed that as the orientation when viewed from MD direction increases the tear resistance in MD direction decreases. The worst tear resistance in MD direction was observed at 20% LDPE content. The TD Elmendorf tear resistance was observed to increase with increase in blend ratio up to a blend ratio of 80-20% (LLDPE-LDPE) blend and then decreased with further increase in blend ratio as shown in Figure 5.70. This observation is of great importance as the TD tear resistance increases with increase in LDPE blend percentage. There is a difference between MD and TD tear resistance of the two materials. It is observed that the TD tear resistance for pure h-

LLDPE is almost twice that of MD tear resistance. On the contrary, LDPE is having a reverse trend where the TD tear resistance is almost three times lower when compared to MD tear resistance. There are two different structure development processes for the individual materials and this controversy shows in the structure development of the blends. In both cases, it has deviated from the linearity rule. It shows that the TD direction tear resistance has improved with an increase in blend ratio. It almost doubled from 200KN/m to 400 KN/m, whereas in the MD direction the tear resistance has been reduced to relatively low values. According to the tear resistance properties, the blend has modified the structure-morphology of the material as it is obvious from the tear results. On one hand it has improved the TD direction properties and on the other deteriorated the MD direction properties. It has played a big role in modifying the structure development and orientation in the material which has to be supported by the morphological study. However, this has been already mentioned earlier that this is beyond the scope of this study. The pure LDPE film has lower TD tear resistance when compared to pure h-LLDPE. There are two competing factors here, at first; we have the blends of the polymer and their properties to be incorporated. The second, we have the molecular orientation during the process which can be due to the alignment of the molecules. This can be observed on the low blend percentages of h-LLDPE/LDPE. This low blend molecular characteristic is shown in Figure 5.69 for MD direction blends upto 20%. However, in Figure 5.52, we have seen that the increase in blend percentage leads to increase in orientation, whereas, in this case, the MD tear resistance decreased lower than LLDPE and which can be attributed to the material properties being significantly incorporated. Therefore, it observed that the TD tear resistance improved by almost 100% by addition

of LDPE for the low blend percentages up to 80-20% blend ratio. Zhang et al [32] from their studies have associated the difference in tear resistance of the two individual materials with the crystalline lamellar structure formed in the film blowing process. The relationship between structure and tear anisotropy in the LDPE film was attributed to the twisted lamellae from the adjacent row nuclei being strongly connected, resulting in an interlocking lamellae structure. For LLDPE films a relatively balanced tear resistance was observed from their study, due to the involvement of less oriented structure. The local preferential orientation of lamellae along TD tear resistance was greater than MD tear resistance for LLDPE.

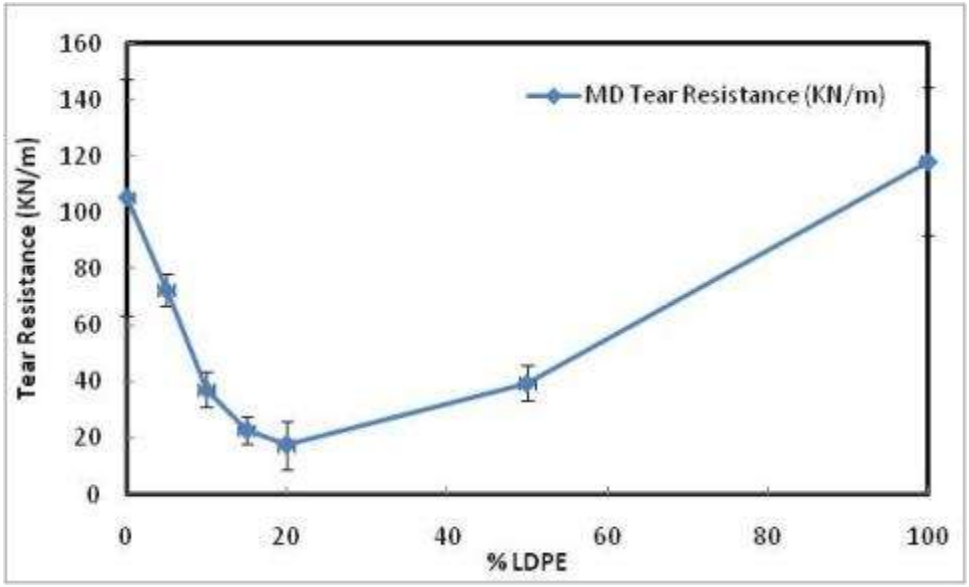

Figure 5.69. MD tear resistance of h-LLDPE/LDPE blends.

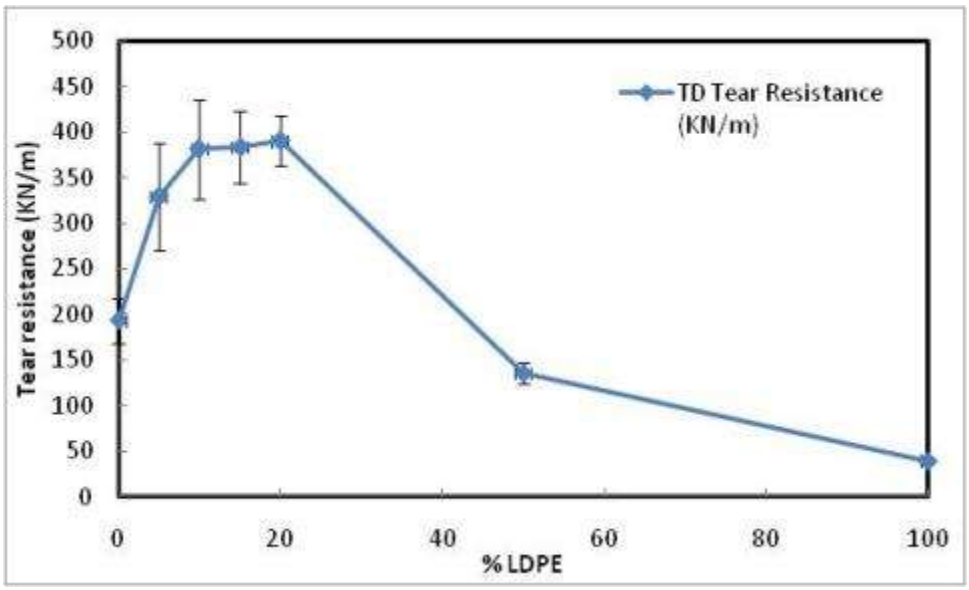

Figure 5.70. TD tear resistance of h-LLDPE /LDPE blends.

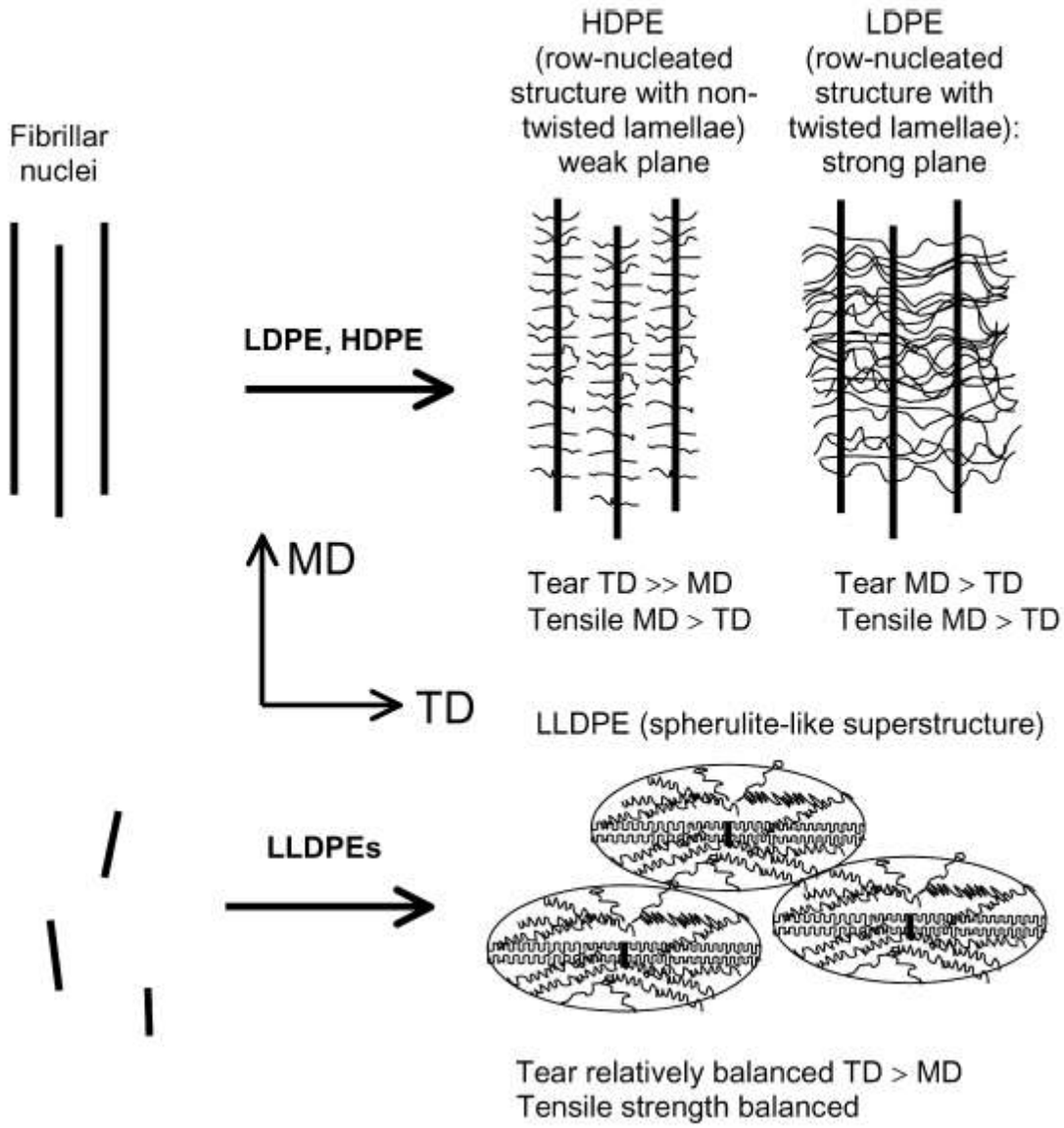

Figure 5.71. Schematic of morphological developments and structure-tear resistance relationship for LDPE, LLDPE and HDPE [32].

5.5 Effect of Blending on the Processability of the Process

In general, the processability of the process was increased with the addition of LDPE to the h-LLDPE as the torque required to turn the screw decreased with an increase in the LDPE blend percentage as shown in Figure 5.72. The processability of the processes was measured in terms of the torque required to turn the extruder screw. Thus this way the mechanical properties of h-LLDPE are further enhanced by addition of small percentages

of LDPE with a lower torque requirement except for the 5% LDPE blend, which resulted in a slightly higher torque. This implies that the h-LLDPE / LDPE blend produces a film of better mechanical properties with a lower production cost. With addition of up to 20% LDPE blend, many mechanical properties improved. There is no fixed blend percentage where all the mechanical properties increase simultaneously. For blend ratios in the range of 5%-20% of LDPE, it was observed that the optimum mechanical properties such as tensile, tear and impact strength properties of the film increased. An individual increase in performance at 15% LDPE in MD tensile strength as observed from Figure 5.54. Optimum TD tensile strength was observed for 10% LDPE as shown in Figure 5.59. An optimum impact test result was obtained by addition of 5% LDPE as shown in Figure 5.65 and Figure 5.68. An optimum MD tear property was obtained by addition of 5% LDPE as shown in Figure 5.69. An optimum TD tear resistance was obtained by addition of 5% LDPE as shown in Figure 5.70. Wong et al. [1] have reported that the energy consumption for extrusion of LLDPE is much higher than that of LDPE and this has been correlated to the presence of long chain branches. In conclusion, the material with long chain branches has lower energy consumption when compared to the one without it, and a relationship has been established for the energy requirement for blends of these two materials.

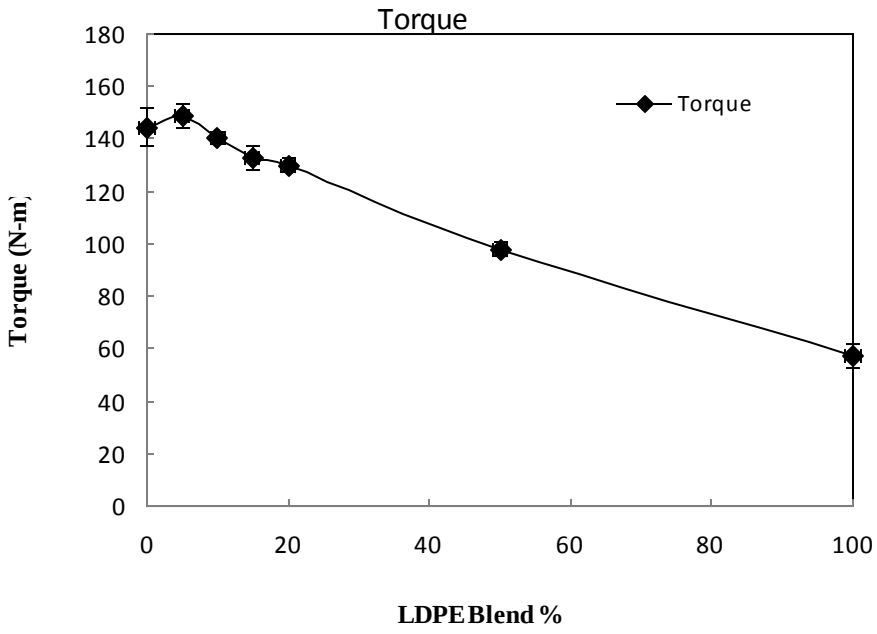

Figure 5.72. Torque required in turning the extruder screw against increasing blend percentage.

CHAPTER 6

CONCLUSION

6.1 Preliminary Studies

During the preliminary studies a temperature profile of 120/150/180/200/200/200/200 °C was maintained in the seven successive zones of the extruder. This temperature profile was used considering the instrument limitations and to avoid degradation of the material. An extruder screw speed of 12 rpm was used and a constant pressure of 14 to 16 bar was maintained at the extruder die exit. This was the maximum screw speed which could be achieved with h-LLDPE, anything beyond this value led to the automatic shutting off of the machine because of an increase in the torque required to turn the screw. The melt pump speed was set to a constant feeding rate of 10 rpm at 210 °C to pump the material to the film blowing die. The maximum melt flow rate at these feed rates was around 8 g/min. The bubble stability window for h-LLDPE and LDPE was evaluated by varying the BR and DR while keeping the mass flow rate and the extruder temperature profile constant. The die temperature was varied from 210 °C to 270 °C and its effect on the operating window of h-LLDPE and LDPE polymer was determined. It can be concluded from the study of effect of die temperature on the processability that the operating window is the largest for h-LLDPE at a die temperature of 230 °C.

6.2 Blend Effect

The process parameters such as the melt flow rate, die temperature, DR, and BR were fixed to their optimum values of 8 g/min, 230 °C, 21, and 1.6 respectively. Pure h-LLDPE, LDPE and their blends (5%, 10%, 15%, 20% and 50%) were processed at the above constant processing conditions and the effect of blending was studied on the thermal and mechanical properties of the films. The crystallinity for different blends was determined using DSC. In general, there was not much change in the cystallinity percentage up to 50% of the blends, and later decreased for LDPE material. The birefringence of the blends has been studied using an optical microscope and an index of orientation has been reported. There is an increase from $-3x10^{-3}$ to $5x10^{-3}$ when the blend ratio increases from 0 to 50%, and then the birefringence decreases to $3x10^{-3}$ for the pure LDPE. Mechanical tests such as tensile, impact and Elmendorf tear test were also conducted on the blended films processed at constant die temperatures, DRs and BRs. The tensile and tear tests were conducted in both MD (machine) and TD (transverse) directions for the blended films. With addition of up to 20% LDPE blend, many mechanical properties improved. There was a 20% enhancement in MD yield strength by small addition of LDPE without any decrement in the MD ductility. The MD toughness also observed an increment of around 43% in its properties with this small addition of LDPE. Thus indicating that small amount of LDPE content could enhance the toughness in MD. The enhancement in TD tensile strength was more than 75% for blend ratio of 90-10% h-LLDPE/LDPE. The TD ductility improved slightly in comparison to pure h-LLDPE. With blend ratio up to 50%, the toughness in the TD direction has shown small increase in the properties. There is some 20% enhancement in failure energy due to 5%

blend followed by a decrease of about 40% for higher blend ratios. The tear resistance also shows some kind of decrease in MD direction, but there is a huge improvement for tear resistance in TD direction. The TD tear resistance improved by almost 100% by addition of LDPE for the low blend percentages upto 80-20% blend ratio. With addition of up to 20% LDPE blend content, many mechanical properties improved. This is of great importance as the processability was improved with the addition of LDPE. As the processability increases there was a reduction (around 15%) in the torque required to process the material. With this decrement in torque requirement the power consumption would also decrease. Thus, by blending with small percentages of LDPE the productivity increases without any deterioration in the quality, rather it helps in improving the quality in many cases. The normalized peak force values during impact tests were also observed to be higher when compared to the pure h-LLDPE and LDPE. The normalized MD tear resistance was observed to decrease at low blend percentages whereas it increased for normalized TD tear resistance.

The die temperature was kept constant at 230 °C and the DR was varied by changing the take up speed. The samples at different DRs (7 to 86) were then tested on the instrumented impact tester. It can be concluded from the study of DR that the DR 21 resulted in higher impact resistance to failure of films, and it was selected as the optimum DR. The BR of 1.6 was selected based on the equipment limitation.

CHAPTER 7

FUTURE WORK

- Future work could be carried out on the morphological structure of the films using rheological instruments.
- The effect of viscosity on the mechanical and structural properties of the films can be studied.
- More insight about the structure development process can be studied using SEM and TEM.
- The effect of various other branch types of LLDPE could be studied by blending them with LDPE.
- Effect of extrusion temperature on the size of the operating window could be studied.

REFERENCE

1 C. M. Wong, Shih H. H. and Huang C. J., *"Effect of various polyethylene structures on film extrusion"*, Journal of Reinforced Plastics and Composites, Vol.17, No.10, (1998), P.945-954

2 Donald G. Baird and I. Collias Dimitris, *"Polymer Processing"*, Wiley-Interscience, (1998)

3 R. J. Crawford, *"Plastics Engineering"*, Butterworth Heinemann, (2005)

4 I.M Ward and J. Sweeney, *"An Introduction to The Mechanical Properties of Solid Polymers"*, Wiley Interscience, (2004)

5 S. Muke, Connell H., Sbarski I. and Bhattacharya S. N., *"Numerical modelling and experimental verification of blown film processing"*, Journal of Non-Newtonian Fluid Mechanics, Vol.116, No.1, (2003), P.113-138

6 Darin Huizenga, Chornoby Kurt and Engelmann Paul V., *"Optimized Lldpe/Ldpe Film Properties Through Correlation of Blend Analyses"*, Journal of Plastic Film and Sheeting, Vol.6, No.4, (1990), P.318-326

7 A. S. Bawa S. Nadanasabapathi J. H. Jagannath, *"Effect of starch on thermal mechanical, and barrier properties of low density polyethylene film"*, Journal of Applied Polymer Science, Vol.99, No.6, (2006), P.3355-3364

8 S. N. Bhattacharya P. Micic, G. Field,, *"Transient elongational viscosity of LLDPE/LDPE blends and its relevance to bubble stability in the film blowing process"*, Polymer Engineering & Science, Vol.38, No.10, (1998), P.1685-1693

9 P. Micic and Bhattacharya S. N., *"Rheology of LLDPE, LDPE and LLDPE/LDPE blends and its relevance to the film blowing process"*, Polymer International, Vol.49, No.12, (2000), P.1580-1589

10 P. Miller, Sbarski I., Kosior E., Masood S. and Iovenitti P., *"Correlation of rheological and mechanical properties for blends of recycled HDPE and virgin polyolefins"*, Journal of Applied Polymer Science, Vol.82, No.14, (2001), P.3505-3512

11 Y. L. Fang, Carreau P. J., Lafleur P. G. and Ymmel S., *"Properties of mLLDPE/LDPE blends in film blowing"*, Polymer Engineering and Science, Vol.45, No.3, (2005), P.343-353

12 C. Silvestre, Cimmino S., Raimo M., Duraccio D., Fernandez B. D., Lafuente P. and Sanz V. L., *"Structure and morphology development in films of mLLDPE/LDPE blends during blowing"*, Macromolecular Materials and Engineering, Vol.291, No.12, (2006), P.1477-1485

13 J. Lu, Sue H. J. and Rieker T. P., *"Dual crystalline texture in HDPE blown films and its implication on mechanical properties"*, Polymer, Vol.42, No.10, (2001), P.4635-4646

14 M. van Gurp, Kip B.J., van Heel J.P.C. and de Boer S., *"On the Development of Orientation in LDPE Blown Films*

10.1177/875608799401000206", Journal of Plastic Film and Sheeting, Vol.10, No.2, (1994), P.156-176

15 A. Ghaneh-Fard, *"Effects of film blowing conditions on molecular orientation and mechanical properties of polyethylene films"*, Journal of Plastic Film & Sheeting, Vol.15, No.3, (1999), P.194-218

16 Y. L. Fang, Carreau P. J. and Lafleur P. G., *"Rheological effects of polyethylenes in film blowing"*, Polymer Engineering and Science, Vol.43, No.7, (2003), P.1391-1406

17 S. Kim, Fang Y. L., Lafleur P. G. and Carreau P. J., *"Dynamics and criteria for bubble instabilities in a single layer film blowing extrusion"*, Polymer Engineering and Science, Vol.44, No.2, (2004), P.283-302

18 J. J. Lu and Sue H. J., *"Morphology and mechanical properties of blown films of a low-density polyethylene/linear low-density polyethylene blend"*, Journal of Polymer Science Part B-Polymer Physics, Vol.40, No.6, (2002), P.507-518

19 Donald G. Baird, *"The role of extensional rheology in polymer processing"*, Korea-Australia Rheology Journal, Vol.11, No.4, (1999), P.305-311

20 H. Munstedt, Kurzbeck S. and Stange J., *"Importance of elongational properties of polymer melts for film blowing and thermoforming"*, Polymer Engineering and Science, Vol.46, No.9, (2006), P.1190-1195

21 James E Mark, *"Physical properties of polymers"*, American institute of physics.AIP Press, (1996)

22 Q. Fu, Men Y. and Strobl G., *"Understanding of the tensile deformation in HDPE/LDPE blends based on their crystal structure and phase morphology"*, Polymer, Vol.44, No.6, (2003), P.1927-1933

23 J. Morawiec, Pawlak A., Slouf M., Galeski A., Piorkowska E. and Krasnikowa N., *"Preparation and properties of compatibilized LDPE/organo-modified montmorillonite nanocomposites"*, European Polymer Journal, Vol.41, No.5, (2005), P.1115-1122

24 ASTM-D882, *"Annual Book of ASTM Standards"*, ASTM, (1995)

25 ASTM-D1709, *"Annual Book of ASTM Standards"*, ASTM, (1995)

26 ISO-7765-1, *"Plastics Film and Sheeting - Determination of Impact Resistance by Free-Falling Dart Method - Part 1: Staircase Method"*, ISO - 1994(E), (1994)

27 ISO-7765-2, *"Plastics Film and Sheeting - Determination of Impact Resistance by Free-Falling Dart Method - Part 2: Instrumented Puncture Test"*, ISO -1994(E), (1994)

28 ASTM-D3798, *"Annual Book of ASTM Standards"*, ASTM, (1995)

29 ASTM-D1922, *"Annual Book of ASTM Standards"*, ASTM, (1995)

30 A. L. Bobovitch, Elkoun S. and Ajji A., *"Orientation,Structure and Properties of Double-Bubble Oriented Lldpe Films"*, Journal of Plastic Film and Sheeting, Vol.22, No.2, (2006), P.133-143

31 M. Nouri, Morshedian J., Rabbani A., Ghasemi I. and Ebrahimi M., *"Investigation of LLDPE/LDPE blown films by response surface methodology"*, Iranian Polymer Journal, Vol.15, No.2, (2006), P.155-162

32 X. M. Zhang, Elkoun S., Ajji A. and Huneault M. A., *"Oriented structure and anisotropy properties of polymer blown films: HDPE, LLDPE and LDPE"*, Polymer, Vol.45, No.1, (2004), P.217-229

VITAE

Name: Sarfaraz Ahmed Furquan

Present & Permanent Address:

HNo: 5-9-848/1, Gunfoundry,

Hyderabad. Andhra Pradesh - 500001

India.

Phone : +966-556183317

Email Address : sarfaraz123_7@yahoo.co.in

Date of Birth: 19 August 1983

Nationality Indian

Education:

Master of Science (M.S.) May 2009

Department of Mechanical Engineering

King Fahd University of Petroleum & Minerals

Dhahran - Saudi Arabia.

Bachelor of Engineering (B.E.) May 2005

Department of Mechanical Engineering

Muffakham Jah College of Engineering & Technology

Osmania University

Hyderabad – India